REACTIONS OF ACETYLENE AND ALLENE WITH AMIDODIPHOSPHINE IRIDIUM COMPLEXES

by

CAMERON EDWARD FORDE

B. Sc., Trinity Western University, 1990

A THESIS SUBMITTED IN PARTIAL FULFILLMENT OF
THE REQUIREMENTS FOR THE DEGREE OF
MASTER OF SCIENCE

in

THE FACULTY OF GRADUATE STUDIES

Department of Chemistry

We accept this thesis as conforming
to the required standard

THE UNIVERSITY OF BRITISH COLUMBIA

AUGUST 1992

In presenting this thesis in partial fulfillment of the requirements for an advanced degree at the University of British Columbia, I agree that the Library shall make it freely available for reference and study. I further agree that permission for extensive copying of this thesis for scholarly purposes may be granted by the head of my department or by his or her representatives. It is understood that copying or publication of this thesis for financial gain shall not be allowed with out my written permission.

Cameron E. Forde

Department of Chemistry

The University of British Columbia

Vancouver, Canada

September 3, 1992

Abstract

The reaction of the alkyl halide complexes Ir[N($SiMe_2CH_2PPh_2$)$_2$](CH_2R)X (**2**; R = H, X = I: **3**; R = H, X = Br: **4**; R = Ph, X = Br) with one equivalent of acetylene produces the corresponding allyl (or phenylallyl) complexes Ir[N($SiMe_2CH_2PPh_2$)$_2$](η^3-C_3H_4R)X (**6**; R = H, X = I: **7**; R = H, X = I: **8**; R = Ph, X = Br). A deuterium labeling study indicates that the allyl complexes form by vinylidene migratory insertion into the iridium-alkyl bonds. Using excess acetylene produces the isoprenyl complexes Ir[N($SiMe_2CH_2PPh_2$)$_2$](C_5H_7)X (**10**; X = I: **11**; X = Br) from the methyl derivatives **2** and **3**. The reactivity of these complexes is blocked by an agostic interaction of a methyl group with the metal. Complex **10** reacts with trimethylphosphine to generate a new compound, Ir[N($SiMe_2CH_2PPh_2$)$_2$](PMe_3)(C_5H_7)I, in which the tridentate ligand has changed from meridional to facial coordination. The addition of excess acetylene to the benzyl bromide complex, **4**, results in elimination of the benzyl ligand as toluene and a dual vinylidene insertion process to produce Ir[C(CH_2)N($SiMe_2CH_2PPh_2$)$_2$](C(CH_2)CCH). An X-ray structure determination shows that one vinylidene unit has inserted into the iridium-amide linkage and the other vinylidene unit has inserted into an in situ iridium acetylide bond.

The η^2-allene complex Ir[N($SiMe_2CH_2PPh_2$)$_2$](η^2-C_3H_4) previously reported from this laboratory was found to exist in a dynamic equilibrium with a new complex which has two incorporated molecules of allene. This new complex is proposed to be the iridacyclopentane complex, Ir[N($SiMe_2CH_2PPh_2$)$_2$](C_6H_8), based on NMR evidence and literature precedent. This iridacyclopentane complex is stable only in the presence of allene. Attempts to stabilize this complex by coordinative saturation with the potent Lewis base trimethylphosphine produced the trimethylphosphine iridacyclopropane complex, Ir[N($SiMe_2CH_2PPh_2$)$_2$](PMe_3)(C_3H_4). This complex could also be prepared directly from the iridacyclopropane complex, Ir[N($SiMe_2CH_2PPh_2$)$_2$](η^2-C_3H_4). The introduction of allene to the alkyl halide complexes **2-4** was found to result in the reductive elimination of the alkyl halide and to form an equilibrium mixture of the iridacyclopropane and iridacyclopentane complexes. The kinetics of the reductive

elimination of benzyl bromide from complex **4** was studied by phosphorus-31 NMR spectroscopy. The reaction was found to have a pseudo-first order dependence upon metal complex concentration when excess allene was employed. The activation parameters were found to be $\Delta H^{\ddagger} = 67$ (9) kJ mol^{-1} and $\Delta S^{\ddagger} = -260$ (30) J mol^{-1} K^{-1}. The rate-determining step of this process is proposed to be the associative step.

Table of Contents

Abstract ii

Table of contents iv

List of tables vii

List of figures viii

List of abbreviations ix

Acknowledgments x

Dedication xi

Chapter 1: Introduction

1. Phosphine and mixed-donor ligands in organometallic chemistry 1
2. The oxidative addition reaction 4
3. The reductive elimination reaction 6
4. Migratory insertion 6
5. Scope of this Thesis 7
6. References 7

Chapter 2: Reactions of Acetylene With Iridium(III) Alkyl Halide Complexes

1. General introduction and background 10
2. Literature survey 12
3. Reactions with one equivalent of acetylene 15
4. Reactions with excess acetylene 20
   - A. Methyl derivatives 21
   - B. Benzyl derivative 25

5. General observations and mechanistic considerations. 30

6. Summary. 31

7. Future work 32

8. References 32

Chapter 3: Reactions of Allene with Amidodiphosphine Iridium Complexes

1. Introduction. 35

2. Literature survey 35

3. Previous work on amidodiphosphine iridium complexes. 38

4. Allene coupling and decoupling at amidodiphosphine iridium centres. 39

5. Reactions with trimethylphosphine 41

6. Allene reactivity with alkyl halide amidodiphosphine iridium complexes. 47

7. Summary. 51

8. Future work 52

9. References 52

Chapter 4: Experimental

1. General. 55

2. Solvents. 55

3. Reagents 56

4. Syntheses of metal complexes. 56

5. NMR measurements. 57

6. Syntheses of new compounds. 57

mer-Ir[N($SiMe_2CH_2PPh_2$)$_2$](η^3-C_3H_5)X 57

mer-Ir[N(SiMe$_2$CH$_2$PPh$_2$)$_2$](η^3-C$_3$H$_5$)I, **6** 58

mer-Ir[N(SiMe$_2$CH$_2$PPh$_2$)$_2$](η^3-C$_3$H$_5$)Br, **7** 58

mer-Ir[N(SiMe$_2$CH$_2$PPh$_2$)$_2$](η^3-C$_3$H$_4$-1-Ph)Br, **8** 58

mer-Ir[N(SiMe$_2$CH$_2$PPh$_2$)$_2$](η^3-C$_3$H$_2$D$_2$-1-Ph)Br, **8-*d*$_2$** 59

mer-trans-Ir[N(SiMe$_2$CH$_2$PPh$_2$)$_2$](Me)I(PMe$_3$), **9A-C** 60

mer-Ir[N(SiMe$_2$CH$_2$PPh$_2$)$_2$][η^1-C(CH$_2$)C(CH$_2$)CH$_3$]X 62

mer-Ir[N(SiMe$_2$CH$_2$PPh$_2$)$_2$][η^1-C(CH$_2$)C(CH$_2$)CH$_3$]I, **10** 62

mer-Ir[N(SiMe$_2$CH$_2$PPh$_2$)$_2$][η^1-C(CH$_2$)C(CH$_2$)CH$_3$]Br, **11** 63

fac-Ir[N(SiMe$_2$CH$_2$PPh$_2$)$_2$](PMe3)[C(CH$_2$)C(CH$_2$)CH$_3$]I, **12** 63

mer-Ir[C(CH$_2$)N(SiMe$_2$CH$_2$PPh$_2$)$_2$][η^1,η^2-C(CH$_2$)CCH]Br, **13** 64

mer-Ir[N(SiMe$_2$CH$_2$PPh$_2$)$_2$](η^2-C$_3$H$_4$), **14** 65

mer-Ir[N(SiMe$_2$CH$_2$PPh$_2$)$_2$](C$_6$H$_8$), **15** 66

fac-Ir[N(SiMe$_2$CH$_2$PPh$_2$)$_2$](PMe$_3$)(η^2-C$_3$H$_4$), **16** 67

7. References 68

Appendix A: X-Ray Crystallographic Analysis

1. Experimental details 70

A. Crystal data 70

B. Intensity measurements 71

C. Structure solution and refinement 71

2. Tabulated data 72

Appendix B: Kinetic Data 77

List of Tables

Table 2.I. Selected bond lengths (Å) for Ir[C(CH_2)N($SiMe_2CH_2PPh_2$)$_2$]-($C(CH_2)CCH$), **13**. 29

Table 2.II. Selected bond angles (degrees) for Ir[C(CH_2)N($SiMe_2CH_2PPh_2$)$_2$]-($C(CH_2)CCH$), **13**. 30

Table 3.I. Kinetic data for the reductive elimination of benzyl bromide. 48

Table A.Ia. Final atomic coordinates (fractional) and B_{eq} ($Å^2$). 72

Table A.Ib. Hydrogen atom coordinates (fractional) and B_{iso} ($Å^2$). 73

Table A.II. Selected bond lengths (Å) with standard deviations. 75

Table A.III. Selected bond angles (degrees) with standard deviations. 75

Table B.I. Run 1: Kinetic data at T = 35.0 ± 0.1 °C. 77

Table B.II. Run 2: Kinetic data at T = 35.3 ± 0.2 °C. 78

Table B.III. Run 3: Kinetic data at T = 35.3 ± 0.1 °C. 79

Table B.IV. Run 4: Kinetic data at T = 45.2 ± 0.1 °C. 80

Table B.V. Run 5: Kinetic data at Temp = 45.2 ± 0.1 °C. 81

Table B.VI. Run 6: Kinetic data at T = 55.2 ± 0.2 °C. 82

Table B.VII. Run 7: Kinetic data at T = 55.1 ± 0.2 °C. 82

Table B.VIII. Run 8: Kinetic data at T = 55.2 ± 0.2 °C with added 1,4-cyclohexadiene. 83

Table B.IX. Run 9: Kinetic data at T = 55.0 ± 0.2 °C with added 1.4-cyclohexadiene. 84

Table B.X. Kinetic data summarized. 85

List of Figures

Figure 1.1. Some representative multidentate phosphine ligands. 2

Figure 1.2. Chiral (β-aminoalkyl)phosphine ligands. 3

Figure 1.3. Free, A, and coordinated, B, $-N(SiMe_2CH_2PPh_2)_2$. 4

Figure 1.4. The trimethylenemethane, methylidene and vinylidene amidodiphosphine iridium complexes 4

Figure 2.1. Free, A, and metal-coordinated, B, vinylidene 10

Figure 2.2. The 300 MHz ^1H NMR spectrum of $Ir[N(SiMe_2CH_2PPh_2)_2](C_5H_7)Br$, **11**..... 22

Figure 2.3. Two possible geometric isomers of $Ir[N(SiMe_2CH_2PPh_2)_2](C_5H_7)(PMe_3)I$, **12**. 24

Figure 2.4. The 300 MHz 1H NMR spectrum of Ir[C(CH2)N(SiMe2CH2PPh2)2]-[C(CH2)CCH]Br, **13**. 26

Figure 2.5. The molecular structure of $Ir[C(CH_2)N(SiMe_2CH_2PPh_2)_2](C(CH_2)CCH)$, **13**. 27

Figure 3.1. Cyclic oligomers of allene 37

Figure 3.2. The 3,4-dimethylenemetallacyclopentane moiety 37

Figure 3.3. $Rh(acac)(C_6H_8)py_2$ and $Ir(acac)(C_6H_8)(\eta^2\text{-}C_3H_4)py$ 37

Figure 3.4. η^2-π, A, and η^2-σ, B, modes of allene coordination 38

Figure 3.5. The 300 MHz ^1H NMR spectrum of $Ir[N(SiMe_2CH_2PPh_2)_2](C_6H_8)$, **15**..... 40

Figure 3.6. Five possible structures of $Ir[N(SiMe_2CH_2PPh_2)_2](PMe_3)(C_3H_4)$, **16**..... 43

Figure 3.7. The 300 MHz ^1H NMR spectrum of $Ir[N(SiMe_2CH_2PPh_2)_2](PMe_3)(C_3H_4)$, **15**. 44

Figure 3.8. The Eyring plot of the kinetic data for the reaction of $Ir[N(SiMe_2CH_2PPh_2)_2]$-$(CH_2Ph)Br$, **4**, with excess allene 49

List of Abbreviations

Aside from the standard IUPAC and SI abbreviations the following abbreviations are used in this Thesis.

acac	acetylacetonato	
BDH	British Drug House	
br	broad	
Bu^t	*tert*-butyl	$-C(CH_3)_3$
cis	cisoidal coordination geometry	
Δ	heat	
$\Delta S^{\ddagger}$	change in entropy of activation	
$\Delta H^{\ddagger}$	change in enthalpy of activation	
δ	chemical shift	
d	doublet	
fac	facial coordination geometry	
gem	geminal disposition	
J	coupling constant	
m-	*meta*-	
m	multiplet	
Me	methyl	$-CH_3$
mer	meridional coordination geometry	
MSD	Merck-Sharp-Dohme	
NMR	nuclear magnetic resonance	
o-	*ortho*-	
p-	*para*-	
Ph	phenyl	$-C_6H_5$
Pr^i	isopropyl	$-CH(CH_3)_2$
py	pyridine	
s	singlet	
t	triplet	
trans	transoidal coordination geometry	
vt	virtual triplet	

Acknowledgments

First and foremost I would like to thank Dr. Michael Fryzuk for instilling in me a sense of the scope and importance of organometallic chemistry. It has been a pleasure to work under his supervision and I have learned much from him in the course of our daily interaction, only a fraction of which could be presented in this Thesis.

I would like to thank Dr. Steve Rettig for his excellent work on the X-ray crystal structure analysis, especially in that he went out of his way to have the results ready for the Edmonton CIC conference.

The onerous and time-consuming task of proof-reading this Thesis was borne by many individuals and I would like thank each one for their unique contributions: Dr. Craig Montgomery, Dr. Lucio Gelmini, Dr. Martin Ehlert, Mr. Richard Schutte, Mr. Kevin Ross, Ms. Lisa Rosenberg, Mr. Myl Mylvaganam, Mr. Jeff Debad, Mr. Guy Clentsmith, and Mr. Eric Brouwer.

In addition I would like to thank Eric Brouwer and Pauline Chow for our many helpful discussions, both chemistry related and otherwise. I wish you both success in your respective endeavours and look forward to our continued friendship.

A thumbnail sketch, a jewelers stone

I need an idea to call my own.

Old man don't lay so still

You're not yet young there's time to teach.

Point to point, point observation

Children carry reservations.

Standing on the shoulders of giants

Leaves me cold, leaves me cold.

I need an idea to call my own

A hundred million birds fly away.

- M. Stipe -

CHAPTER 1

INTRODUCTION

1. Phosphine and mixed-donor ligands in organometallic chemistry.

The formation of metal-carbon bonds and the transformations that can be wrought to organic fragments at a metal centre comprise much of the subject matter of organometallic chemistry.[1] Formally, only those complexes containing a metal-carbon bond can be considered organometallic complexes, but many ligands in organometallic chemistry involve coordination to a metal through elements other than carbon. These ancillary ligands are only rarely involved in the reactivity of the complex and are used to manipulate the steric and electronic properties of the complex. The phosphine family of ligands is quite commonly used as ancillary ligands since the desired steric and electronic properties can be adjusted by appropriate choice of the phosphine.

One way in which phosphine ligands can be modified is by altering the size of the substituents. The cone angle[2] has been introduced as a measure of the steric bulk of a phosphine ligand, and phosphine ligands of a wide range of cone angles have been prepared. Phosphine ligands with large cone angles (eg. tri-*t*-butylphosphine and tricyclohexylphosphine) have been used to stabilize coordinatively unsaturated complexes.

The electron-donating ability of the substituents on phosphorus changes the Lewis basicity of the ligand. For example, alkyl substituents are better electron donors and produce more Lewis-

References p. 7

basic phosphines than the corresponding aryl analogues. Thus the electron density at a metal centre can be controlled to some extent by the choice of substituent on the phosphine.

The ubiquitary presence of phosphine ligands in organometallic chemistry is due in part to the NMR activity of the phosphorus nucleus. The ^{31}P nucleus is has a nuclear spin of one half and is 100 % abundant and has adequate sensitivity for NMR measurement (about one one-thousandth that of proton). The magnitude of two-bond phosphorus-phosphorus coupling constants across a metal ($^2J_{PP}$)[3] as well as the one-bond metal-phosphorus coupling constants ($^1J_{MP}$, where M is a spin-half nucleus)[4] are useful stereochemical probes. The chemical shift can also be used to determine the oxidation state of the phosphorus nucleus; however, there are a number of parameters involved and such assignments should be made carefully.

Phosphine ligands with more than one phosphorus atom available for coordination to a metal have also found much use in organometallic chemistry. Such ligands that coordinate through more than one atom are called chelating ligands (from the Greek *chēlē*, claw). The donor atoms can be separated by any number of atoms, although two and three member backbones have been the most common since the resulting ring systems are five- and six-membered. With this method chelating phosphorus ligands can be constrained to certain geometries about a metal (eg.

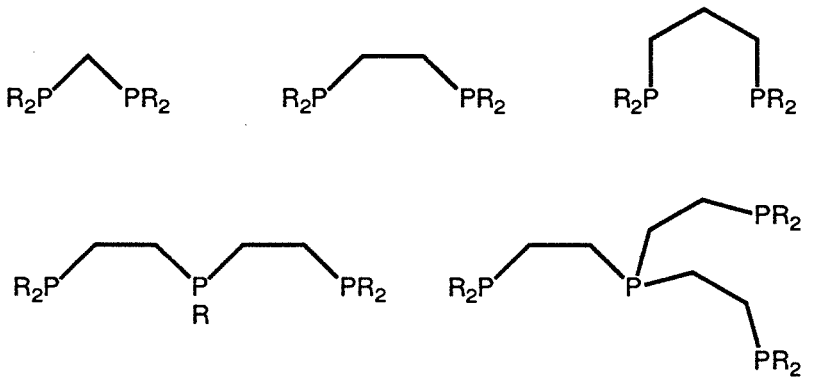

Figure 1.1. Some representative multidentate phosphine ligands.

References p. 7

cis or facial). Some representative examples of multidentate phosphine ligands are shown in Figure 1.1.

Chelating ligands which have the ability to coordinate to metal atoms through disparate nuclei have also been prepared. This class of ligands is known as mixed-donor ligands and they can have some advantages over multidentate ligands of the same donor type. The mixed-donor ligands used in the preparation of the catalysts for the catalytic asymmetric cross-coupling reaction provide a good example of some of the advantages. The chiral (β-aminoalkyl)phosphine ligands[5] have been prepared from optically active amino acids (Figure 1.2). Nickel and palladium complexes with these ligands have been used in the catalytic asymmetric Grignard cross-coupling of secondary alkyl magnesium reagents with alkyl and aryl halide compounds.[6] The nitrogen donor of these ligands aids in the orientation of the attack of the Grignard reagent and results in the formation of optically active products.

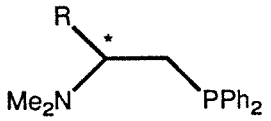

Amino acid	R	Ligand	Amino acid	R	Ligand
S-alanine	Me	S-Alaphos	S-phenylalanine	CH_2Ph	S-Phephos
S-leucine	Bu^i	R-Leuphos	R-phenylglycine	Ph	R-PhGlyphos
S-valine	Pr^i	S-Valphos	R-cyclohexylglycine	C_6H_{11}	R-ChGlyphos
S-isoleucine	Bu^s	S-Ilephos	R-*t*-leucine	Bu^t	R-*t*-Leuphos

Figure 1.2. Chiral (β-aminoalkyl)phosphine ligands.

A tridentate amidodiphosphine family of mixed-donor ligands has been prepared in these laboratories (Figure 1.3). This family of ligands has been used to make many exceptional compounds; examples are amide complexes of the later transition elements[7] and phosphine complexes of the early transition series and lanthanide group.[8] Some unusual organic fragments have been stabilized at an iridium complex with this ligand. Three examples are shown in Figure 1.4; the trimethylenemethane,[9] methylidene,[10] and vinylidene[11,12] complexes. The starting

References p. 7

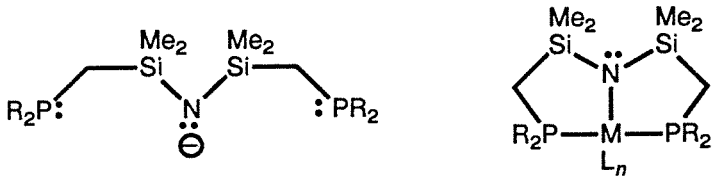

A B

Figure 1.3. Free, **A**, and coordinated, **B**, $^{-}N(SiMe_2CH_2PPh_2)_2$.

material for the formation of these complexes is the iridium amidodiphosphine cyclooctene complex, **1**, the preparation of which is shown in Reaction 1.1.[13-15]

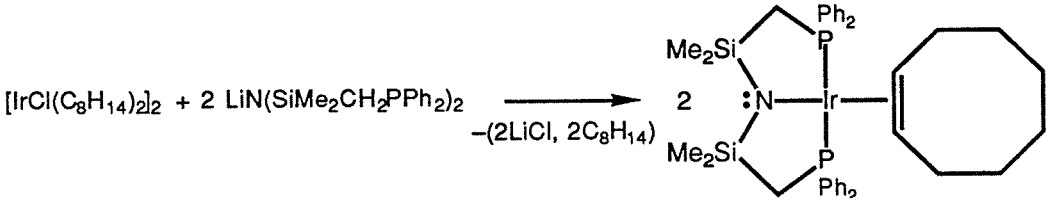

(1.1)

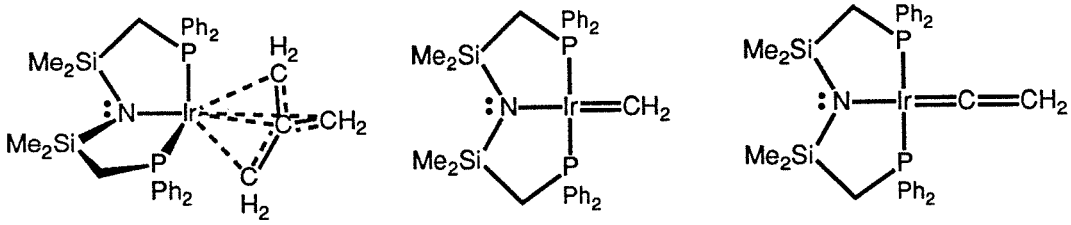

Figure 1.4. The trimethylenemethane, methylidene and vinylidene amidodiphosphine iridium complexes.

2. The oxidative addition reaction.

The oxidative addition reaction is important in many catalytic and stoichiometric reactions in organometallic chemistry.[16] The reaction involves the addition of the two parts of a molecule, A-B, to a metal. The A-B bond breaks and new bonds between the metal and A and B form. The metal complex needs to have available an oxidation state that is two higher than before the addition and also have available sites for coordination. The reagents which oxidatively add to metal complexes can be separated into three categories:[17] nonpolar reagents, electrophilic reagents and

Scheme 1.I

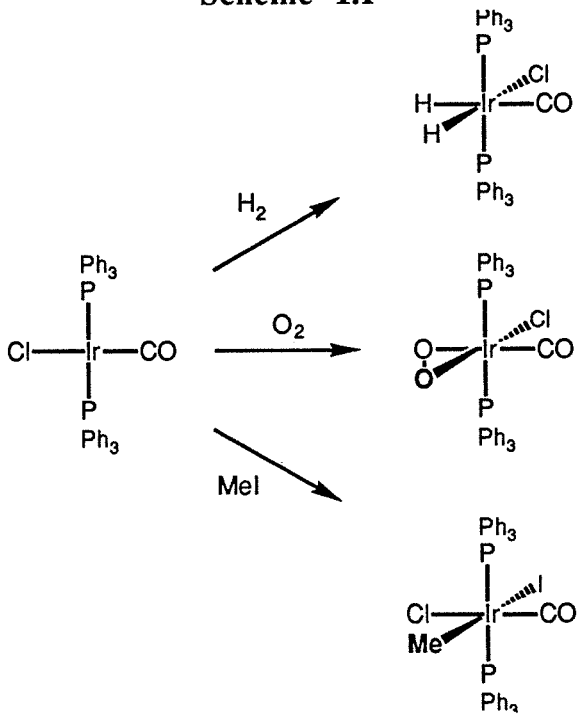

reagents where a bond remains between the two added parts. The reactivity of the iridium complex, *trans*-$Ir(PPh_3)_2(CO)Cl$, with each of these classes of compounds is summarized in Scheme 1.I. The amidodiphosphine iridium complex, **1**, mentioned above is quite similar to this iridium complex; there are two phosphine donors trans to one another and a uninegative ligand. The oxidative addition of alkyl halides to the iridium cyclooctene complex, **1**, was found to produce coordinatively unsaturated complexes, **2**,[15,18] **3**[15] and **4**[19] (Reaction 1.2).

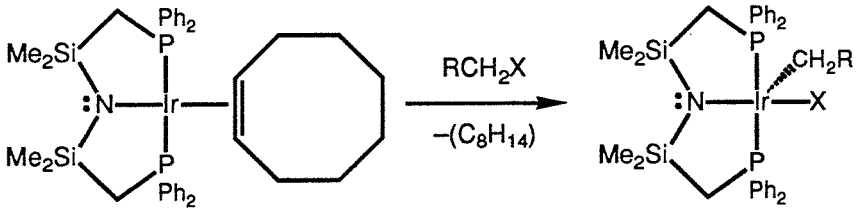

1

2: R = H, X = Br
3: R = H, X = I
4: R = Ph, X = Br

(1.2)

3. The reductive elimination reaction.

The reverse of the oxidative addition reaction is the reductive elimination reaction. Reductive elimination is important in organometallic chemistry since carbon-carbon bonds can be formed and many catalytic cycles include reductive elimination steps.[16] In order for reductive elimination to occur two substituents need to be cis to each other in the coordination sphere of a metal. Reductive elimination of alkyl halides is observed in the reactivity studies presented in Chapter 3.

4. Migratory insertion.

Another mode of reactivity that is of importance to organometallic chemistry is migratory insertion.[20] The migratory insertion reaction is vital to many catalytic cycles and to stoichiometric formation of organic molecules. In order for migratory insertion to occur the two substituents need to be cis to each other in the coordination sphere of the metal and the process is usually aided

Scheme 1.2

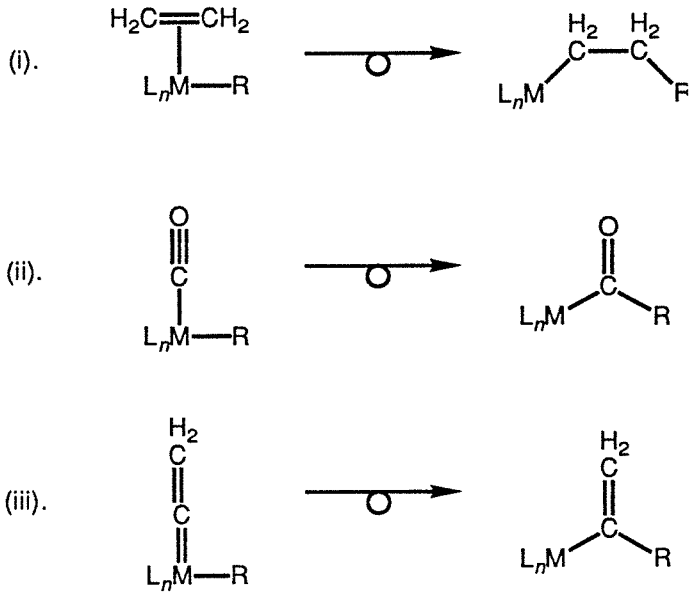

References p. 7

by the addition of some ligand to stabilize the resulting complex. Many olefin polymerization reactions are proposed to proceed by olefin insertion into metal-alkyl bonds (Scheme 1.2i).[21] Carbon monoxide is a ligand which quite commonly undergoes migratory insertion into metal-carbon bonds (Scheme 1.2ii). The migratory insertion of the vinylidene moiety (Scheme 1.2iii) is observed in the acetylene reactions reported in Chapter 2.

5. Scope of this Thesis.

The study of the reactivity of d^6, amidodiphosphine iridium alkyl halide complexes is presented in this Thesis. The addition of unsaturated hydrocarbons, acetylene and allene, to these iridium complexes results in the formation of carbon-carbon bonds and thus transformations of organic molecules at the metal centre. The addition of acetylene to the amido diphosphine complexes is reported in Chapter 2. The rearrangement of acetylene to vinylidene and subsequent migratory insertion of the vinylidene moiety into iridium-alkyl bonds is observed. Chapter 3 extends this reactivity to the three carbon diene, allene. The reductive elimination of alkyl halide compounds from the iridium(III) alkyl halide complexes occurs when allene is introduced. The experimental details of the work are reported in Chapter 4. Some ideas for future work are presented at the ends of Chapters 2 and 3.

6. References.

(1) Collman, J. P.; Hegedus, L. S.; Norton, J. R.; Finke, R. G. *Principles and Applications of Organotransition Metal Chemistry*; University Science Books: Mill Valley, CA, 1987, pp 1-2.

(2) Tolman, C. A. *Chem. Rev.* **1977**, *77*, 313.

(3) Finer, E. G.; Harris, R. K. *Prog. NMR Spectroscopy* **1970**, *6*, 61.

(4) Pregosin, P. S.; Kunz, R. W. *NMR Basic Principles and Progress*; Springer-Verlag: Heidelberg, 1979; Vol. 16, pp 55ff.

(5) Hayashi, T.; Fukushima, M.; Konishi, M.; Kumada, M. *Tetrahedron Lett.* **1980**, *21*, 79.

(6) Hayashi, T.; Konishi, M.; Fukushima, M.; Kanehira, K.; Hioki, T.; Kumada, M. *J. Org. Chem.* **1983**, *48*, 2195.

(7) Fryzuk, M. D.; Montgomery, C. D. *Coord. Chem. Rev.* **1989**, *95*, 1.

(8) Fryzuk, M. D.; Haddad, T. S.; Berg, D. J. *Coord. Chem. Rev.* **1990**, *99*, 137.

(9) Fryzuk, M. D.; Joshi, K.; Rettig, S. J. *Organometallics* **1991**, *10*, 1642.

(10) Fryzuk, M. D.; MacNeil, P. A.; Rettig, S. J. *J. Am. Chem. Soc.* **1985**, *107*, 6708.

(11) Fryzuk, M. D.; McManus, N. T.; Rettig, S. J.; White, G. S. *Angew. Chem., Int. Ed. Engl.* **1990**, *29*, 73.

(12) Fryzuk, M. D.; Huang, L.; McManus, N. T.; Paglia, P.; Rettig, S. J.; White, G. S. *Organometallics* **1992**, *11*, in press.

(13) Fryzuk, M. D.; MacNeil, P. A. *Organometallics* **1983**, *2*, 355.

(14) Fryzuk, M. D.; MacNeil, P. A. *Organometallics* **1983**, *2*, 682.

(15) Fryzuk, M. D.; MacNeil, P. A.; Rettig, S. J. *Organometallics* **1986**, *5*, 2469.

(16) reference 1, pp 279-343.

(17) reference 1, pp 281-284.

(18) Fryzuk, M. D.; MacNeil, P. A.; Rettig, S. J. *Organometallics* **1985**, *4*, 1145.

(19) Fryzuk, M. D.; MacNeil, P. A.; Massey, R. L.; Ball, R. G. *J. Organomet. Chem.* **1989**, *368*, 231.

(20) reference 1, pp 355-394.

(21) reference 1, pp 383-393.

CHAPTER 2

REACTIONS OF ACETYLENE WITH IRIDIUM(III) ALKYL HALIDE COMPLEXES

1. General introduction and background.

One of the key features of organometallic chemistry is the stabilization of reactive organic molecules at a transition-metal centre.[1] Many molecules are unstable at normal temperatures and pressures, requiring special conditions to stabilize them or special conditions to produce them. One reactive molecule that has been stabilized by coordination to transition metals is vinylidene, the tautomer of acetylene (Figure 2.1). While free vinylidene has been generated thermally by modulated beam dynamic mass spectroscopy at 820 K[2] and has an estimated life-time of 10 ps,[3] many examples of stable transition-metal vinylidene complexes and their methods of preparation are reported in the literature.[4,5]

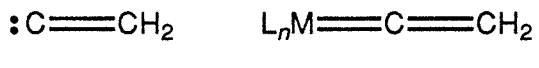

A **B**

Figure 2.1. Free, **A**, and metal-coordinated, **B**, vinylidene.

The most common route of vinylidene formation within the coordination sphere of a metal is the rearrangement of coordinated terminal alkynes. This rearrangement can proceed via two distinct pathways: (i) a concerted route which involves a η^2- to η^1- slip of the alkyne

Scheme 2.I

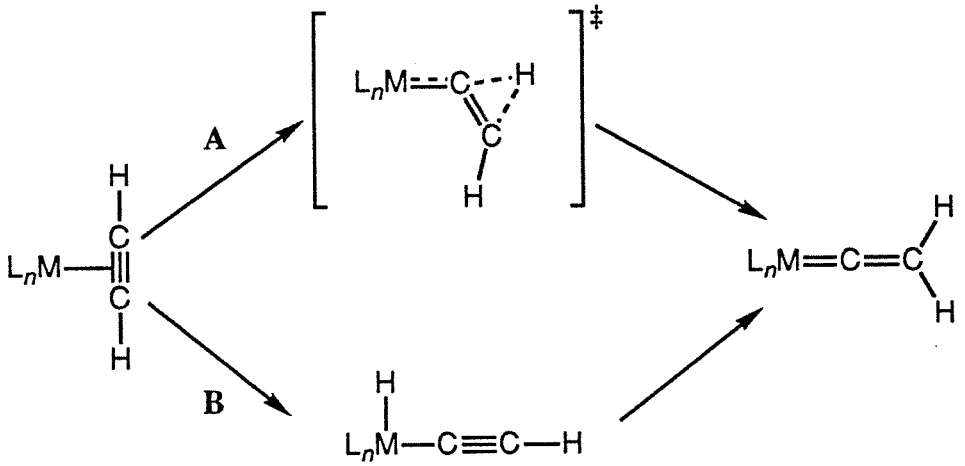

with concomitant α, β proton shift (Scheme 2.IA); or, (ii) an alkynyl(hydrido) route which involves the oxidative addition of the alkyne C-H bond followed by a 1,3-hydrogen shift (Scheme 2.IB). Even though theoretical studies[6] have shown that the alkynyl(hydrido) route is energetically disfavoured, iridium (Scheme 2.II)[7] and rhodium (Scheme 2.III)[8] systems have been reported that proceed by this route. After a brief literature survey of rhodium and iridium systems in which vinylidene intermediates are invoked, the reactions of d^6 iridium alkyl halide complexes with acetylene will be presented and the evidence for vinylidene intermediates in this system of complexes will be discussed.

Scheme 2.II

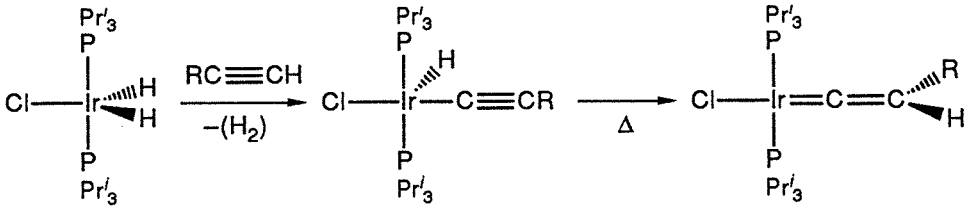

R = $SiMe_3$, COOMe

References p. 32

Scheme 2.III

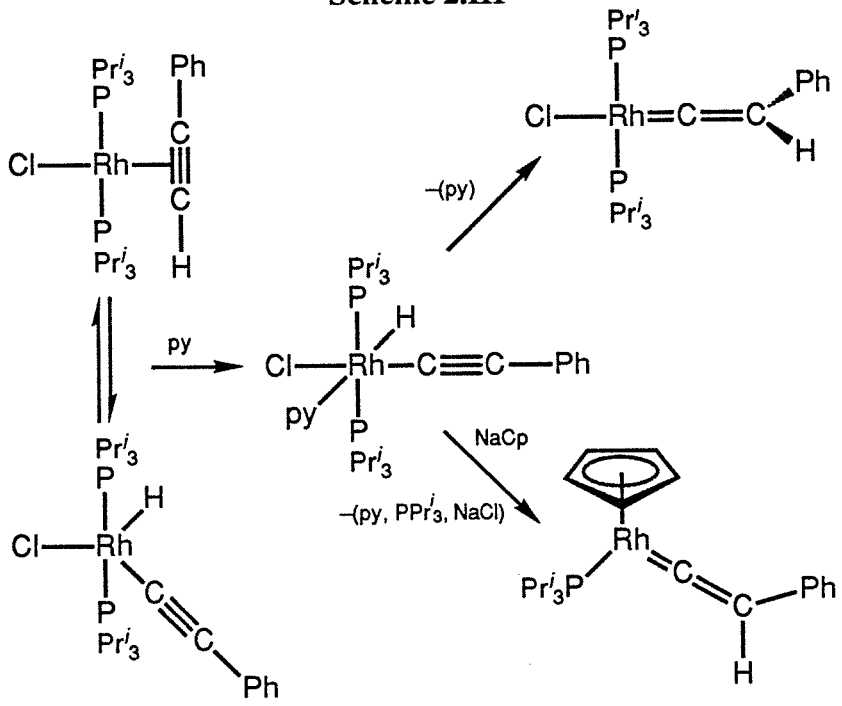

2. Literature survey.

A rhodium vinylidene intermediate is proposed in the reaction of phenylacetylene with chlorotris(triphenylphosphine)rhodium(I) (Scheme 2.IV). The reaction with excess

Scheme 2.IV

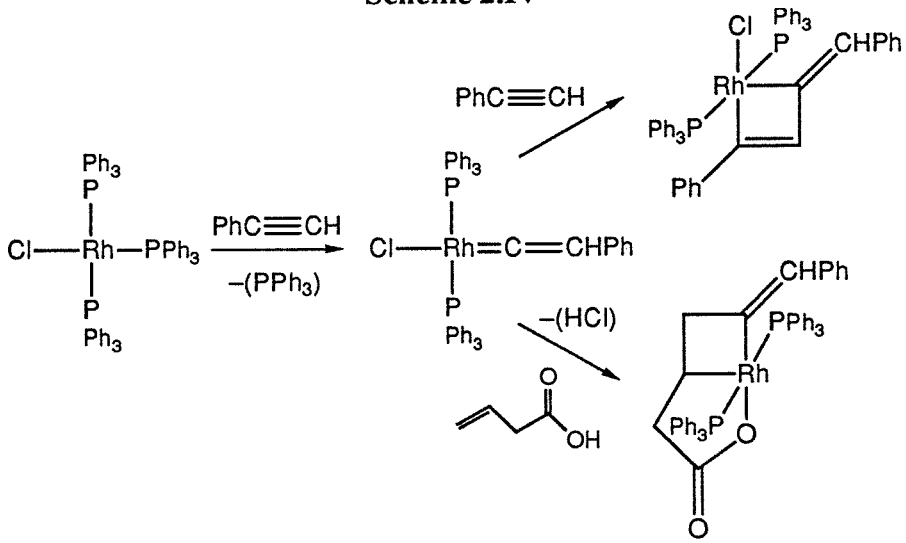

Scheme 2.V

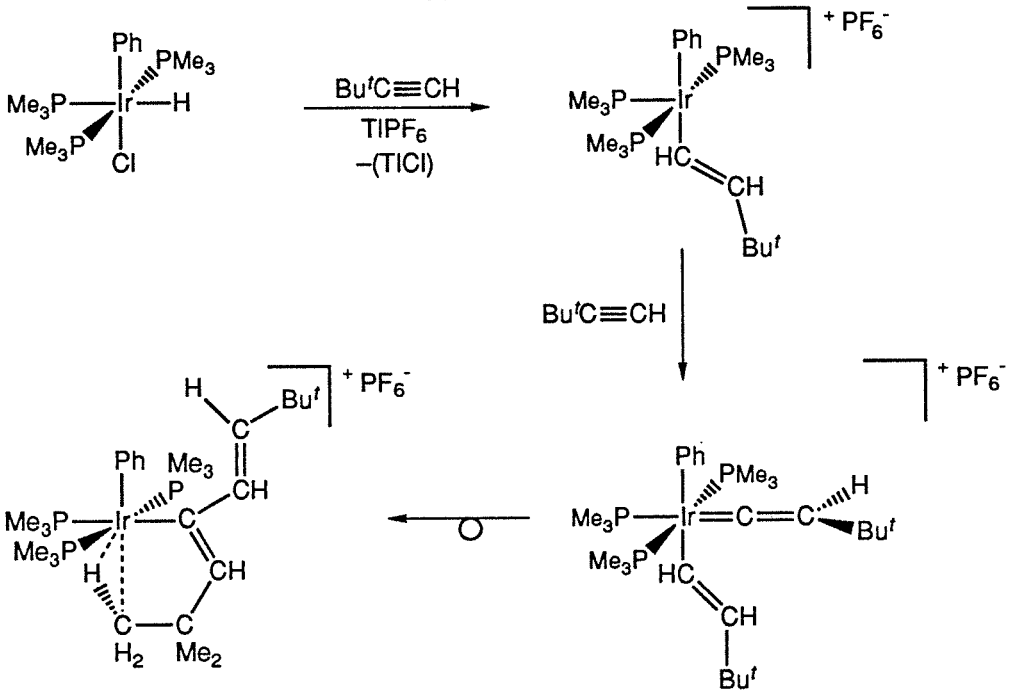

phenylacetylene produces the substituted rhodacyclobutene, while the addition of 3-butenoic acid generates the bicyclic compound shown.[9] The insertion step in each case involves the insertion of either the alkyne or the alkene into the rhodium-vinylidene unit.

The reaction of *mer-trans*-Ir(PMe_3)$_3$(Ph)(Cl)H with phenylacetylene involves migratory insertion of a vinylidene unit (Scheme 2.V). While it has not been shown that the vinyl intermediate formed is produced by vinylidene insertion into the iridium-hydride bond, the final product is formed by vinylidene migratory insertion into the iridium-vinyl group.[10]

The vinylidene complex **5** has been prepared in our laboratories[11] by the addition of acetylene to the cyclooctene complex, **1**; the reaction proceeds via an unstable η^2-acetylene intermediate, which undergoes an acetylene to vinylidene rearrangement (Scheme 2.VI). The reactivity of this complex with Group 13 alkyl compounds[11,12] and with alkyl halides[12] has recently been reported. Relevant to this Thesis is the reaction of **5** with methyl iodide which

Scheme 2.VI

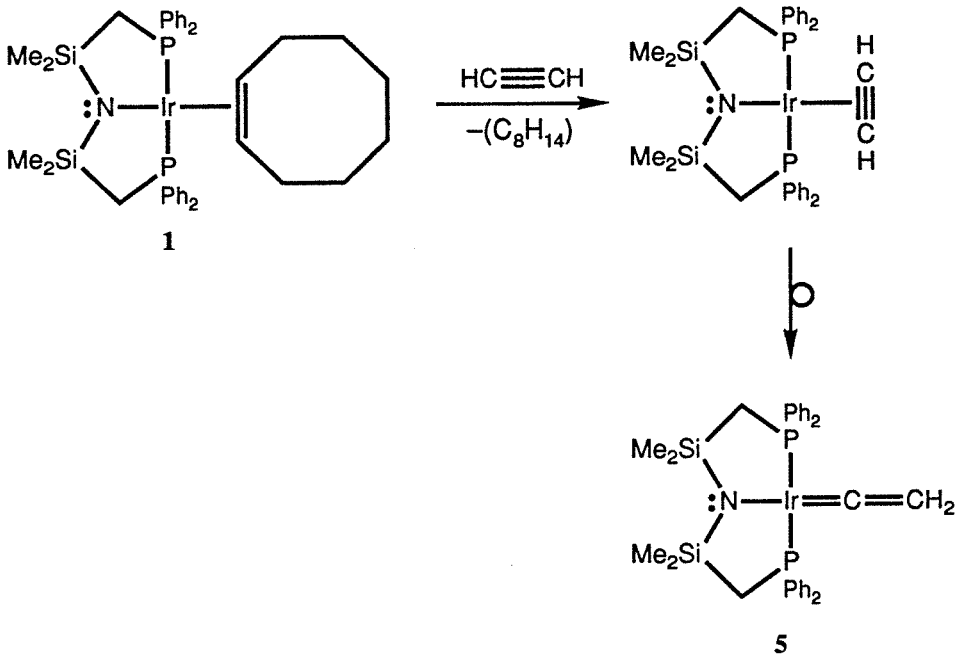

1 **5**

produces the η^3-allyl complex **6**; the progress of this transformation was studied by phosphorus-31 NMR spectroscopy and the proposed mechanism is summarized in Scheme 2.VII. The first step of the proposed mechanism involves the *trans*-oxidative addition of methyl iodide[13,14] to the vinylidene complex **5**. Migratory insertion of the vinylidene unit into the iridium-methyl bond generates an isopropenyl ligand which produces the η^3-allyl complex, **6**, by a 1,2-hydrogen shift.

The intermediate **A** in Scheme 2.VII might be accessible by reaction of acetylene with the alkyl halide complex Ir[N($SiMe_2CH_2PPh_2$)$_2$](Me)I, **2**. The potential for the in situ formation of the vinylidene unit and subsequent migratory insertion invited further study. This route would also make multiple insertions of the vinylidene moiety possible, and could lead to new oligomerization or polymerization products. With this goal in mind a study of the reaction of acetylene with three suitable alkyl halide complexes, which had already been prepared and characterized in our laboratories, Ir[N($SiMe_2CH_2PPh_2$)$_2$](Me)I,[15,16] **2**, Ir[N($SiMe_2CH_2PPh_2$)$_2$]-

Scheme 2.VII

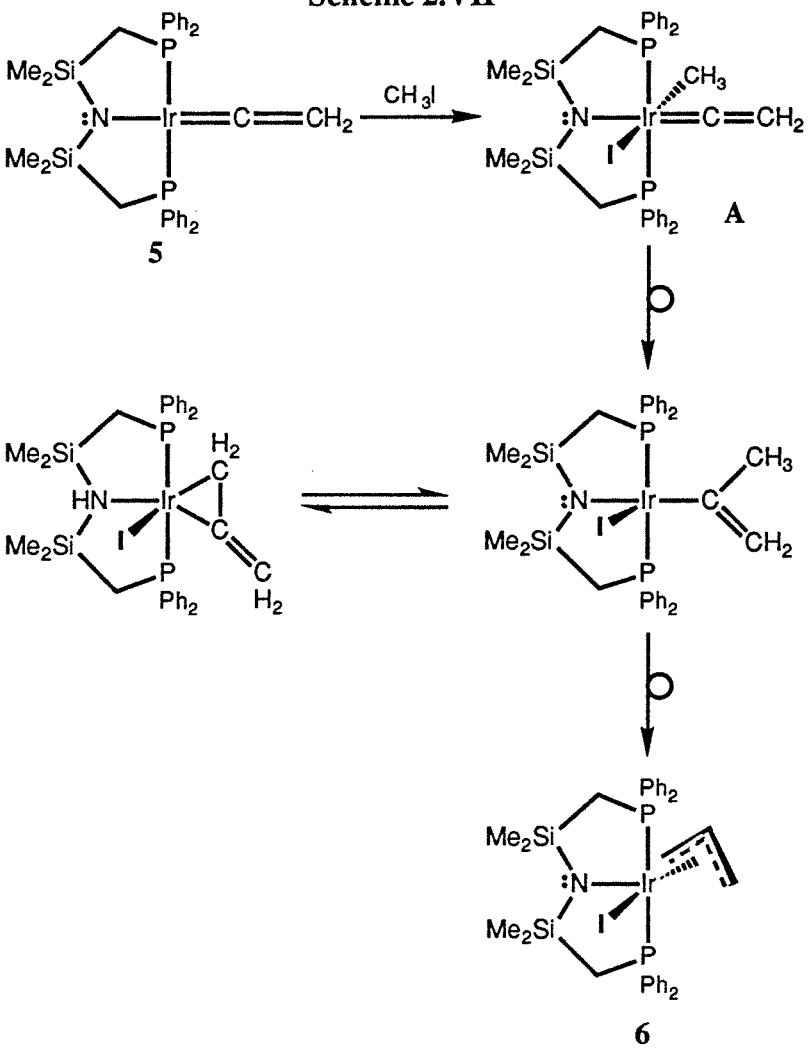

(Me)Br[16] **3**, and Ir[N(SiMe$_2$CH$_2$PPh$_2$)$_2$](CH$_2$Ph)Br,[17] **4** , was undertaken.

3. Reactions with one equivalent of acetylene.

The introduction of one equivalent of acetylene into solutions of the alkyl halide complexes **2-4** produces the allyl complexes, **6-8** (Reaction 2.1). The phosphorus-31 NMR spectra of these complexes exhibit two signals, each of which is a doublet. It has been observed that the magnitude of phosphorus-phosphorus coupling constants is dependant on the cis or

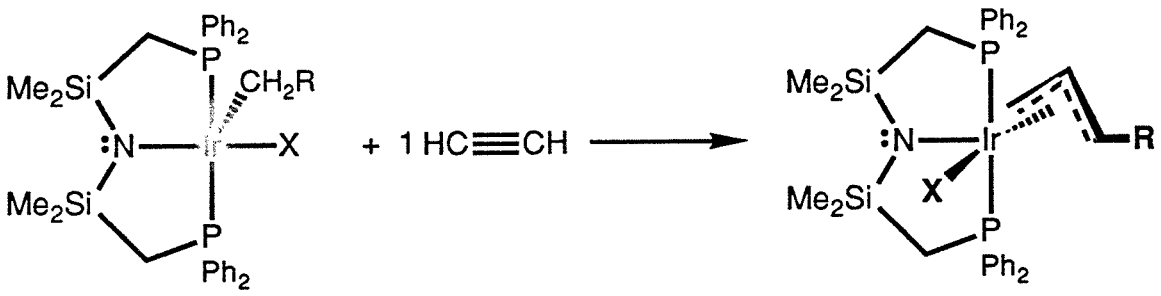

(2.1)

2: R = H, X = I
3: R = H, X = Br
4: R = Ph, X = Br

6: R = H, X = I
7: R = H, X = Br
8: R = Ph, X = Br

trans orientation of the phosphine donors;[18] *cis*-phosphine ligands produce coupling constants less than 100 Hz, while *trans*-phosphine donors have coupling constants greater than 100 Hz. The magnitude of the phosphorus-phosphorus coupling constants for the allyl complexes **6-8** are between 400 and 500 Hz and this strongly indicates a *trans*-orientation of the phosphorus nuclei, which then requires meridional coordination of the tridentate ligand. This is also evidenced in the proton NMR spectra where the separation of the *ortho*- from the *meta*- and *para*-phenyl resonances is greater than 0.5 ppm in each case (a separation of less than 0.5 ppm would suggest *cis*-diphenylphosphines).[19] The allyl complexes **6-8** exhibit the expected resonances for allyl ligands in the proton NMR spectra[20,21] (or phenylallyl resonances[22,23] for **8**). The phenylallyl complex could not be formed by the reaction of benzyl bromide with the vinylidene complex **5**.[12]

Two possible mechanisms can be proposed for the formation of the allyl ligand: (i) direct acetylene insertion, and (ii) acetylene to vinylidene rearrangement, followed by vinylidene insertion. In the first mechanism the direct insertion of the acetylene into the iridium-alkyl bond generates a propenyl ligand which then requires a 1,3-hydrogen shift to generate the allyl ligand (Scheme 2.VIIIA). The alternative mechanism proceeds by

References p. 32

Scheme 2.VIII

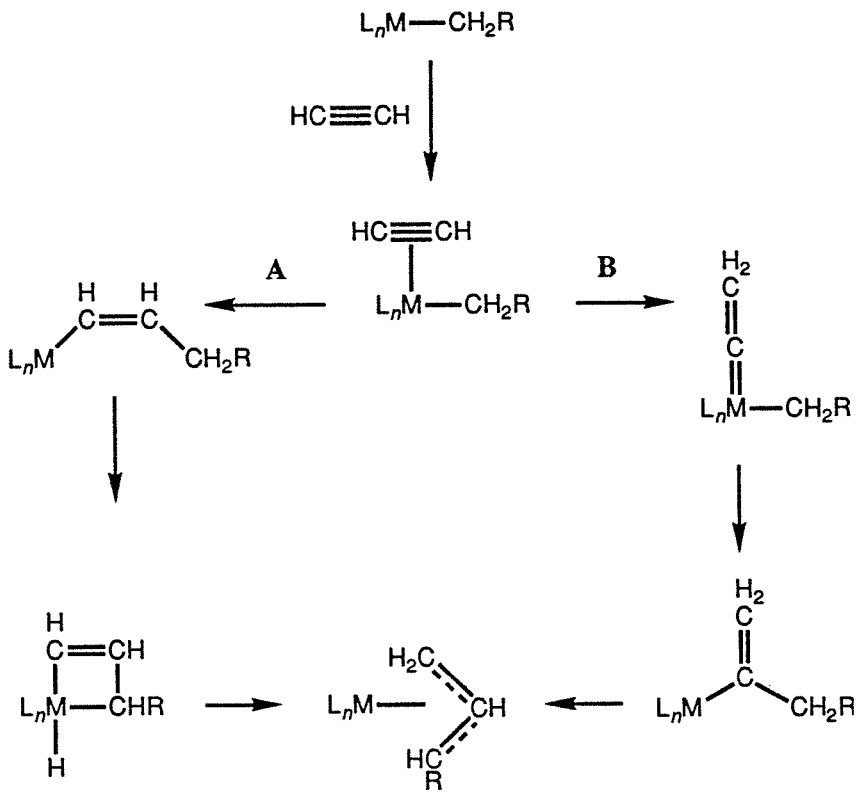

rearrangement of η^2-coordinated acetylene to a vinylidene ligand which then requires migratory insertion of the vinylidene unit into the iridium-alkyl bond and a 1,2-hydrogen shift to produce the allyl ligand (Scheme 2.VIIIB).

In order to discern the applicable mechanism a labeling study was undertaken. Doubly deuterium-labeled acetylene, DC≡CD, was employed as the position of the labels in the final product would differentiate the two mechanisms. Scheme 2.IX delineates the two mechanisms and the product that would be produced by each pathway. The acetylene insertion route (Scheme 2.IXA) results in the central position of the allyl being deuterium-labeled while the vinylidene mechanism (Scheme 2.IXB) leaves this position unaffected. The benzyl bromide complex, **4**, was reacted with one equivalent of acetylene-d_2 and the proton NMR spectrum of

Scheme 2.IX

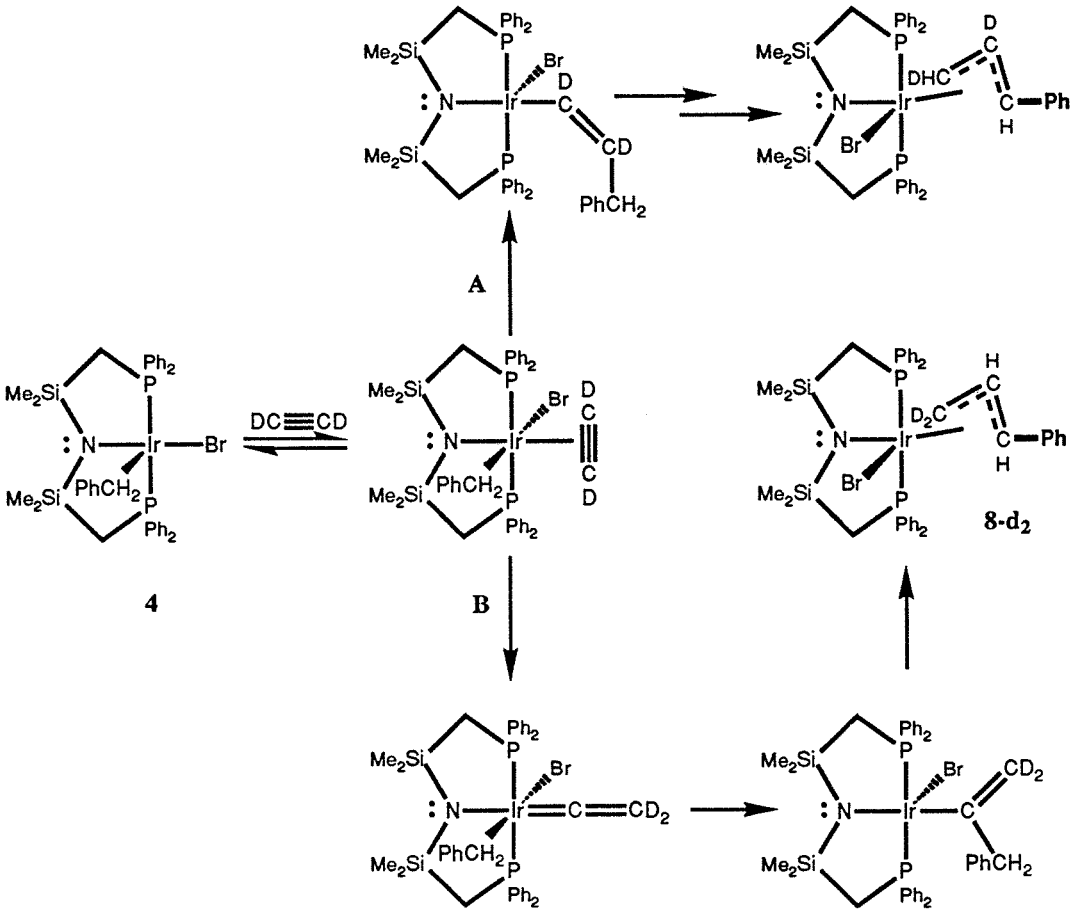

the product, Ir[N(SiMe$_2$CH$_2$PPh$_2$)$_2$](η^3-C$_3$H$_2$D$_2$Ph)Br, **8-*d*$_2$**, exhibits the resonance of the central proton. This evidence supports the proposal of a vinylidene intermediate in the reaction pathway.

The proposed mechanism for the reaction of one equivalent of acetylene with the alkyl halide complexes, **2-4**, is shown in Scheme 2.IXB. The first step is the η^2-coordination of the acetylene. The coordinated acetylene rearranges to a vinylidene moiety, which then inserts into the iridium-alkyl bond. The resultant isopropenyl ligand undergoes a 1,2-hydrogen shift to yield the observed allyl product.

With this mechanism the initial coordination of the acetylene must be cis to the alkyl group in order for the subsequent migratory insertion to be viable. Alternatively, coordination of the alkyne trans to the alkyl group followed by a rearrangement at the metal centre such that the acetylene (or vinylidene) ligand ends up cis to the alkyl group is possible. This rearrangement could potentially occur by phosphine or alkyne dissociation and rearrangement of the resulting five-coordinate complex. The assignment of the structure of five-coordinate d^6 complexes as square-based pyramids is based both on NMR spectroscopic,[16,17,24-26] X-ray crystallographic,[16,17,25-27] and theoretical[28-30] studies. In order to determine if these five-coordinate, d^6 alkyl halide complexes, **2-4**, are fluxional in solution, thus allowing for coordination of the acetylene cis to the alkyl group to occur, the reaction of the methyl iodide complex, **2**, with a strong Lewis base was performed.

Introducing trimethylphosphine into a solution of Ir[N(SiMe$_2$CH$_2$PPh$_2$)$_2$](Me)I, **2**, results in immediate coordination of the phosphine as evidenced by the colour change from

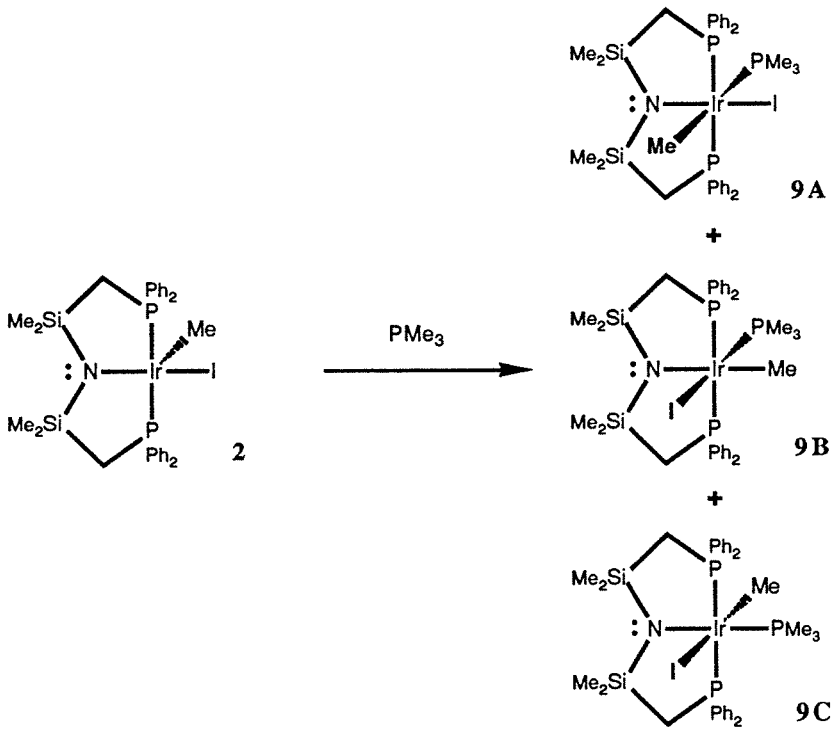

(2.2)

green (five-coordinate Ir(III)) to yellow (six-coordinate Ir(III)) (Reaction 2.2). The phosphorus-31 NMR spectrum indicates the presence of three compounds, **9A-C**, which are shown in Reaction 2.2. In each of these complexes the tridentate ligand has maintained a meridional geometry.

One set of signals can be unambiguously assigned based on an independent synthesis of that compound. The complex with the trimethylphosphine trans to the amide, **9C**, was prepared by the addition of trimethylphosphine to the cyclooctene adduct **1**,[16] which, followed by the *trans*-oxidative addition of methyl iodide,[13,14] generates complex **9C**. The other two products could not be unambiguously assigned. A mixture of the three products was found to convert quantitatively to complex **9C** on warming to 65°C in benzene-d_6 for two days. This rearrangement likely proceeds by dissociation of one ligand, rearrangement of the five-coordinate intermediate and then reassociation of the dissociated ligand.

The presence of three complexes on addition of trimethyl phosphine and the rearrangement of the six-coordinate complexes **9A-C** all suggests that iridium complexes of this type are fluxional in solution. Not only is there the possibility that the incoming acetylene ligand can coordinate cis to the alkyl group, there is also the possibility that the coordinatively saturated complex can undergo some sort of rearrangement that results in the *cis*-orientation of these ligands which is required for migratory insertion.

4. Reactions with excess acetylene.

When excess acetylene is employed, more than one equivalent of acetylene is incorporated in the final products. The methyl and benzyl compounds were found to exhibit different reactivities under these conditions and the results for each will be presented separately. In each case vinylidene intermediates are invoked based on product analysis. The products of

the acetylene reactions with the methyl complexes will be discussed first, followed by a proposed mechanism for the formation of these complexes and then the results of some reactivity studies. The product of the reaction of acetylene with the benzyl analogue and the proposed mechanism for the formation of this compound will then be considered.

A. Methyl derivatives.

The addition of excess acetylene to the methyl halide complexes, $Ir[N(SiMe_2CH_2PPh_2)_2](Me)X$ (**2**: X = I; **3**: X = Br) results in the formation of two new complexes, **10** (X = I) and **11** (X = Br), which have incorporated two equivalents of acetylene. Based on NMR spectroscopic evidence these complexes are proposed to have the structures indicated in Reaction 2.3.

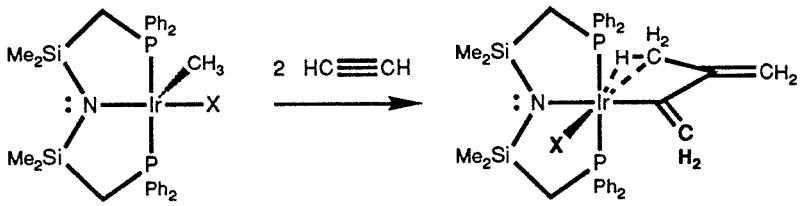

2: X = I
3: X = Br

10: X = I
11: X = Br

(2.3)

The proton NMR spectra of these two complexes exhibit four olefinic proton resonances in the region of 4.8 to 5.9 ppm (Figure 2.2). For the peaks in which couplings can be distinguished, the magnitude of the coupling constants is small (ca. 0.5 Hz) and suggests geminal rather than vicinal disposition of the protons. This assignment is consistent with the rearrangement of the acetylene ligands to vinylidene units prior to insertion into the iridium-methyl bond. The methyl resonance is observed at higher than usual field for methyl resonances (–0.95 ppm for **10** and –0.86 for **11**). The upfield shift of these methyl resonances is proposed to be due to an agostic interaction[31] of the C-H bonds with the metal. The double vinylidene insertion into the iridium-methyl bond produces the isoprenyl ligand depicted in

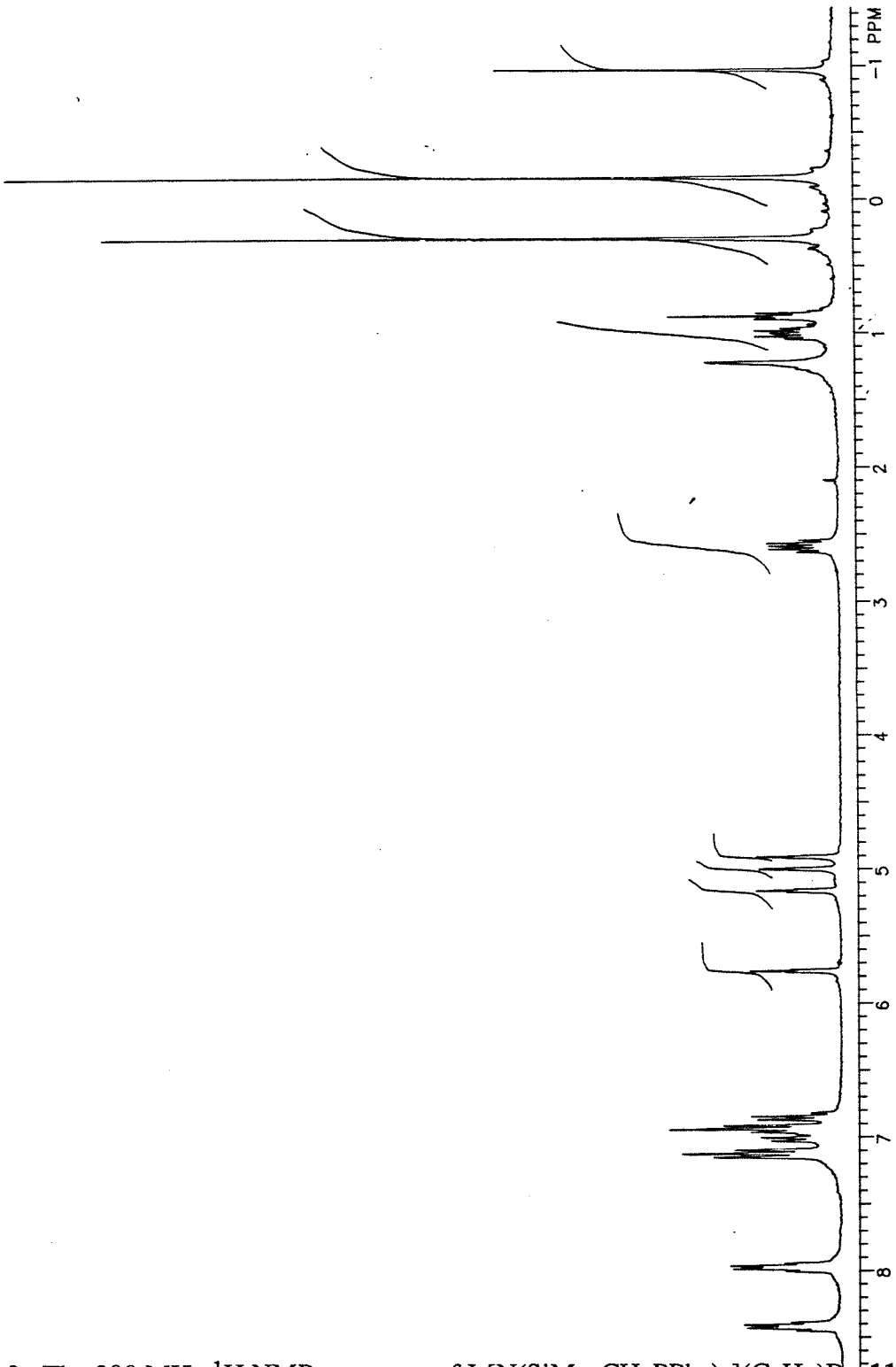

Figure 2.2. The 300 MHz ^{1}H NMR spectrum of $Ir[N(SiMe_2CH_2PPh_2)_2](C_5H_7)Br$, **11**.

Scheme 2.X

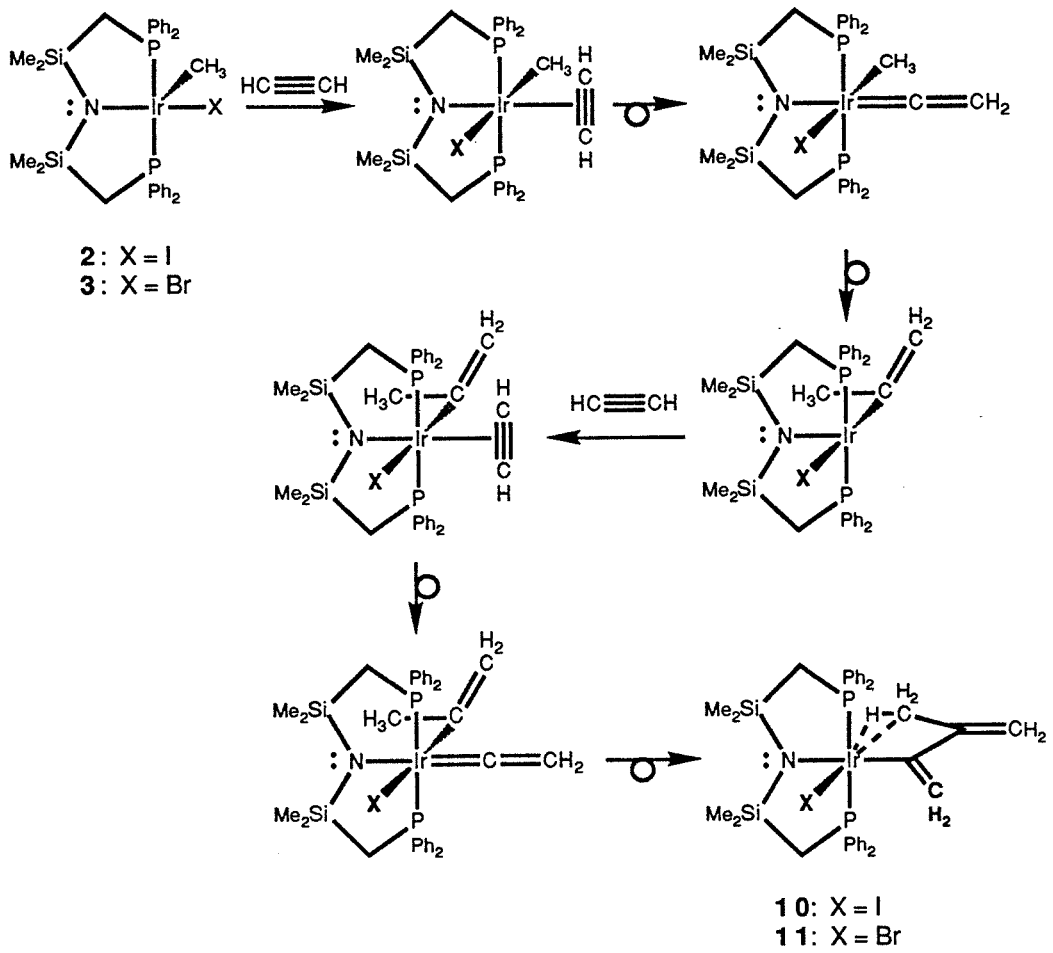

Reaction 2.3.

The proposed mechanism is based on the mechanism proposed for the formation of the allyl ligands. As shown in Scheme 2.X, the first step is the η^2-coordination of the acetylene which rearranges to a vinylidene ligand at the metal. The migratory insertion of the vinylidene unit into the iridium-methyl bond produces an isopropenyl intermediate. Before this ligand rearranges to an allyl ligand, another equivalent of acetylene coordinates to the metal and rearranges to a vinylidene ligand. Migratory insertion of this vinylidene unit into the iridium-

isopropenyl ligand generates the observed final products with isoprenyl ligands, **10** and **11**.

The agostic interaction of the methyl C-H bonds with the metal apparently blocks much of the anticipated reactivity of complexes **10** and **11**. The introduction of small molecules (hydrogen, carbon monoxide, acetylene and allene) results in no reaction. Maleic anhydride, a common dienophile, fails to react, possibly due to distortion of the planarity of the diene, or loss of conjugation. Another possibility is that the metal complex could act as a sterically demanding protecting group. A low-temperature proton NMR spectroscopic study[32] was performed to determine whether or not the exchange of the agostic methyl protons with the metal could be slowed down. However, even at –80 °C, no resolution of the two species, free and agostic C-H, was observed.

Trimethylphosphine does react with $Ir[N(SiMe_2CH_2PPh_2)_2](C_5H_7)I$, **10**. Addition of excess trimethylphosphine to a solution of **10** in toluene resulted in an immediate reaction . The phosphorus-31 NMR spectrum indicated that there was complete conversion to a single new compound, **12**, with three different phosphorus environments. The highest field resonance is attributed to the coordinated trimethylphosphine ligand. The coupling pattern of this signal is a doublet of doublets. The two doublet couplings are indicative of coupling to a *cis*- (9 Hz) and to a *trans*-phosphine (388 Hz). One of the phosphines of the tridentate ligand is trans to the trimethylphosphine ligand while the other is cis to this ligand and the resonances of these two

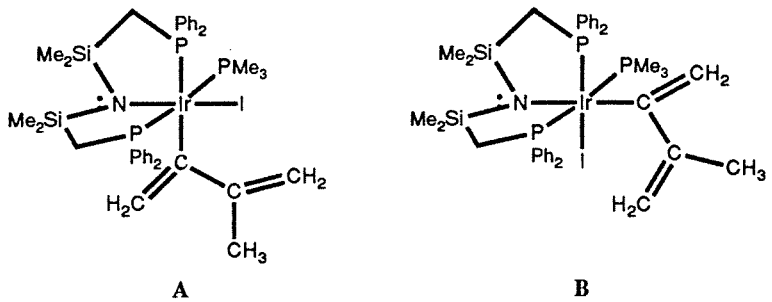

Figure 2.3. Two possible geometric isomers of $Ir[N(SiMe_2CH_2PPh_2)_2](C_5H_7)(PMe_3)I$, **12**.

References p. 32

nuclei appear as two doublets of doublets. The pendant arms of the tridentate amidodiphosphine ligand are therefore cis to one another, which then requires this ligand to assume facial coordination. The two remaining sites of the octahedron are occupied by the isoprenyl and the iodo ligands. Two isomers are then possible: one isomer has the iodo group trans to the amido group (Figure 2.3 **12A**) while the other has the isoprenyl ligand trans to the amide (Figure 2.3 **12B**). These two isomers should be able to be distinguished by carbon-13 NMR spectroscopy; the isomer with isoprenyl ligand trans to the amide should result in the presence of a large, trans phosphorus-carbon coupling constant in the carbon-13 spectrum. But due to time constraints this experiment was not performed.

B. Benzyl derivative.

The reaction of excess acetylene with the benzyl bromide complex, Ir[N($SiMe_2CH_2$-$PPh_2)_2$](CH_2Ph)Br, **7**, produced a new compound, **13**, with only a singlet in the phosphorus-31 NMR spectrum. The two phosphine donors must therefore exist in magnetically equivalent environments. The proton NMR spectrum of this compound is quite complex (Figure 2.4). The presence of two silyl methyl resonances indicates the formation of a molecule with low symmetry, while the separation of the *ortho*- from the *meta*- and *para*-phenyl proton resonances indicates that the diphenylphosphino donors have maintained a trans coordination geometry, which implies a meridional coordination of the tridentate ligand. The set of olefinic resonances in the region of 3.7 to 5.8 ppm suggests that a compound like **10** or **11** has not formed in this case and the resonances of the benzylic protons were not present.

In order to elucidate the structure of the new compound an X-ray structure determination was undertaken. Complex **13** belongs to the triclinic space group $P\bar{1}$ (#2), with unit cell dimensions, a = 11.044 (2) Å, b = 19.520 (3) Å, c = 10.062 (1) Å, α = 89.99 (1)°, β = 109.72 (1)°, γ = 76.50 (1)° (Z = 2; R_w = 0.028). The molecular structure of this compound, **13**, is

References p. 32

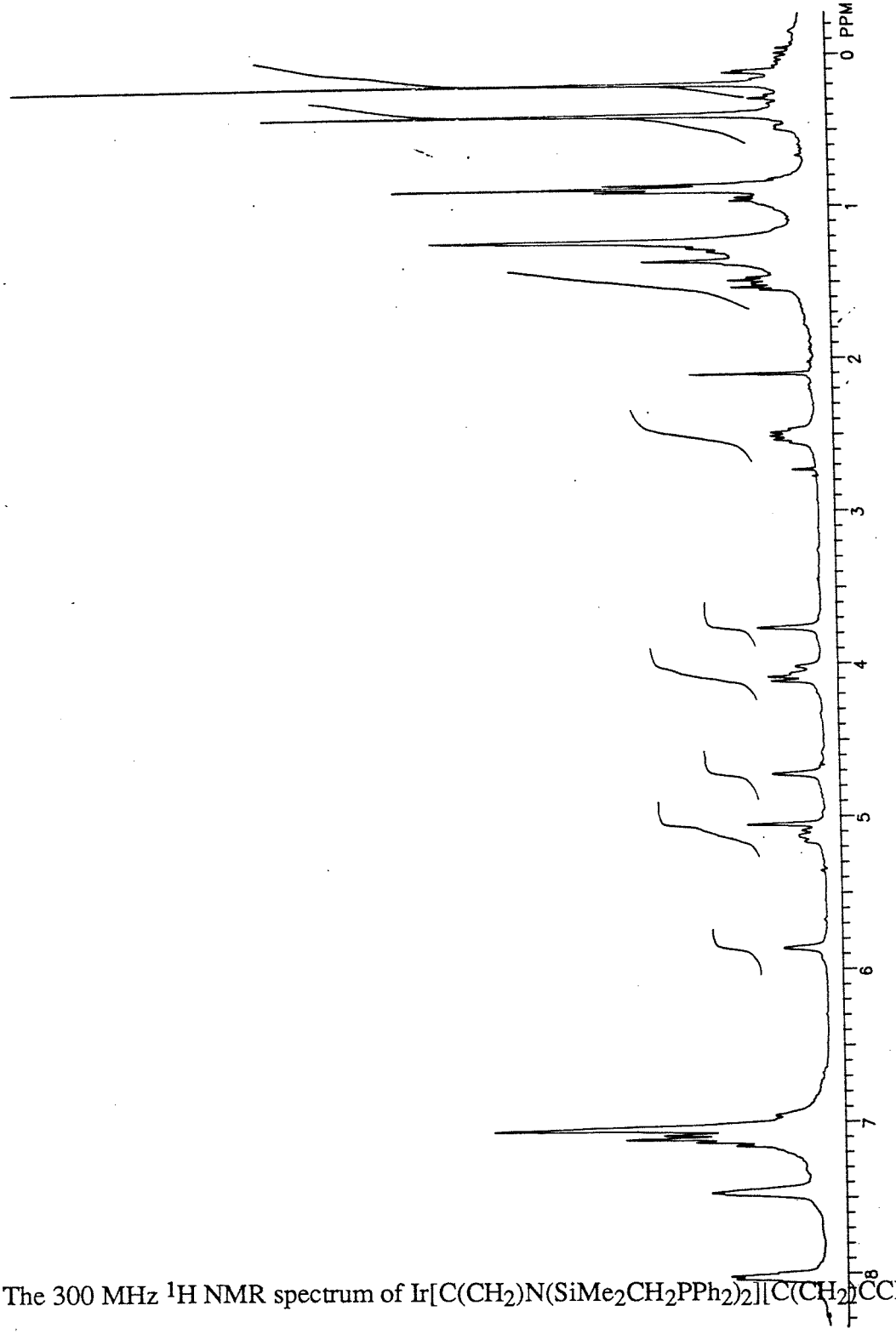

Figure 2.4. The 300 MHz ^{1}H NMR spectrum of $Ir[C(CH_2)N(SiMe_2CH_2PPh_2)_2][C(CH_2)CCH]$-Br, **13**.

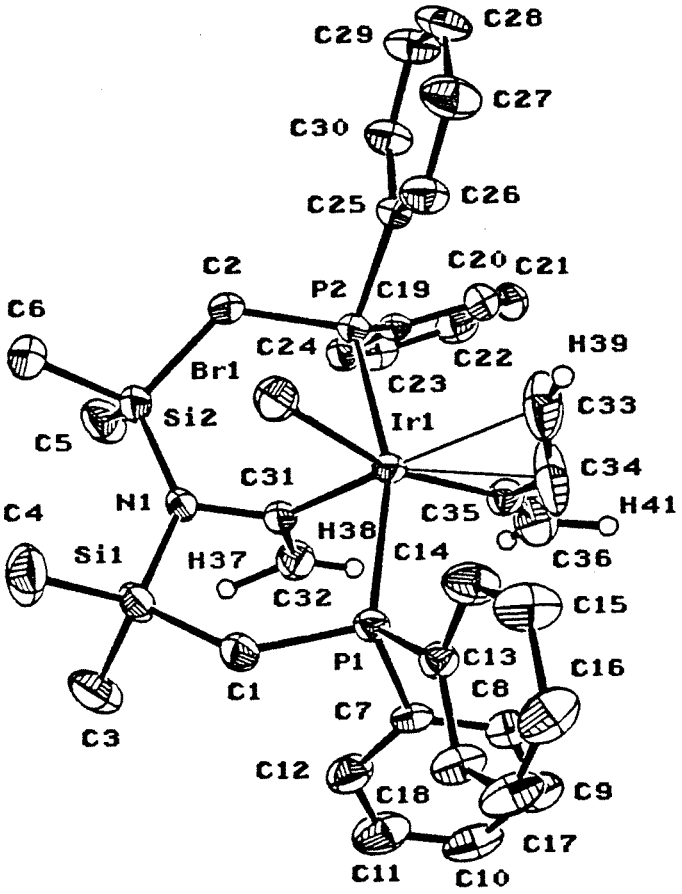

Figure 2.5. The molecular structure of $Ir[C(CH_2)N(SiMe_2CH_2PPh_2)_2](C(CH_2)CCH)$, **13**.

References p. 32

Scheme 2.XI

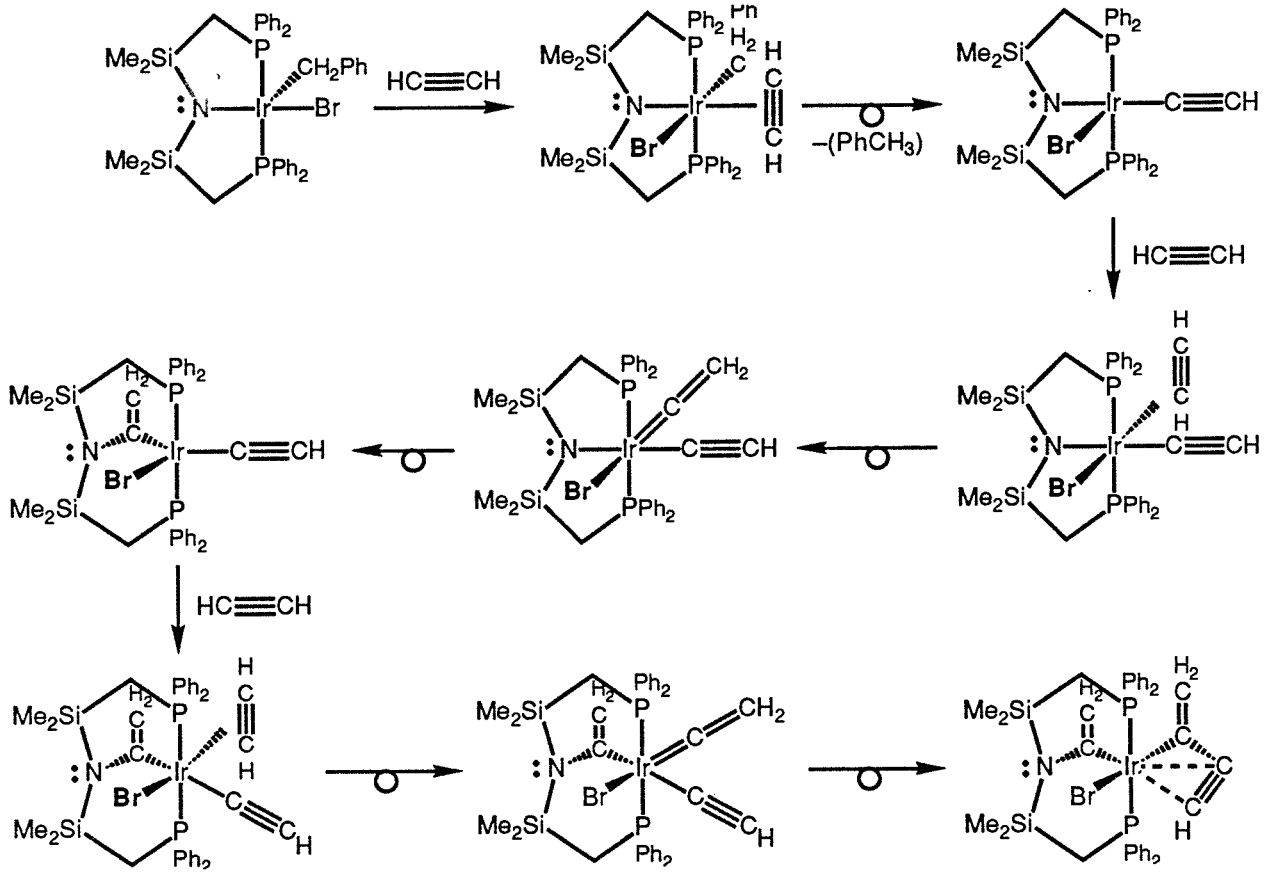

shown in Figure 2.5. Selected bond lengths and bond angles are listed in Tables 2.I and 2.II respectively (see **Appendix A**). The structure determination revealed that three equivalents of acetylene have been incorporated into the compound. The protons associated with the incorporated acetylene were all located and were refined with isotropic thermal parameters. The carbon-carbon bond lengths in the C_4H_3 ligand support the triple (1.174 (9) Å) and double (1.265 (9) Å) bond formalism of a vinylidene unit inserting into an iridium-acetylide moiety. The acetylenic unit is not linear; the angle about the C-C-H linkages is 144 (4)°. This deviation from linearity is due to interaction with the metal in the form of the donation of electron density from a bonding ligand molecular orbital to unfilled orbitals on the metal and subsequent back-

donation of electron density from filled metal-based orbitals into antibonding orbitals on the ligand.

Based on the aforementioned mechanisms, the proposed mechanism for the formation of **13** is depicted in Scheme 2.XI. The first equivalent of acetylene oxidatively adds to the metal across the C-H bond to form an alkynyl(hydrido) complex. The hydride ligand and the benzyl ligand reductively eliminate as a molecule of toluene. An equivalent of acetylene is then coordinated to the vacant coordination site and rearranges to the vinylidene moiety. There are two possible insertion pathways now possible; insertion into the metal-alkynyl unit and insertion into the metal-amide linkage. The insertion into the metal-alkynyl moiety would block the second insertion needed to produce the product, so the vinylidene unit must insert into the metal-amide bond preferentially. In the formation of the allyl complexes it was seen that the vinylidene unit inserted into the metal alkyl bonds and not the metal-nitrogen bond.

Table 2.I. Selected bond lengths (Å) for $Ir[C(CH_2)N(SiMe_2CH_2PPh_2)_2](C(CH_2)CCH)$, **13**.

Atom	Atom	Distance	Atom	Atom	Distance
Ir (1)	Br (1)	2.6401 (7)	C (31)	C (32)	1.330 (7)
Ir (1)	P (1)	2.339 (1)	C (32)	H (37)	1.19 (6)
Ir (1)	P (2)	2.337 (1)	C (32)	H (38)	0.92 (5)
Ir (1)	C (31)	2.053 (4)	C (33)	C (34)	1.174 (9)
Ir (1)	C (33)	2.389 (6)	C (33)	H (39)	0.83 (4)
Ir (1)	C (34)	2.230 (6)	C (34)	C (35)	1.476 (8)
Ir (1)	C (35)	2.039 (5)	C (35)	C (36)	1.265 (9)
C (36)	H (41)	1.05 (6)	C (36)	H (40)	0.63 (5)

References p. 32

Table 2.II. Selected bond angles (degrees) for $Ir[C(CH_2)N(SiMe_2CH_2PPh_2)_2](C(CH_2)CCH)$, **13.**

Atom	Atom	Atom	Angle	Atom	Atom	Atom	Angle
P (1)	Ir (1)	P (2)	160.61 (4)	Ir (1)	C (35)	C (34)	76.9 (3)
C (31)	Ir (1)	C (33)	166.9 (2)	C (31)	C (32)	H (37)	110 (3)
C (31)	Ir (1)	C (34)	141.4 (2)	C (31)	C (32)	H (38)	119 (3)
C (31)	Ir (1)	C (35)	103.4 (2)	H (37)	C (32)	H (38)	130 (4)
C (33)	Ir (1)	C (34)	29.2 (2)	Ir (1)	C (33)	C (34)	67.9 (4)
C (33)	Ir (1)	C (35)	64.4 (2)	Ir (1)	C (33)	H (39)	133 (4)
C (34)	Ir (1)	C (35)	40.1 (2)	C (34)	C (33)	H (39)	144 (4)
Ir (1)	C (31)	N (1)	117.3 (3)	C (33)	C (34)	C (35)	127.2 (8)
Ir (1)	C (31)	C (32)	123.7 (4)	C (34)	C (35)	C (36)	133.7 (6)
N (1)	C (31)	C (32)	118.9 (4)	C (35)	C (36)	H (40)	114 (7)
Ir (1)	C (34)	C (33)	82.9 (5)	C (35)	C (36)	H (41)	116 (3)
Ir (1)	C (34)	C (35)	62.9 (3)	H (40)	C (36)	H (41)	127 (7)
Ir (1)	C (35)	C (36)	149.3 (5)				

5. General observations and mechanistic considerations.

The presence of an acetylenic unit and the elimination of toluene from complex **13**, support the alkynyl(hydrido) mechanism of vinylidene formation in this system. The two proposed mechanisms for the conversion of a metal-bound alkyne to a coordinated vinylidene are shown in Scheme 2.I.[4] When only one equivalent of acetylene was employed there was rearrangement to the vinylidene and then migratory insertion of the vinylidene into the iridium benzyl bond. In the methyl system, the reductive elimination of methane must proceed at a

References p. 32

Scheme 2.XII

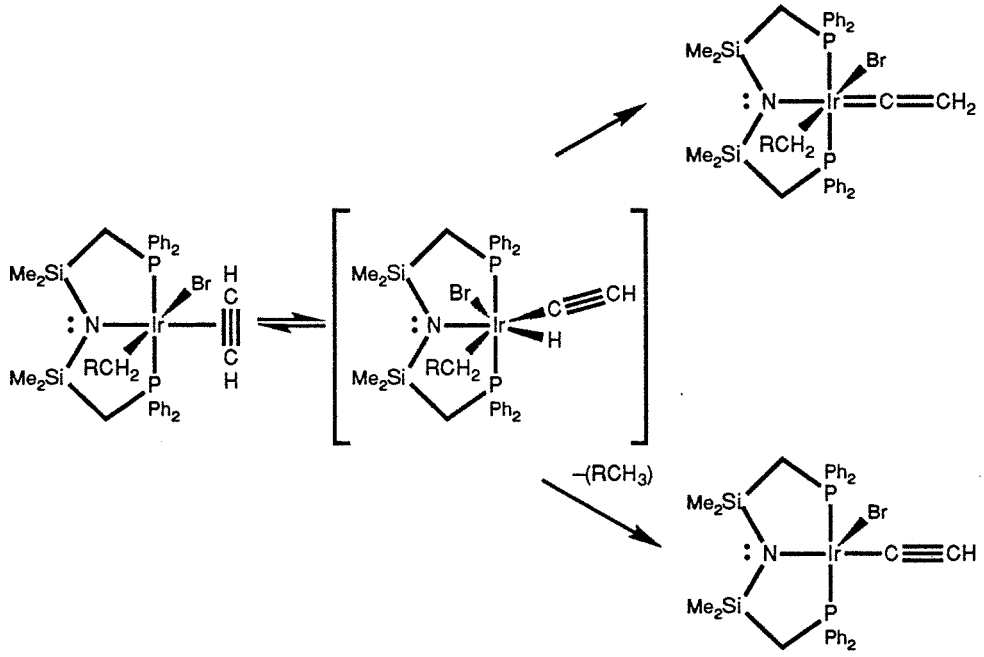

slower rate than the rearrangement to the vinylidene.

6. Summary.

The reaction of the alkyl halide complexes **2-4** with one equivalent of acetylene produces the corresponding allyl (or phenylallyl) complexes **6-8**. A deuterium labeling study indicates that the allyl complexes form by vinylidene migratory insertion into the iridium-alkyl bonds. Using excess acetylene produces the isoprenyl complexes **10** and **11** from the methyl derivatives **2** and **3** respectively. The reactivity of these complexes is blocked by an agostic interaction of a methyl group with the metal. Complex **10** reacts with trimethylphosphine to generate a new compound, **12**, in which the tridentate ligand has changed from meridional to facial coordination. The addition of excess acetylene to the benzyl bromide complex, **4**, results in elimination of the benzyl ligand as toluene and a dual vinylidene insertion process to produce **13**. An X-ray structure determination shows that one vinylidene unit has inserted into the

References p. 32

iridium-amide linkage and the other vinylidene unit has inserted into the iridium acetylide bond.

7. Future work.

Though it has been shown that vinylidene intermediates are involved in the reactions of acetylene with the alkyl halide amidodiphosphine iridium complexes studied, more questions have been raised from this study. The reactivity of the isobutenynyl complex, **13**, has not yet been investigated. The mechanism of the formation of this molecule is another area that requires further study. The reason for the change in mechanism that results from the change of the stoichiometry, from one equivalent to excess acetylene, is not known. The extension of this chemistry to other alkyl groups and the investigation of the reactions of acetylene with the aryl halide analogues may clear up some of the confusion that persists. Dialkyl amidodiphosphine iridium complexes have also been prepared in our laboratories[17] and the reactions of these complexes with acetylene would also be instructive. In particular, the competition of insertion products that would arise from utilizing mixed alkyl or alkyl-aryl complexes would lead to an understanding of the ranking of preference of insertion of the vinylidene ligand. The synthetic utility of the vinylidene insertion reaction is yet to be realized. The potential for multiple (more than two) insertions still exists if the interference of the agostic interaction and the elimination reaction can be avoided. It may be possible to form long chains of vinylidene units and potentially to form poly(vinylidene).

8. References.

(1) Collman, J. P.; Hegedus, L. S.; Norton, J. R.; Finke, R. G. *Principles and Applications of Organotransition Metal Chemistry*; University Science Books: Mill Valley, CA, 1987, pp 57ff.

(2) Durán, R. P.; Amorebieta, V. T.; Colussi, A. J. *J. Am. Chem. Soc.* **1987**, *109*, 3154.

(3) Scheiner, A. C.; Schaefer, H. F. I. *J. Am. Chem. Soc.* **1985**, *107*, 4451.

(4) Bruce, M. I. *Chem. Rev.* **1991**, *91*, 197.

(5) Bruce, M. I.; Swincer, A. G. *Adv. Organomet. Chem.* **1983**, *22*, 59.

(6) Silvestre, J.; Hoffmann, R. *Helv. Chim. Acta.* **1985**, *68*, 1461.

(7) Höhn, A.; Otto, H.; Dziallas, M.; Werner, H. *J. Chem. Soc., Chem. Commun.* **1987**, 852.

(8) Alonso, F. J. G.; Höhn, A.; Wolf, J.; Otto, H.; Werner, H. *Angew. Chem., Int. Ed. Engl.* **1985**, *24*, 406.

(9) Chiusoli, G. P.; Salerno, G.; Giroldini, W.; Pallini, L. *J. Organomet. Chem.* **1981**, *219*, C16.

(10) Selnau, H. E.; Merola, J. S. *J. Am. Chem. Soc.* **1991**, *113*, 4008.

(11) Fryzuk, M. D.; McManus, N. T.; Rettig, S. J.; White, G. S. *Angew. Chem., Int. Ed. Engl.* **1990**, *29*, 73.

(12) Fryzuk, M. D.; Huang, L.; McManus, N. T.; Paglia, P.; Rettig, S. J.; White, G. S. *Organometallics*. **1992**, *11*, in press.

(13) Collman, J. P.; Sears, C. T. J. *Inorg. Chem.* **1968**, *7*, 27.

(14) Labinger, J. A.; Osborn, J. A. *Inorg. Chem.* **1980**, *19*, 3230.

(15) Fryzuk, M. D.; MacNeil, P. A.; Rettig, S. J. *Organometallics* **1985**, *4*, 1145.

(16) Fryzuk, M. D.; MacNeil, P. A.; Rettig, S. J. *Organometallics* **1986**, *5*, 2469.

(17) Fryzuk, M. D.; MacNeil, P. A.; Massey, R. L.; Ball, R. G. *J. Organomet. Chem.* **1989**, *368*, 231.

(18) Finer, E. G.; Harris, R. K. *Prog. NMR Spectroscopy* **1970**, *6*, 61.

(19) Moore, D. S.; Robinson, S. D. *Inorg. Chim. Acta.* **1981**, *53*, L 171.

References p. 32

(20) Wakefield, J. B.; Stryker, J. M. *Organometallics* **1990**, *9*, 2428.

(21) Tjaden, E. B.; Stryker, J. M. *Organometallics* **1992**, *11*, 16.

(22) Tulip, T. H.; Ibers, J. A. *J. Am. Chem. Soc.* **1979**, *101*, 4201.

(23) Tulip, T. H.; Ibers, J. A. *J. Am. Chem. Soc.* **1978**, *100*, 3252.

(24) Ashworth, T. V.; Chalmers, A. A.; Singleton, E. *Inorg. Chem.* **1985**, *24*, 2125.

(25) Hoffman, P. R.; Caulton, K. G. *J. Am. Chem. Soc.* **1975**, *97*, 4221.

(26) Fryzuk, M. D.; MacNeil, P. A.; Ball, R. G. *J. Am. Chem. Soc.* **1986**, *108*, 6414.

(27) Troughton, P. G. H.; Skapski, A. C. *J. Chem. Soc., Chem. Commun.* **1968**, 575.

(28) Rossi, A. R.; Hoffmann, R. *Inorg. Chem.* **1975**, *14*, 365.

(29) Rachidi, I. E.; Eisenstein, O.; Jean, Y. *New J. Chem.* **1990**, *14*, 671.

(30) Dotz, K. H.; Fisher, H.; Hoffmann, P.; Kreissel, F. R.; Schubert, U.; Weiss, K. *Transition Metal Carbene Complexes*; Verlag Chemie: Weinheim, 1983.

(31) Brookhart, M.; Green, M. L. H. *J. Organomet. Chem.* **1983**, *250*, 395.

(32) Cracknell, R. B.; Orpen, A. G.; Spencer, K. L. *J. Chem. Soc., Chem. Commun.* **1984**, 326.

CHAPTER 3

REACTIONS OF ALLENE WITH AMIDODIPHOSPHINE IRIDIUM COMPLEXES

1. Introduction.

This chapter extends the chemistry presented in the previous chapter to allene (propadiene, $H_2C=C=CH_2$). Allene has been reported to insert into metal-halide,[1-3] metal-hydride[4] and metal-carbon[5] bonds to form η^3-allyl ligands. However, this method of forming η^3-allyl ligands was not found to be viable for the iridium alkyl complexes studied. The reaction of allene with alkyl halide amidodiphosphine iridium complexes was found to result in the reductive elimination of the alkyl halide and the incorporation of one or two equivalents of allene to produce an equilibrium mixture of two complexes. After a brief survey of the literature, the investigation of these two allene complexes, and the studies of the reductive elimination of alkyl halides will be reported.

2. Literature survey.

The insertion of allene into metal-carbon, metal hydride, and metal-halide bonds are routes by which allyl complexes have been formed. Allene is proposed to insert into palladium-aryl bonds based on product analysis.[5] The aryl group is transferred to the β-carbon of the allene to form the allyl ligand in situ (Reaction 3.1).

References p. 52

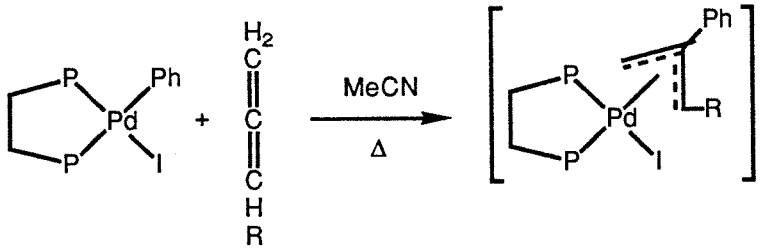

(3.1)

A similar insertion of allene into palladium-chloride[1,2] and -bromide[3] bonds is shown in Reaction 3.2.

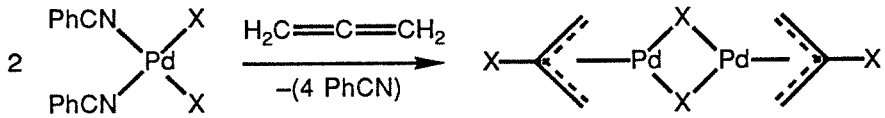

X = Cl, Br

(3.2)

The insertion of allene into rhodium- and iridium-hydride bonds has also been reported and is shown in Reaction 3.3.[4]

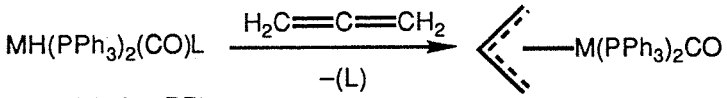

M = Rh; L = PPh_3
M = Ir; L = CO

(3.3)

The rearrangement of a σ-butenyl ligand to a methylallyl ligand at an iridium centre has been proposed to proceed by an intermediate allene hydride complex (Reaction 3.4).[6]

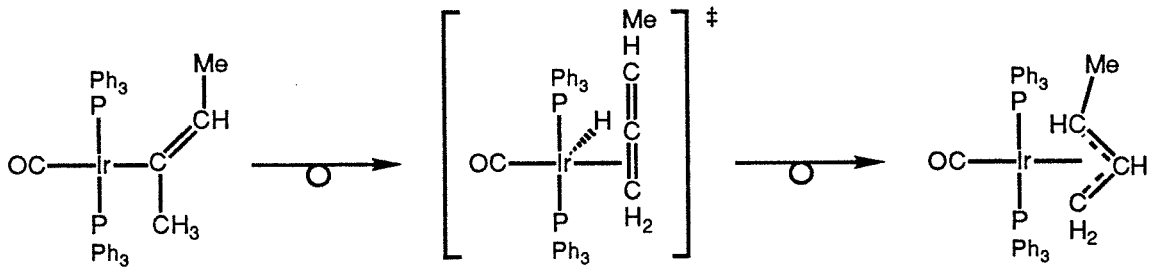

(3.4)

Stable allene complexes of the formula $M(PPh_3)_2$(allene) have been prepared for the nickel triad (allene is $H_2C=C=CH_2$ as well as the substituted derivatives, $H_2C=C=CHMe$,

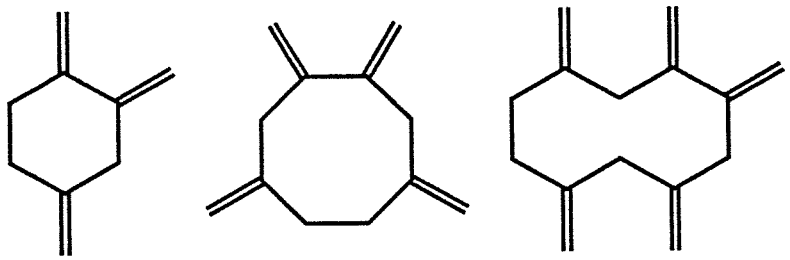

A B C

Figure 3.1. Cyclic oligomers of allene.

$H_2C{=}C{=}CMe_2$, $Me_2C{=}C{=}CMe_2$ and $PhHC{=}C{=}CHPh$).[7] In the nickel case only substituted-allene complexes can be isolated. Reaction of unsubstituted allene with nickel(0) complexes results in the catalytic coupling of allene units to form exo-methylene substituted cyclic trimers (**A**), tetramers (**B**) and pentamers (**C**, Figure 3.1)[8,9] The analogous reactivity with platinum(0)

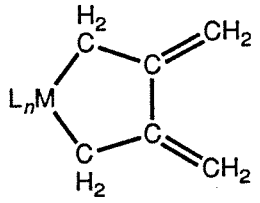

Figure 3.2. The 3,4-dimethylenemetallacyclopentane moiety.

species resulted in the formation of a platinacyclopentane moiety like that shown in Figure 3.2.[10] The oxidative coupling of two allene molecules on rhodium[11-14] and iridium[15-17] complexes has also been reported. The pyridine adducts were isolated and X-ray diffraction studies confirm the formation of metallacyclopentane moieties (Figure 3.3).

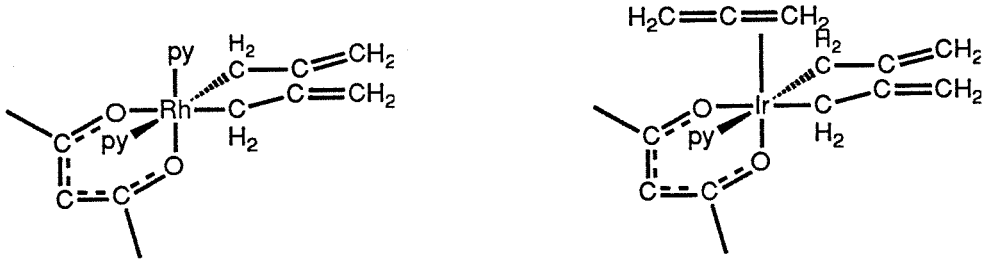

Figure 3.3. $Rh(acac)(C_6H_8)py_2$ and $Ir(acac)(C_6H_8)(\eta^2\text{-}C_3H_4)py$.

3. Previous work on amidodiphosphine iridium complexes.

Previous work in our laboratories has shown that the cyclooctene iridium amidodiphosphine complex, **1**, is a versatile starting material for both low and high oxidation state iridium chemistry.[18-26] For example, reaction of excess allene with **1** yields an allene complex, **14** (Reaction 3.5).[27]

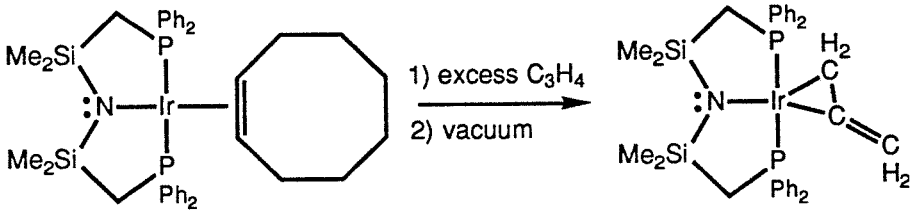

1 **14** (3.5)

The coordination of the allene molecule in **14** can either be described as a η^2-π (Figure 3.4A) or η^2-σ (Figure 3.4B), depending on the degree of backbonding from the metal to the olefin. The iridium-bound α-carbon gives rise to a resonance at –3.82 ppm in the carbon-13 NMR spectrum which is diagnostic of the η^2-σ coordination mode.[27] Compound **14** is therefore best described as an iridacyclopropane complex.

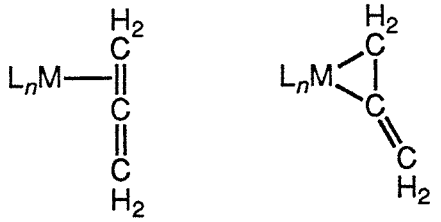

A **B**

Figure 3.4. η^2-π, **A**, and η^2-σ, **B**, modes of allene coordination.

The possibility that an iridacyclopentane unit like that found for the platinum, rhodium and iridium systems mentioned above (Figure 3.2) could have formed was not considered. In an

effort to compare the earlier work in our laboratory with the literature systems this reaction was investigated further.

4. Allene coupling and decoupling at amidodiphosphine iridium centres.

When complex **1** was sealed in an NMR tube with excess allene (Reaction 3.6), complete conversion of **1** to a new species, different from **14**, was evident from the proton and phosphorus-31 NMR spectra. This new species is proposed to be the iridacyclopentane complex **15**. The proton NMR spectrum (Figure 3.5) displays signals at δ 6.17, 5.79 and 1.25 ppm in a ratio of 2:2:4. The high field resonance is attributable to the protons on the α-carbon. The pattern of this signal is a triplet of triplets attributable to coupling to two magnetically equivalent phosphorus nuclei and to equivalent coupling to the two terminal exo-methylene protons. The two low-field multiplets are assigned to the two terminal exo-methylene protons.

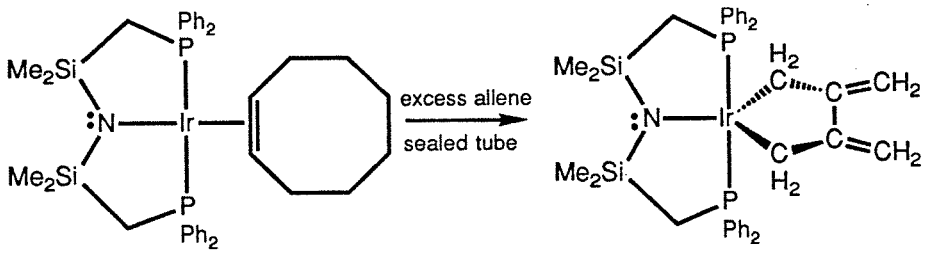

1 **15** **(3.6)**

The iridacyclopentane complex, **15**, is unstable to loss of allene. Removal of solvent and excess allene *in vacuo* results in complete conversion of complex **15** to the iridacyclopropane complex, **14** (Reaction 3.7). The previously reported formation of complex **14** from the cyclooctene complex **1** and excess allene must have gone through the in situ generation and subsequent decomposition of the iridacyclopentane complex **15**. This conversion of **14** to **15** is as facile as the reverse reaction. The addition of excess allene to the iridacyclopropane complex **14** results in the complete conversion of **14** to **15** as monitored by proton and phosphorus-31

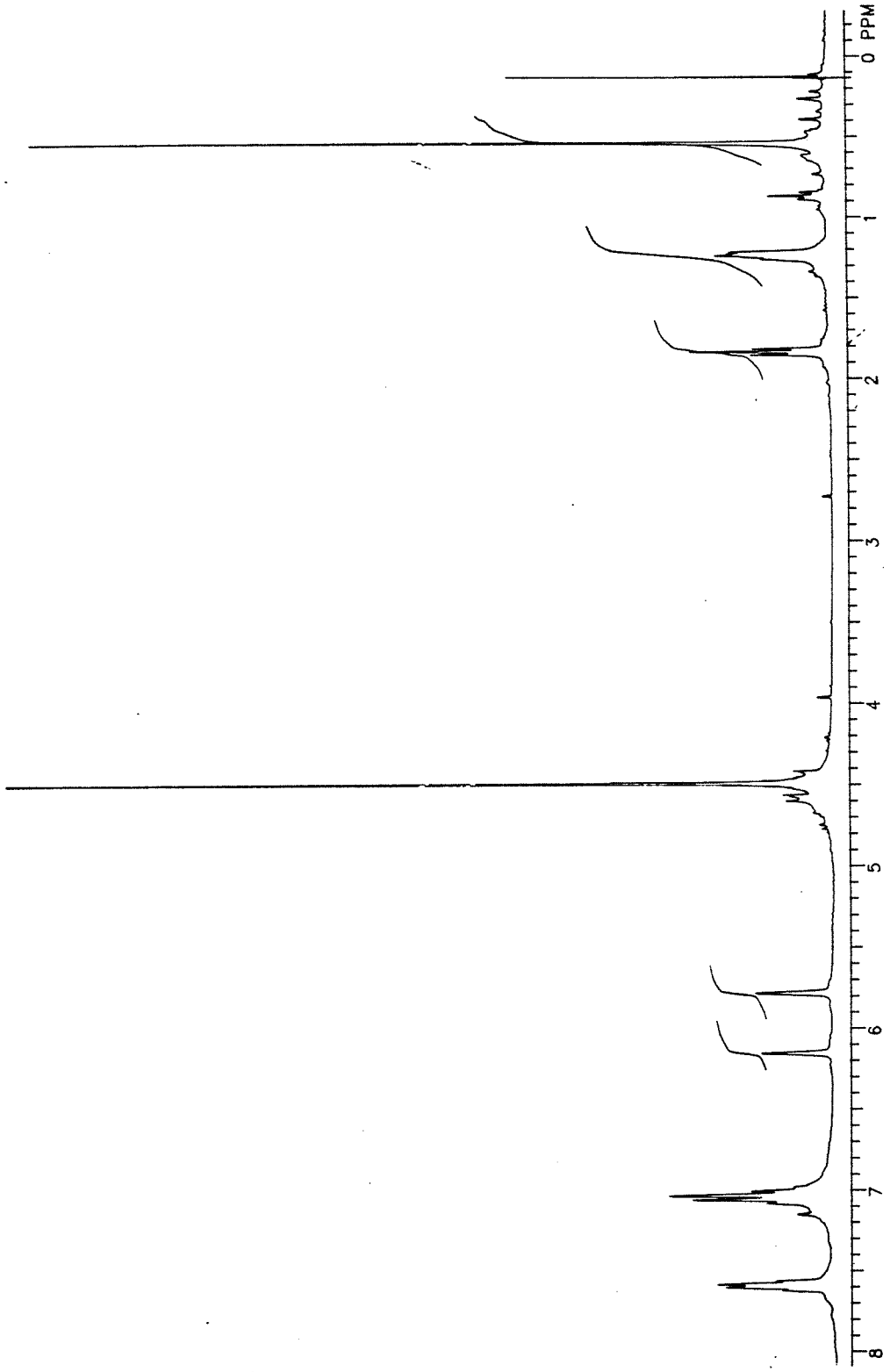

Figure 3.5. The 300 MHz ^1H NMR spectrum of $Ir[N(SiMe_2CH_2PPh_2)_2](C_6H_8)$, **15**.

References p. 52

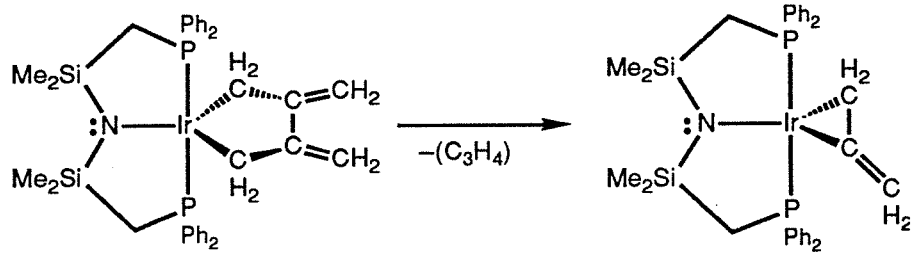

15 14 (3.7)

NMR spectroscopy (Reaction 3.8). The coupling of two allene molecules at this iridium centre is reversible and the two complexes **14** and **15** exist in a dynamic equilibrium.

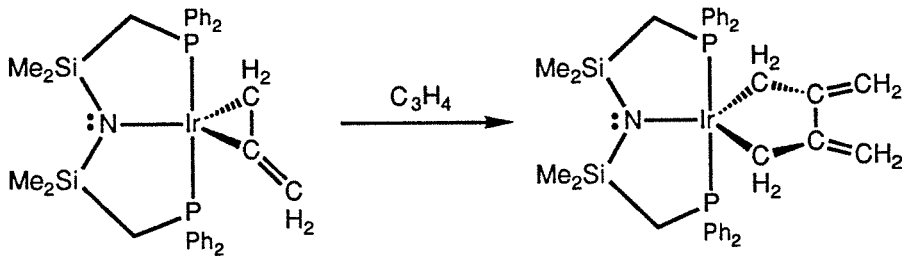

14 15 (3.8)

The relationship between the cyclooctene complex **1** and the two allene derivatives **14** and **15** is summarized in Scheme 3.I. The cyclooctene complex **1** can be converted to either **14** or **15** by judicious setting of the stoichiometry. These reactions of **1** are irreversible; the cyclooctene complex **1** cannot be regenerated.

5. Reactions with trimethylphosphine.

The ready conversion of the iridacyclopentane complex **15** to the iridacyclopropane complex **14** by allene elimination prevented the isolation of the iridacyclopentane complex. The stabilization of the rhodium and iridium metallacyclopentane complexes by the introduction of pyridine,[11,12,16,17] mentioned above, indicated that the metallacyclopentane moiety could be

Scheme 3.I

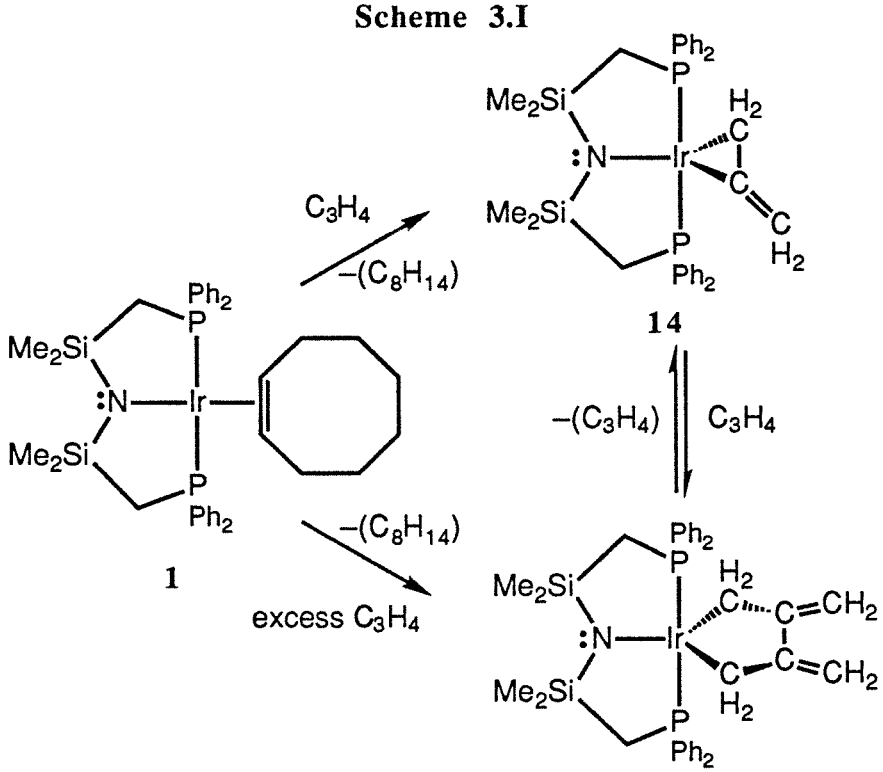

stabilized by coordinative saturation of the metal. It seemed possible that the iridacyclopentane complex **15** might be stabilized in a similar manner.

One Lewis base that binds readily to complexes of this type is trimethylphosphine. This ligand has the additional benefit of producing a signal in the phosphorus-31 NMR spectrum that, combined with the two phosphines of the amidodiphosphine ligand, aids in stereochemical assignment. The trimethylphosphine signal is sufficiently different (much higher field) from the signals of the phosphine arms of the tridentate ligand that its position in the NMR spectrum is readily assigned. The magnitude of the phosphorus-phosphorus coupling constants allows for the *cis* - and *trans*-phosphines to be distinguished: *trans*-disposed phosphines typically produce

coupling constants greater than 100 Hz, while *cis*-disposed phosphines results in smaller coupling constants; $|\ ^2J_{PP}^{cis}\ | < 100\ Hz < |\ ^2J_{PP}^{trans}\ |$.[28]

The addition of one equivalent of trimethylphosphine to the iridacyclopentane complex, $Ir[N(SiMe_2CH_2PPh_2)_2](C_6H_8)$, **15**, generated in situ, results in the quantitative formation of a trimethylphosphine adduct, **16**. The phosphorus-31 NMR spectrum of the new compound consists of two doublets of doublets for the diphenylphosphino nuclei and a high field triplet for the trimethylphosphine. The fact that there are two signals for the diphenylphosphino nuclei rules out the formation of the trimethylphosphine adduct of the iridacyclopentane complex. All couplings are less than 20 Hz, which indicates the three phosphorus nuclei are in a mutually cis geometry. The tridentate amidodiphosphine ligand has adopted a facial coordination with the trimethylphosphine ligand trans to the amide donor atom. Four of the six coordination sites have been accounted for, leaving the remaining two sites for the allene ligand. Five possible structures of this compound are shown in Figure 3.6. Structures **A** and **A'** have meridional coordination geometries of the tridentate ligand and are thus not applicable. Structures **B** and **B'** are not

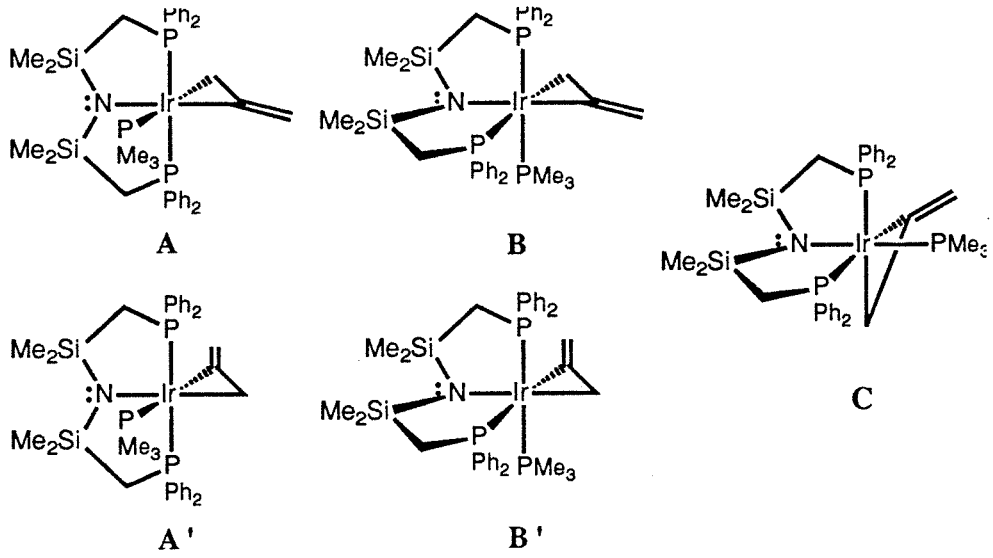

Figure 3.6. Five possible structures of $Ir[N(SiMe_2CH_2PPh_2)_2](PMe_3)(C_3H_4)$, **16**.

References p. 52

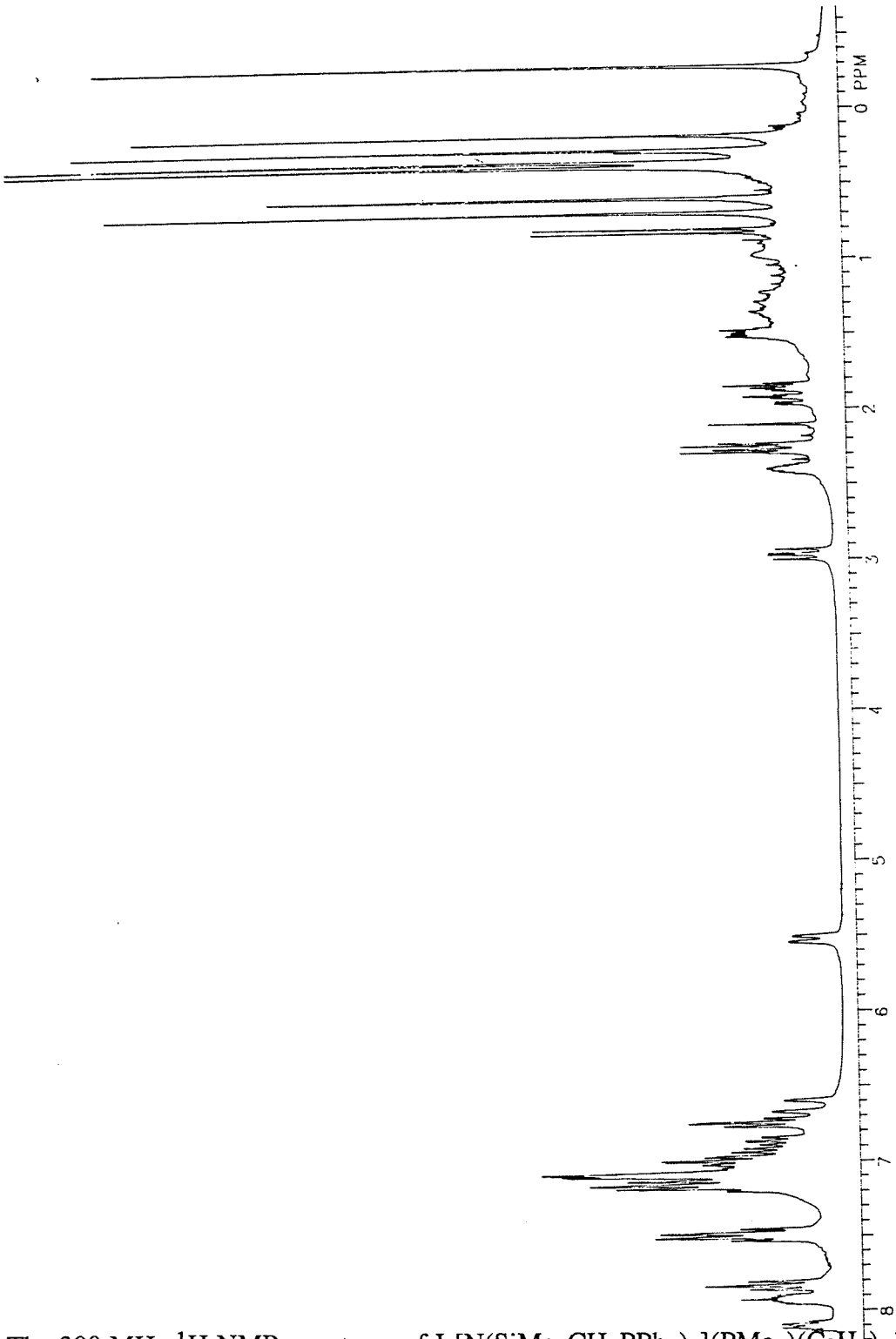

Figure 3.7. The 300 MHz ^{1}H NMR spectrum of $Ir[N(SiMe_2CH_2PPh_2)_2](PMe_3)(C_3H_4)$, **15**.

distinguishable by NMR spectroscopy, but in these structures the trimethylphosphine is trans to one of the diphenylphosphino donors, and this is not supported by the phosphorus-phosphorus coupling constants. The structure represented by **C** in Figure 3.6 is thus the appropriate structure of this compound.

The ^{1}H NMR spectrum of this complex, shown in Figure 3.7, contains the expected multiplets for the protons on the α-carbon; one centred at δ 2.38 ppm and another at δ 1.48 ppm. The two vinylidene protons also give rise to multiplets. The expected coupling pattern for each of these would be a doublet of doublets of doublets. This would ideally be observed as an eight line pattern and the coupling constants easily distinguishable. In this case though the coupling constants are too small to yield a distinct pattern.

Complex **16** could also be synthesized from the iridacyclopropane complex, **14** (Reaction 3.9). The addition of trimethylphosphine to a solution of **14** resulted in the formation of **16**, as verified by proton and phosphorous-31 NMR spectroscopy.

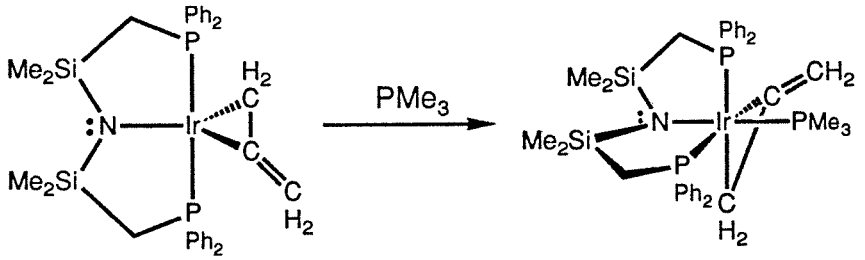

14 **16** **(3.9)**

The addition of allene to complex **16** does not generate an iridacyclopentane complex. Presumably the conversion of the iridacyclopropane complex, **14**, to the iridacyclopentane complex, **15**, involves a coordinatively saturated intermediate. Saturating the metal centre with a sixth ligand (like trimethylphosphine) blocks this associative pathway. A proposed mechanism is given in Scheme 3.II. The metallacyclopropane complex, **14**, coordinates an equivalent of allene

Scheme 3.II

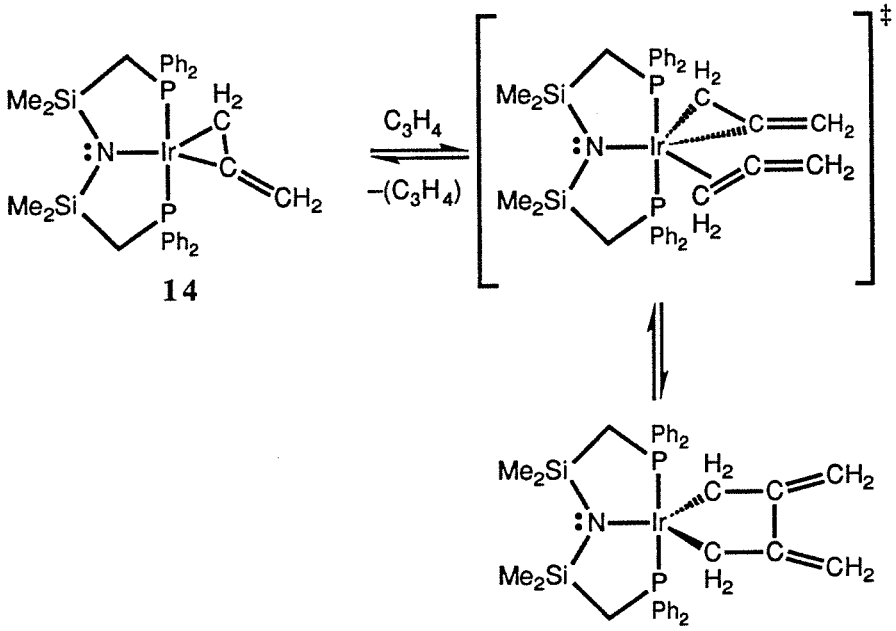

14 **15**

Scheme 3.III

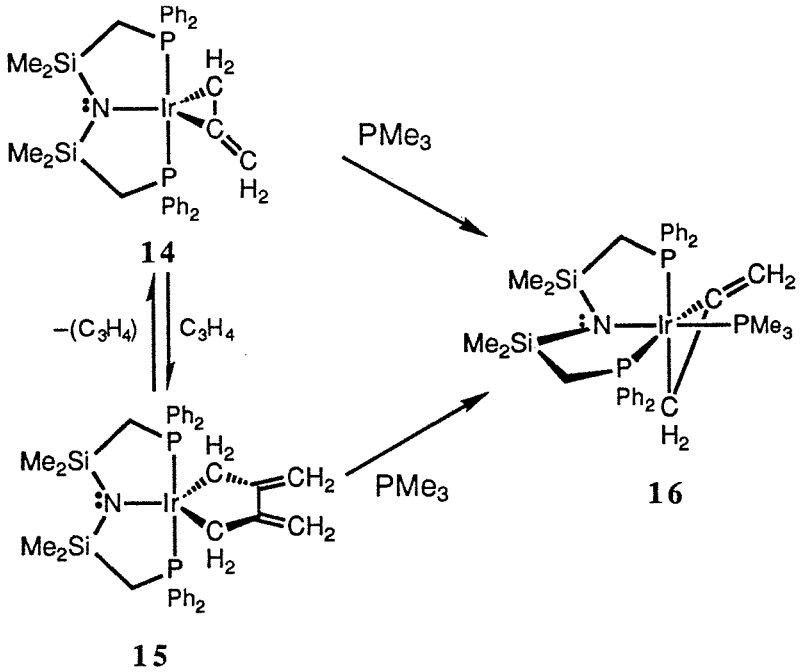

14 **15** **16**

References p. 52

to produce a coordinatively saturated intermediate that contains two η^2-allene molecules; one bound η^2-σ while the incoming ligand is bound η^2-π. The two allene units couple at the metal to form the observed iridacyclopentane complex, **15**.

The relationship between the iridacyclopropane, **14**, iridacyclopentane, **15**, complexes and the trimethylphosphine adduct, **16**, is summarized in Scheme 3.III.

6. Allene reactivity with alkyl halide amidodiphosphine iridium complexes.

The reactivity of the alkyl halide amidodiphosphine iridium complexes with allene was investigated in an attempt to form allyl complexes by insertion of allene into metal-carbon or metal-halide bonds in direct analogy with the palladium systems mentioned above. Despite the availability of both iridium-carbon and iridium-halide bonds for potential allene insertion, no allyl

Scheme 3.IV

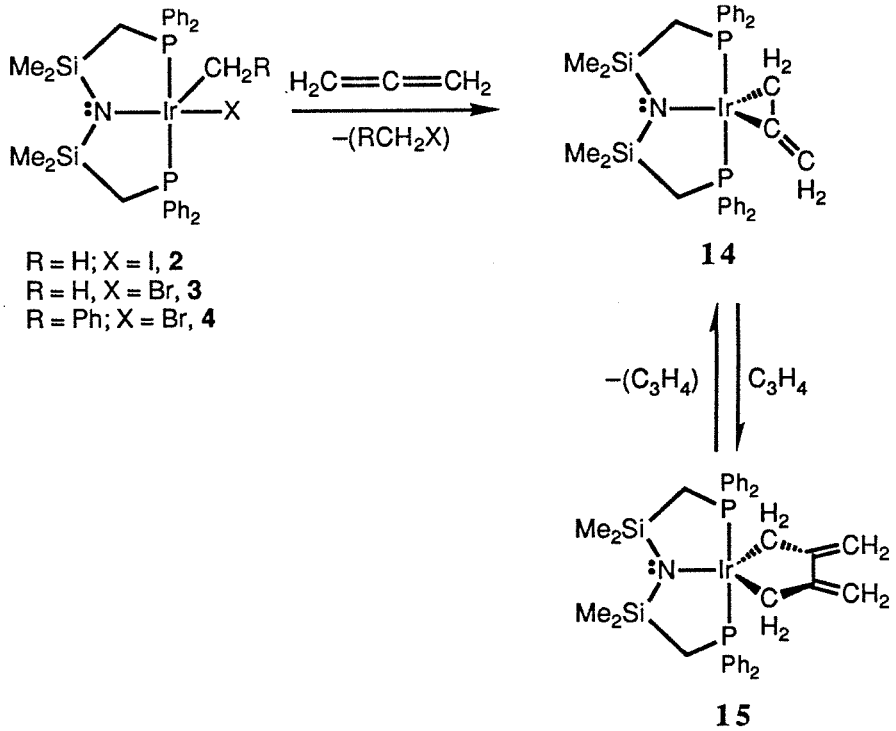

R = H; X = I, **2**
R = H, X = Br, **3**
R = Ph; X = Br, **4**

14

15

References p. 52

complexes were formed. The addition of allene to benzene solutions of **2-4** was found to result in the reductive elimination of the alkyl halide and the formation of the allene complexes **14** and **15** described above (Scheme 3.IV). As mentioned above the position of the equilibrium between **14** and **15** depends on the amount of allene introduced.

While oxidative addition of alkyl halide compounds to iridium complexes is well documented,[29-32] the reverse reaction, reductive elimination, is not as well studied. Hence, in order to better understand this phenomenon a study of the kinetics of this transformation were undertaken. The allene dependence was nulled by using greater than ten-fold excess of allene. The reactants and products give rise to well separated signals in the phosphorus-31 NMR spectrum and consequently this spectroscopic technique was chosen to monitor the reaction. The methyl derivatives, **2** and **3**, react too rapidly to be monitored by NMR spectroscopy, while the benzyl-bromide complex, **4**, reacted at a rate amenable to such a study. The reaction of the benzyl-bromide complex, **4**, with excess allene at three different temperatures (35, 45 and 55°C) has a pseudo-first order dependence upon metal complex concentration. The observed pseudo-first order rate constants, k, at the various temperatures are collected in Table 3.I (see Chapter 4 and Appendix B).

Table 3.I. Kinetic data for the reductive elimination of benzyl bromide.

Run (#)	T (°C)	k (min^{-1})	$t_{1/2}$ (min)
1	35.0 (1)	$2.0\ (1) \times 10^{-4}$	937 (2)
2	35.3 (2)	$9.4\ (1) \times 10^{-4}$	737 (8)
3	35.3 (1)	$9.6\ (3) \times 10^{-4}$	720 (20)
4	45.2 (1)	$2.34\ (4) \times 10^{-3}$	296 (5)
5	45.2 (1)	$2.40\ (1) \times 10^{-3}$	289 (1)

References p. 52

6	55.2 (2)	3.57 (3) x 10^{-3}	194 (2)
7	55.1 (2)	4.87 (7) x 10^{-3}	142 (2)

The activation parameters, $\Delta H^{\ddagger}$ and $\Delta S^{\ddagger}$, were obtained from a plot of $\ln\left(\frac{k}{T}\right)$ versus $\frac{1}{T}$ (Figure 3.8). The enthalpy of activation, $\Delta H^{\ddagger}$, calculated from the slope of this Eyring plot, was found to be 67 (9) kJ mol^{-1}, while the entropy of activation , $\Delta S^{\ddagger}$, calculated from the y-intercept, was found to be –263 (2) J mol^{-1} K^{-1}. The proposed mechanism of this reaction is shown in Scheme 3.V.

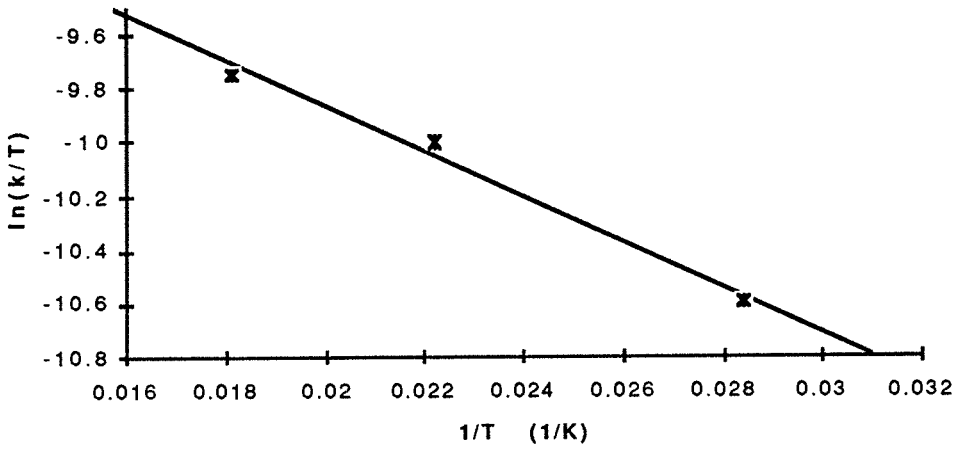

Figure 3.8. The Eyring plot of the kinetic data for the reaction of Ir[$N(SiMe_2CH_2PPh_2)_2$]-(CH_2Ph)Br, **4**, with excess allene.

The rate of change of concentration of **4** with respect to time can be expressed algebraically,

$$-\frac{d[4]}{dt} = k_1\,[4]\,[C_3H_4] - k_{-1}\,[A] \qquad \textbf{(3.a)}$$

Scheme 3.V

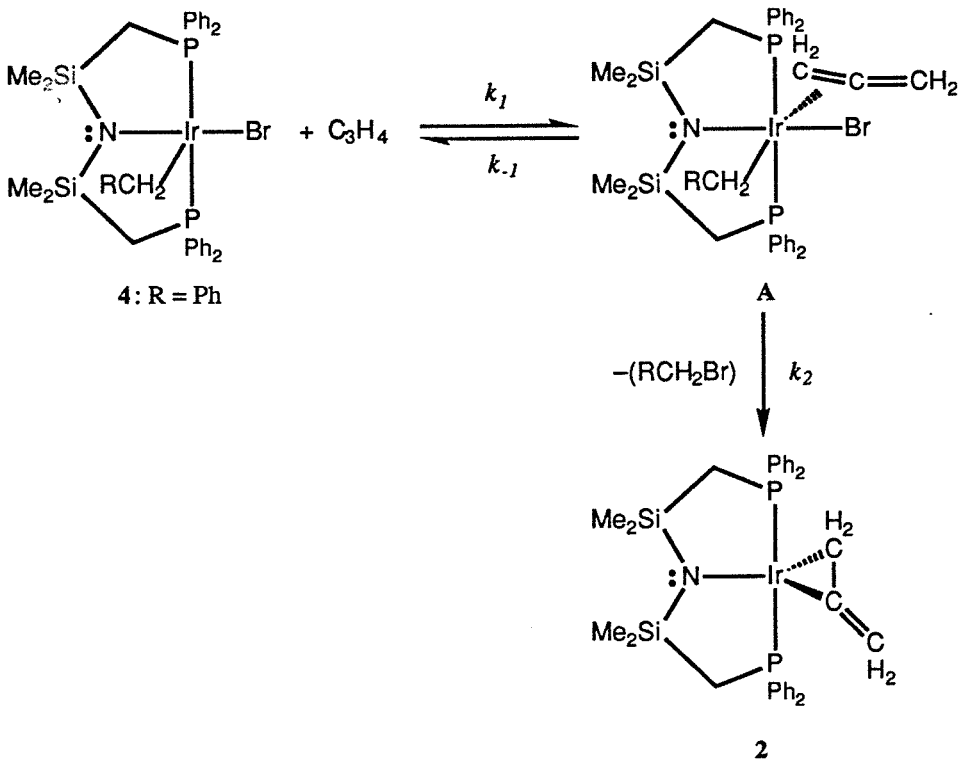

Applying the steady state approximation, that the concentration of **A** (Scheme 3.V) is invariant with time, results in the following expression:

$$\frac{d[\mathbf{A}]}{dt} = k_1\,[\mathbf{4}]\,[C_3H_4] - k_{-1}\,[\mathbf{A}] - k_2\,[\mathbf{A}] = 0 \qquad \textbf{(3.b)}$$

Rearrangement of equation **3.b** and substitution into equation **3.a** results in equation **3.c**.

$$-\frac{d[\mathbf{4}]}{dt} = \frac{k_1\,k_2}{k_{-1} + k_2}\,[\mathbf{4}]\,[C_3H_4] \qquad \textbf{(3.c)}$$

If the k_{-1} step is much faster than the opposing step, k_2, then the observed rate constant becomes;

$$k_{obs} = K_1\,k_2\,[C_3H_4] \qquad \textbf{(3.d)}$$

where, $K_1 = \frac{k_1}{k_{-1}}$

If the converse is true then,

$$k_{obs} = k_1 [C_3H_4] \qquad (3.e)$$

The negative value obtained for $\Delta S^{\ddagger}$ suggests that the rate-determining step involves the associative step. The first, reversible step, k_1, is thus proposed to be rate determining and the appropriate observed pseudo-first order rate constant is, $k_{obs} = k_1[C_3H_4]$ (equation **3.e**).

7. Summary.

The η^2-allene complex **14** previously reported from this laboratory was found to exist in a dynamic equilibrium with a new complex which has two incorporated molecules of allene. This new complex is proposed to be the iridacyclopentane complex, **15**, based on NMR evidence and literature precedent. The iridacyclopentane complex **15** is stable only in the presence of allene. Attempts to stabilize this complex by coordinative saturation with the potent Lewis base trimethylphosphine produced the trimethylphosphine iridacyclopropane complex, **16**. This complex could also be prepared directly from the iridacyclopropane complex, **14**. The introduction of allene to the alkyl halide complexes **2-4** was found to result in the reductive elimination of the alkyl halide and to form an equilibrium mixture of the iridacyclopropane and iridacyclopentane complexes **14** and **15**. The kinetics of the reductive elimination of benzyl bromide from complex **4** was studied by phosphorus-31 NMR spectroscopy. The reaction was found to have a pseudo-first order dependence upon metal complex concentration when excess allene was employed. The activation parameters were found to be $\Delta H^{\ddagger}$ = 67 (9) kJ mol^{-1} and $\Delta S^{\ddagger}$ = –263 (2) J mol^{-1} K^{-1}. The rate-determining step of this process is proposed to be the associative step.

References p. 52

8. Future work.

The generality of the reductive elimination reaction still requires investigation. The extension of this reaction to bis(alkyl), bis(aryl) or even mixed alkyl, mixed aryl or alkyl-aryl complexes could lead to the formation of carbon-carbon bonds. The study of the kinetics of these reactions would make an interesting comparative study. The effect of light on this reaction is also in need of further investigation. Preliminary results suggest that in the presence of light the rate of the reaction is nearly doubled. Presumably the light induces a radical chain mechanism. The comparison of the kinetics of the reaction in the presence and absence of light would result in better understanding of the two mechanisms. The present mechanism could possess some radical nature since two experiments in the presence of a radical trapping agent, 1,4-cyclohexadiene, resulted in lower pseudo-first order rate constants (see Appendix B, runs 8 and 9).

9. References.

(1) Schultz, R. G. *Tetrahedron* **1964**, *20*, 2809.

(2) Schultz, R. G. *Tetrahedron Lett* **1964**, *6*, 301.

(3) Lupin, M. S.; Shaw, B. L. *Tetrahedron Lett* **1964**, 883.

(4) Brown, C. K.; Mowat, W.; Yagupsky, G.; Wilkinson, G. *J. Chem. Soc. (A)* **1971**, 850.

(5) Shimizu, I.; Tsuji, J. *Chem Lett* **1984**, 233.

(6) Schwartz, J.; Hart, D. W.; McGiffert, B. *J. Am. Chem. Soc.* **1974**, *96*, 5613.

(7) Otsuka, S.; Nakamura, A. *Adv. Organomet. Chem.* **1976**, *14*, 245.

(8) Otsuka, S.; Nakamura, A.; Tani, K.; Ueda, S. *Tetrahedron Lett* **1965**, *5*, 297.

(9) Otsuka, S.; Tani, K.; Yamagata, T. *J. Chem. Soc., Dalton Trans.* **1973**, 2491.

(10) Barker, G. K.; Green, M.; Howard, J. A. K.; Spencer, J. L.; Stone, F. G. A. *J. Chem. Soc., Dalton Trans.* **1978**, 1839.

(11) Ingrosso, G.; Immirzi, A.; Porri, L. *J. Organomet. Chem.* **1973**, *60*, C35.

(12) Immirzi, A. *J. Organomet. Chem.* **1974**, *81*, 217.

(13) Ingrosso, G.; Porri, L. *J. Organomet. Chem.* **1975**, *84*, 75.

(14) Borrini, A.; Ingrosso, G. *J. Organomet. Chem.* **1977**, *132*, 275.

(15) Diversi, P.; Ingrosso, G.; Immirzi, A.; Zocchi, M. *J. Organomet. Chem.* **1975**, *102*, C49.

(16) Diversi, P.; Ingrosso, G.; Immirzi, A.; Zocchi, M. *J. Organomet. Chem.* **1976**, *104*, C1.

(17) Diversi, P.; Ingrosso, G.; Immirzi, A.; Porzio, W.; Zocchi, M. *J. Organomet. Chem.* **1977**, *125*, 253.

(18) Fryzuk, M. D.; MacNeil, P. A. *Organometallics* **1983**, *2*, 355.

(19) Fryzuk, M. D.; MacNeil, P. A. *Organometallics* **1983**, *2*, 682.

(20) Fryzuk, M. D.; MacNeil, P. A.; Rettig, S. J. *Organometallics* **1985**, *4*, 1145.

(21) Fryzuk, M. D.; MacNeil, P. A.; Rettig, S. J. *Organometallics* **1986**, *5*, 2469.

(22) Fryzuk, M. D.; MacNeil, P. A.; Rettig, S. J. *J. Am. Chem. Soc.* **1987**, *109*, 2803.

(23) Fryzuk, M. D.; MacNeil, P. A.; McManus, N. T. *Organometallics* **1987**, *6*, 882.

(24) Fryzuk, M. D.; Bhangu, K. *J. Am. Chem. Soc.* **1988**, *110*, 961.

(25) Fryzuk, M. D.; Joshi, K.; Chadha, R. K. *J. Am. Chem. Soc.* **1989**, *111*, 4498.

(26) Fryzuk, M. D.; Joshi, K. J. *Organometallics* **1989**, *8*, 722.

(27) Joshi, K. Ph D Thesis, University of British Columbia, 1990.

(28) Finer, E. G.; Harris, R. K. *Prog. NMR Spectroscopy* **1970**, *6*, 61.

(29) Vaska, L. *Acc. Chem. Res.* **1968**, *1*, 335.

(30) Mondal, J. U.; Blake, D. M. *Coord. Chem. Rev.* **1982**, *47*, 205.

(31) Labinger, J. A.; Osborn, J. A. *Inorg. Chem.* **1980**, *19*, 3230.

(32) Collman, J. P.; Sears, C. T. J. *Inorg. Chem.* **1968**, *7*, 27.

References p. 52

CHAPTER 4

EXPERIMENTAL

1. General.

Unless stated otherwise all manipulations were performed at room temperature under an atmosphere of air- and moisture-free dinitrogen. Standard glove box and Schlenk techniques were employed in the handling of all compounds. The dinitrogen (Linde) was purified by either passing it through a column of activated molecular sieves and manganese(IV) oxide[1] for vacuum line use or through a MO–40–2H purifier for glove box use. The glove box used was a Vacuum Atmospheres model HE–553–2 workstation equipped with a refrigerator kept at –40°C. The vacuum line used was all glass with Kontes teflon valve ports and mercury manometers on both nitrogen and vacuum manifolds.

2. Solvents.

Solvents were dried and deoxygenated prior to use. Hexanes and tetrahydrofuran (BDH) were dried and deoxygenated by refluxing over calcium hydride for at least 24 hours, distilling onto a mixture of sodium and benzophenone, and then distilling into appropriate containers under argon (Linde) when the purple colour of the diradical benzophenone ketyl was evident. Toluene (BDH) was predried by refluxing over calcium hydride for at least 24 hours, distilling onto sodium and then distilling from molten sodium into appropriate containers under argon.

References p. 68

Methylene chloride (BDH) was predried by refluxing over calcium hydride and dried over phosphorus pentoxide and vacuum transferred before use. Benzene (BDH) was predried over activated 4 Å molecular sieves, dried by distilling from sodium benzophenone ketyl and vacuum transferred into appropritate containers. Acetonitrile (Fisher), 1,4-cyclohexadiene (Aldrich), and deuterated solvents, benzene-d_6 and toluene-d_8 (both MSD Isotopes) were dried overnight over activated 4 Å molecular sieves, degassed with three "freeze-pump-thaw" cycles and vacuum transferred before use.

3. Reagents.

Cyclooctene (Aldrich) was distilled under a nitrogen atmosphere and freeze-pump-thawed three times to exclude oxygen. Alkyl halide reagents (methyl and benzyl bromide and methyl iodide all from Aldrich) were purified of water by storing over 4 Å molecular sieves and purified of oxygen by three "freeze-pump-thaw" cycles. Cinnamyl alcohol (Aldrich) was used as received in the preparation of cinnamyl bromide by the published method.[2] The alkyl lithium reagent, *n*-butyl lithium (1.6 M solution in hexanes, Aldrich) was used as received. Deuterium oxide (MSD Isotopes) was used without purification in the preparation of acetylene-d_2.[3] Acetylene and allene (both Matheson) were purified with an alumina column immediately prior to use. Carbon monoxide (Matheson) was used as received. Hydrogen (Linde) was passed through a column of activated molecular sieves and manganous oxide.[1] Maleic anhydride (Fisher) was purified by sublimation.

4. Syntheses of metal complexes.

Iridium trichloride hydrate ($IrCl_3.xH_20$; on loan from Johnson Matthey) was used as received in the preparation of $[IrCl(C_8H_{14})_2]_2$.[4,5] Preparations of $Ir[N(SiMe_2CH_2PPh_2)_2](C_8H_{14})$, **1**,[6,7] $Ir[N(SiMe_2CH_2PPh_2)_2](Me)I$, **2**,[8,9] $Ir[N(SiMe_2CH_2PPh_2)_2](Me)Br$, **3**,[9] and

$Ir[N(SiMe_2CH_2PPh_2)_2](CH_2Ph)Br$, **4**,[10] were performed according to the indicated published procedures.

5. NMR measurements.

All nuclear magnetic resonance (NMR) spectra were recorded on either a Varian XL–300 instrument at ambient temperature (20°C) unless noted otherwise. Proton spectra were obtained at 299.94 MHz and were referenced to the residual solvent proton peak (C_6D_5H at 7.15 ppm or $C_6D_5CD_2H$ at 2.09 ppm). Phosphorus-31 spectra, $^{31}P\{^1H\}$, were obtained at 121.42 MHz on the Varian and these spectra were referenced externally to trimethylphosphite, $P(OMe)_3$ set at 141.00 ppm realitive to 85% phosphoric acid. Carbon-13 spectra were recorded at 75.43 MHz and were referenced to the solvent peak (C_6D_6) at 128.00 ppm. All chemical shift values, δ, are given in ppm and all coupling constants, *J*, are listed in Hz.

6. Syntheses of new compounds.

The structural depictions given for each compound are the proposed solution structures based on the NMR spectroscopic evidence except for $Ir[C(CH_2)N(SiMe_2CH_2PPh_2)_2][\eta^1, \eta^2\text{-}C(CH_2)CCH]$, **13**, for which a X–ray structure determination was performed.

***mer*-Ir[N(SiMe$_2$CH$_2$PPh$_2$)$_2$](η^3-C$_3$H$_5$)X**

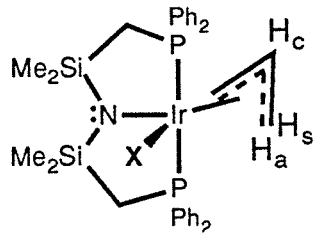

Solutions of $Ir[N(SiMe_2CH_2PPh_2)_2](Me)X$ (**2**, X = I; 0.154 g, 0.178 mmol; **3**, X = Br; 0.162 g, 0.199 mmol) in toluene (10 mL) were degassed on the vacuum line. One equivalent of

acetylene was added to the frozen reaction vessels (77 K) via a constant volume bulb (55 mm Hg in 62.443 mL). The solutions were warmed to room temperature and stirred for 6–7 days. During this time the solutions changed from green to yellow, then to reddish orange and then to yellow. The solvent was then removed *in vacuo* and the resulting powder was washed with hexanes and then extracted with toluene. Insoluble impurities were filtered off and the solution was concentrated and let stand at room temperature, which resulted in the formation of yellow crystals.

***mer*-Ir[N(SiMe$_2$CH$_2$PPh$_2$)$_2$](η^3-C$_3$H$_5$)I, 6**

This compound was previously synthesized by reaction of the vinylidene complex with methyl iodide,[11] and analytical data consistent with that preparation were obtained.

***mer*-Ir[N(SiMe$_2$CH$_2$PPh$_2$)$_2$](η^3-C$_3$H$_5$)Br, 7**

Yield 136 mg (81%). **^{1}H NMR** (C_6D_6, δ, ppm): 0.34 (s, SiCH_3, 3H), 0.40 (s, SiCH_3, 3H), 1.10 (s, SiCH_3, 3H), 0.62 (s, SiCH_3, 3H), 1.53 (dvt, PCH_2Si, 2H, ^2JH,H = 1.5, [$^2J_{H,P}$+$^4J_{H,P}$] ÷ 2 = 9.7), 2.72 (dvt, PCH_2Si, 2H, ^2JH,H = 1.5, [$^2J_{H,P}$+$^4J_{H,P}$] ÷ 2 = 11), 0.75, 1.6 (m, H_s), 2.1, 3.35 (m, H_a), 3.90 (m, H_c), 6.9-7.2 (m, *m,p*-P(C_6H_5)$_2$), 7.2-7.3, (m, *o*-PC_6H_5), 7.5-7.6 (m, *o*-PC_6H_5), 8.2-8.3 (m, *o*-PC_6H_5). **^{31}P{^{1}H} NMR** (C_6D_6, δ, ppm): -3.57 (d, CH_2PPh_2, $^2J_{P,P}$ = 425), -9.86 (d, CH_2PCH_2Si). Due to the tendency of this compound to fail to crystallize accurate analysis of this compound was not obtained.

***mer*-Ir[N(SiMe$_2$CH$_2$PPh$_2$)$_2$](η^3-C$_3$H$_4$-1-Ph)Br, 8**

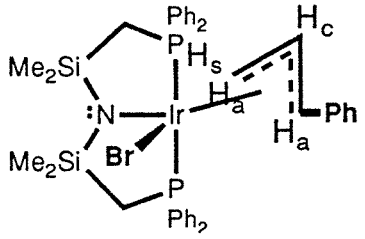

A solution of Ir[N($SiMe_2CH_2PPh_2$)$_2$](CH_2Ph)Br, **4**, (0.110 g; 0.123 mmol) in toluene (10 mL) was degassed on the vacuum line. One equivalent of acetylene was added to the frozen reaction vessel (77 K) via a constant volume bulb (36 mm Hg in 62.443 mL). The solutions were thawed and stirred for eight days. During this time the colour of the solutions changed from green to yellow, then to reddish orange and then back to yellow. The solvent was then removed *in vacuo* and the resulting powder was washed with hexanes and then extracted with toluene. Insoluble impurities were filtered off and the solution was concentrated and let stand at room temperature. The product formed as yellow crystals.

Yield 85 mg (75%). **^{1}H NMR** (C_6D_6, δ, ppm): -0.6, (s, $SiCH_3$, 3H), 0.1 (s, $SiCH_3$, 3H), 0.6, (s, $SiCH_3$, 3H), 0.9 (s, $SiCH_3$, 3H), 1.70 (ddd, PCH_2Si, 2H, $^2J_{H,H}$ = 14.5, $^2J_{H,P}$ = 16.8, $^4J_{H,P}$ = 1.7), 2.49 (ddd, PCH_2Si, 2H, $^2J_{H,P}$ = 11.8, $^4J_{H,P}$ = 4.5), 2.65 (br. s, Ha, 2H), 3.4 (ddd, H_s, 1H, J = 4.7, J = 11.1, J = 13.0), 4.5 (ddd, H_c, J = 3.6, J = 7.4, J = 10.8) 6.6 (m, *o*-$C_3H_4C_6H_5$), 6.8 (m, *m*-$C_3H_4C_6H_5$), 6.9 (m, *p*-$C_3H_4C_6H_5$), 7.0-7.3 (m, *m,p*-$P(C_6H_5)_2$), 7.8-8.1, (m, *o*-PC_6H_5), 8.3-8.4 (m, *o*-PC_6H_5). **^{31}P{^{1}H} NMR** (C_6D_6, δ, ppm): -8.3 (d, CH_2PPh_2, $^2J_{P,P}$ = 440); -13.7 (d; CH_2PPh_2). As mentioned above, this compound could not be crystallized to enable accurate analysis of this compound.

***mer*-Ir[N($SiMe_2CH_2PPh_2$)$_2$](η^3-$C_3H_2D_2$-1-Ph)Br, 8-d_2**

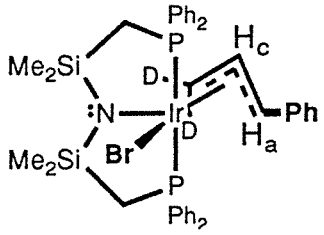

A solution of Ir[N($SiMe_2CH_2PPh_2$)$_2$](CH_2Ph)Br, **4**, (0.100 g; 0.112 mmol) in toluene (10 mL) was degassed on the vacuum line. One equivalent of acetylene-d_2 was added to the frozen reaction vessels (77 K) via a constant volume bulb (37 mm Hg in 62.443 mL). The

solution was thawed and stirred for eight days. During this time the colour of the solution changed from green to yellow, then to reddish orange and then back to yellow. The solvent was removed *in vacuo* and the resulting powder was washed with hexanes and then extracted with benzene-d_6 and the solution transferred to an NMR tube.

^{1}H NMR (C_6D_6, δ, ppm): -0.6, (s, SiCH_3, 3H), 0.1 (s, SiCH_3, 3H), 0.6, (s, SiCH_3, 3H), 0.9 (s, SiCH_3, 3H), 1.70 (ddd, PCH_2Si, 2H, $^2J_{H,H}$ = 14.5, $^2J_{H,P}$= 16.8, $^4J_{H,P}$ = 1.7), 2.49 (ddd, PCH_2Si, 2H, $^2J_{H,P}$ = 11.8, $^4J_{H,P}$ = 4.5), 2.65 (s, H_a, 1H), 4.5 (t, H_c, $^3J_{HD}$ = 4.5) 6.6 (m, *o*-$C_3H_4C_6H_5$), 6.8 (m, *m*-$C_3H_4C_6H_5$), 6.9 (m, *p*-$C_3H_4C_6H_5$), 7.0-7.3 (m, *m,p*-P(C_6H_5)$_2$), 7.8-8.1, (m, *o*-PC_6H_5), 8.3-8.4 (m, *o*-PC_6H_5). **^{31}P{^{1}H} NMR** (C_6D_6, δ, ppm): -8.3 (d, CH_2PPh_2, $^2J_{P,P}$ = 440); -13.7 (d; CH_2PPh_2).

***mer-trans*-Ir[N(SiMe$_2$CH$_2$PPh$_2$)$_2$](Me)I(PMe$_3$), 9A-C**

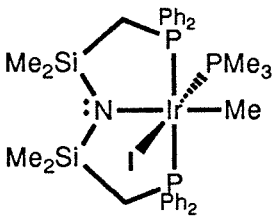

A

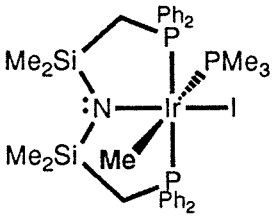

B

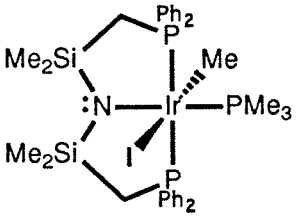

C

Method I: Trimethylphosphine (12 mm Hg in 62.443 mL) was condensed onto a frozen solution of mer-Ir[N(SiMe$_2$CH$_2$PPh$_2$)$_2$](Me)I (0.031 g; 0.036 mmol) in toluene (10 mL). Removal of the solvent *in vacuo* and extraction with benzene-d_6 allowed for the mixture to be analyzed by NMR spectroscopy. The phosphorus-31 NMR spectrum indicated that the solution contained three phosphorus containing components, **9A-C**. Heating a sealed tube of this mixture to 65°C in benzene-d_6 over a two day period resulted in the quantitative conversion to the most stable isomer, proposed to be the isomer with trimethylphosphine trans to the amide,

9C. The identity of this isomer is assigned based on the independent synthesis given below (Method II).

^{1}H NMR (C_6D_6, δ, ppm): *mer-trans*-Ir[$N(SiMe_2CH_2PPh_2)_2$](Me)I(PMe_3): 0.60 (s, $SiCH_3$, 6H), 0.65 (s, $SiCH_3$, 6H), 1.97 (dvt, PCH_2Si, 2H, $^2J_{H,H}$ = 13.6, $[^2J_{H,P}+^4J_{H,P}] \div 2$ = 5.9), 2.17 (dvt, PCH_2Si, 2H, $[^2J_{H,P}+^4J_{H,P}] \div 2$ = 5.4), 0.9 (d, $P(CH_3)_3$, J = 9.7), 0.32 (qrt, $IrCH_3$, $J_{H,P}$ = 5.6), 7.0-7.2 (m, *m,p*-$P(C_6H_5)_2$), 7.5-7.6, (m, *o*-PC_6H_5), 8.3-8.4 (m, *o*-PC_6H_5). *mer-trans*-Ir[$N(SiMe_2CH_2PPh_2)_2$](Me)(PMe_3)I: 0.40, (s, $SiCH_3$, 6H), 0.45 (s, $SiCH_3$, 6H), 1.57 (dvt, PCH_2Si, 2H, $^2J_{H,H}$ = 13, $[^2J_{H,P}+^4J_{H,P}] \div 2$ = 6), 2.2 (obscured, PCH_2Si), 1.13 (d, $P(CH_3)_3$, J = 8), 2.2 (obscured, $IrCH_3$), 6.85-7.0 (m, *m,p*-$P(C_6H_5)_2$), 8.0-8.1, (m, *o*-PC_6H_5), 8.4-8.5 (m, *o*-PC_6H_5). *mer-trans*-Ir[$N(SiMe_2CH_2PPh_2)_2$](PMe_3)I(Me): compound in too low concentration to measure resonances. **$^{31}P\{^1H\}$ NMR** (C_6D_6, δ, ppm): *mer-trans*-Ir[$N(SiMe_2CH_2PPh_2)_2$](Me)I(PMe_3): -9.15 (d; CH_2PPh_2; $^2J_{P,P}$ = 17); -60.66 (t; PMe_3); *mer-trans*-Ir[$N(SiMe_2CH_2PPh_2)_2$](PMe_3)I(Me): -22.7 (d; CH_2PPh_2; $^2J_{P,P}$ = 19); -71.0 (t; PMe_3); *mer-trans*-Ir[$N(SiMe_2CH_2PPh_2)_2$](Me)(PMe_3)I: -19.0 (d; CH_2PPh_2; $^2J_{P,P}$ = 16-18); -50.0 (t; PMe_3).

Method II: Excess trimethylphosphine was vacuum transferred onto a solution of Ir[$N(SiMe_2CH_2PPh_2)_2$](C_8H_{14}) (0.070 g; 0.084 mmol) in toluene (10 mL). After stirring for one hour the excess trimethylphosphine, toluene and liberated cyclooctene were removed *in vacuo*. The resulting powder was taken up in toluene (10 mL) and excess methyl iodide was vacuum transferred onto the solution. The orange colour of the solution was immediately lost as the coordinatively saturated *mer-trans*-Ir[$N(SiMe_2CH_2PPh_2)_2$](Me)I(PMe_3), **9C**, formed. The mixture was stirred for one half hour and the solvent and excess methyl iodide are removed *in vacuo*. The resulting oil was extracted with toluene and crystallization of yellow bricks ensued.

References p. 68

Yield 100% by NMR. **^{1}H NMR** (C_6D_6, δ, ppm) 0.60 (s, SiCH_3, 6H), 0.65 (s, SiCH_3, 6H), 1.97 (dvt, PCH_2Si, 2H, $^2J_{H,H}$ = 13.6, [$^2J_{H,P}$+$^4J_{H,P}$] ÷ 2 = 5.9), 2.17 (dvt, PCH_2Si, 2H, [$^2J_{H,P}$+$^4J_{H,P}$] ÷ 2 = 5.4), 0.9 (d, P(CH_3)$_3$, J = 9.7), 0.32 (qrt, IrCH_3, $J_{H,P}$ = 5.6), 7.0-7.2 (m, *m,p*-P(C$_6H_5$)$_2$), 7.5-7.6, (m, *o*-PC$_6H_5$), 8.3-8.4 (m, *o*-PC$_6H_5$). **^{31}P{^{1}H} NMR** (C_6D_6, δ, ppm): -9.15 (d; CH_2PPh_2; $^2J_{P,P}$ = 17); -60.66 (t; PMe_3). Elemental analysis of this compound was not attempted.

***mer*-Ir[N(SiMe$_2$CH$_2$PPh$_2$)$_2$][η^1-C(CH$_2$)C(CH$_2$)CH$_3$]X**

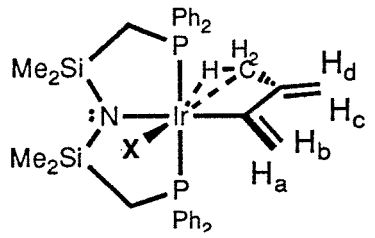

A solution of *mer*-Ir[N(SiMe$_2$CH$_2$PPh$_2$)$_2$](Me)X (**2**, X = I; 0.150 g, 0.173 mmol: **3**, X = Br; 0.268 g, 0.328 mmol) in toluene (10 mL) was degassed and acetylene was added to a pressure of 1 atm. The reaction mixture was stirred overnight, with the pressure of acetylene maintained at 1 atm. The solvent was removed *in vacuo* and the product extracted with toluene. Insoluble polymeric residue was filtered off and the solution was concentrated and left to stand at room temperature.

***mer*-Ir[N(SiMe$_2$CH$_2$PPh$_2$)$_2$][η^1-C(CH$_2$)C(CH$_2$)CH$_3$]I, 10**

Yield 118 mg (75%). **^{1}H NMR** (C_6D_6, δ, ppm) -0.95 (s, C(CH$_2$)C(CH$_2$)CH_3) -0.15 (s, SiCH_3) 0.30 (s, SiCH_3) 1.01 (dvt, PCH_2Si $^2J_{gem}$ = 12.9, [$^2J_{H,P}$+$^4J_{H,P}$] ÷ 2 = 5.3) 2.59 (dvt, PCH2Si, [$^2J_{H,P}$+$^4J_{H,P}$] ÷ 2 = 6.6) 4.91 (td, H_c, $^4J_{P,H}$ = 2.4, $^2J_{gem}$= 0.5) 4.98-5.01 (m, H_d) 5.16 and 5.74 (td, H_a and H_b, $J_{P,H}$ = 2.6 and $J_{P,H}$ = 3.1, J_{gem} = 0.5), 6.85 (m, *p*-PC$_6H_5$), 6.95 (m, *m*-PC$_6H_5$), 7.00 (m, *p*-PC$_6H_5$), 7.13 (m, *m*-PC$_6H_5$), 7.8-8.0 (m, *o*-PC$_6H_5$), 8.45-8.55 (m, *o*-

PC_6H_5). **$^{31}P\{^1H\}$ NMR** (C_6D_6, δ, ppm) -3.06 (s, CH_2PPh_2). Accurate analysis of this compound was previously obtained.[12]

Previous work from our laboratories[12] involved the preparation of the carbon-13 labelled product by reaction of Ir[N($SiMe_2CH_2PPh_2$)$_2$($^{13}CH_3$)I with acetylene. The proton NMR of the resulting complex displays three resonances that are coupled to the carbon-13 nucleus; they are: -0.95 (d, $^{13}CH_3$, $^1J_{C,H}$ = 169), 4.91 (d, H_c, $^3J_{C,H}$ = 13), 4.99 (d, H_d, $^3J_{C,H}$ = 6).

***mer*-Ir[N($SiMe_2CH_2PPh_2$)$_2$][η^1-$C(CH_2)C(CH_2)CH_3$]Br, 11**

Yield 205 mg (72%). **^1H NMR** (C_6D_6, δ, ppm) -0.86 (s, $C(CH_2)C(CH_2)CH_3$) -0.18 (s, $SiCH_3$) 0.32 (s, $SiCH_3$) 1.11 (dvt, PCH_2Si $^2J_{gem}$ = 12.8, [$^2J_{H,P}$+$^4J_{H,P}$] ÷ 2 = 5.4) 2.54 (dvt, PCH_2Si, [$^2J_{H,P}$+$^4J_{H,P}$] ÷ 2 = 6.6) 4.84 (t, $C(CH_2)C(CH_2)CH_3$, $^4J_{P,H}$ = 2.4) 4.98-5.01 (m, $C(CH_2)C(CH_2)CH_3$) 5.24 (t, $C(CH_2)C(CH_2)CH_3$, $J_{P,H}$ = 2.8) 5.90 (t, $C(CH_2)C(CH_2)CH_3$, $J_{P,H}$ = 2.6), 6.83 (m, *p*-PC_6H_5), 6.92 (m, *m*-PC_6H_5), 7.00 (m, *p*-PC_6H_5), 7.03 (m, *m*-PC_6H_5), 7.86-9793 (m, *o*-PC_6H_5), 8.47-8.54 (m, *o*-PC_6H_5). **$^{31}P\{^1H\}$ NMR** (C_6D_6, δ, ppm) -3.66 (s, CH_2PPh_2)

***fac*-Ir[N($SiMe_2CH_2PPh_2$)$_2$](PMe$_3$)[$C(CH_2)C(CH_2)CH_3$]I, 12**

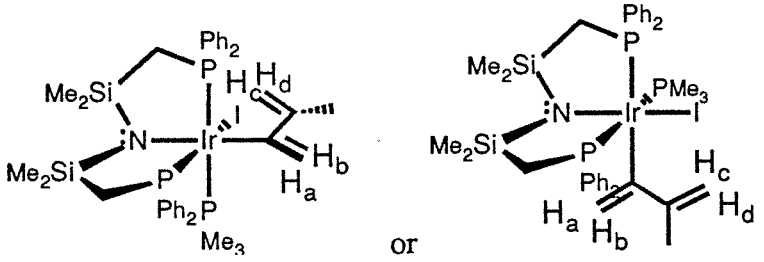

To a stirred, degassed solution of *mer*-Ir[N($SiMe_2CH_2PPh_2$)$_2$][$C(CH_2)C(CH_2)CH_3$]I, **10**, (0.055 g; 0.060 mmol) in toluene (10 mL) was added trimethylphosphine in excess. The solution immediately changed from peach to pale yellow. The solution was stirred for half an

hour and the solvent was removed *in vacuo*. The oil was extracted with benzene-d_6 and the phosphorus-31 and proton NMR spectra were recorded.

Yield 90% by ^{31}P NMR. **^1H NMR** (C_6D_6, δ, ppm) -0.16 (s, SiCH_3), 0.13 (s, SiCH3), 0.27 (s, SiCH_3), 0.64 (s, SiCH_3), 0.37 (d, P(CH_3)$_3$), 1.49 (m, PCH_2Si), 1.17 (m, PCH_2Si), 2.2 (m, $C_4H_4CH_3$), 5.08 (m, H_a), 5.95 (m, H_c), 6.06 (m, H_b), 6.51 (m, H_d), 6.5-7.2 (m, *m,p*-P(C$_6H_5$)$_2$), 7.6-7.7 (m, *o*-P(C$_6H_5$)$_2$), 7.9-8.0 (m, *o*-P(C$_6H_5$)$_2$), 8.2-8.3 (m, *o*-P(C$_6H_5$)$_2$), 8.4-8.5 (m, *o*-P(C$_6H_5$)$_2$). **$^{31}P\{^1H\}$ NMR** (C_6D_6, δ, ppm) -59.15 (dd, *P*Me3, $^2J_{trans}$=387.5 Hz, $^2J_{cis}$=8.5 Hz); -50.54 (dd, CH_2PPh_2 trans to PMe_3, $^2J_{cis}$=19.6 Hz) and -37.69 (dd, CH_2PPh_2 cis to both other phosphines).

***mer*-Ir[C(CH$_2$)N(SiMe$_2$CH$_2$PPh$_2$)$_2$][η^1,η^2-C(CH$_2$)CCH]Br, 13**

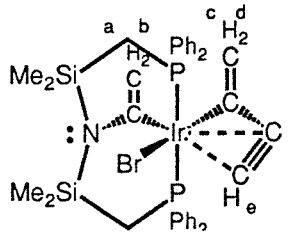

A solution of Ir[N(SiMe$_2$CH$_2$PPh$_2$)$_2$](CH$_2$Ph)Br, **4**, (0.063 g; 0.071 mmol) in toluene (10 mL) was degassed and acetylene was added to a pressure of one atmosphere. The solution was stirred magnetically overnight and the pressure of acetylene was maintained at one atmosphere. The solvent and excess acetylene were removed *in vacuo* and the resulting oil was extracted with toluene. Insoluble polymeric residue was filtered off and the solution was concentrated and left to stand at room temperature and the product crystallized as orange prisms.

Yield 28 mg (43%). **^1H NMR** (C_6D_6, δ, ppm): 0.20, (s, Si(CH_3)$_2$, 6H), 0.40 (s, Si(CH_3)$_2$, 6H), 1.50 (dvt, PCH_2Si, 2H, [$^2J_{H,P}$+$^4J_{H,P}$] ÷ 2 = 5.5, $^2J_{H,H}$ = 14), 2.50 (dvt, PCH_2Si,

2H, $[^2J_{H,P}+^4J_{H,P}] \div 2 = 7.0$), 3.7 (br s, H_e), 4.1 and 4.2 (br s and br s, H_a and H_b), 5.0 and 5.8 (br s and br s, H_c and H_d) 7.0-7.2 (m, *m,p*-P(C_6H_5)$_2$), 7.4-7.5 (m, *o*-P(C_6H_5)$_2$) 7.9-8.0 (m, *o*-P(C_6H_5)$_2$). **$^{31}P\{^1H\}$ NMR** (C_6D_6, δ, ppm): -10.60 (s, CH_2PPh_2). Despite repeated attempts, accurate analysis of this compound was not obtained. The failure of the elemental analysis is likely due to the presence of toluene in the crystal lattice. See Appendix A for details of the X-ray crystallographic analysis.

***mer*-Ir[N(SiMe$_2$CH$_2$PPh$_2$)$_2$](η^2-C$_3$H$_4$), 14**

The preparation of this compound from the cyclooctene precursor, **1**, has been reported previously.[13] A second procedure is reported here.

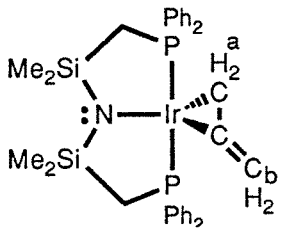

The addition of excess allene to the alkyl halide complexes, Ir[N(SiMe$_2$CH$_2$PPh$_2$)$_2$](CH$_2$R)X (**2**, R = H, X = I; **3**, R = H, X = Br; **4**, R = Ph, X=Br. A typical reaction used about 30 mg of the alkyl halide complex.), in benzene (5 mL) results in reductive elimination of the alkyl halide (within five minutes for the methyl derivatives, **2** and **3**, and longer for the benzyl analogue, **4**) and coordination of the allene. Removal of the excess allene, alkyl halide and solvent *in vacuo* produces the desired adduct with one equivalent of incorporated allene.

Analytical data consistent with that obtained from the first preparation were obtained.[13] The earlier preparation reported the allene and tridentate ligand methylene resonances as multiplets. Coupling patterns of these resonances could be determined and are reported here.

References p. 68

^{1}H NMR (C_6D_6, δ, ppm) 1.13 (ddvt, Ir-CH_2-C=CH_2, $J_{H,P}$ = 5.8, $J_{H,H}$ = 2.3, $J_{H,H}$ = 2.0), 1.73 (dvt, PCH_2Si, $J_{H,H}$ = 13.1, $J_{H,P}$ = 5.0), 1.80 (dvt, PCH_2Si, $J_{H,H}$=13.1, $J_{H,P}$ = 5.1), 5.20 and 5.39 (dvt and dvt, H_b and H_c, $J_{H,H}$ = 2.0, $J_{H,P}$ = 1.3 and $J_{H,P}$ = 1.5). All other resonances were as previously reported.

***mer*-Ir[N(SiMe$_2$CH$_2$PPh$_2$)$_2$](C$_6$H$_8$), 15**

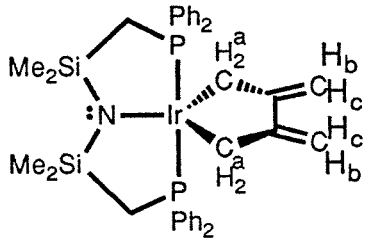

This compound is stable only in the presence of excess allene. There are three methods by which this compound can be prepared.

Method I: A solution of Ir[N(SiMe$_2$CH$_2$PPh$_2$)$_2$](C$_8$H$_{14}$), **1**, (0.030 g; 0.036 mmol) in benzene-d_6 was sealed under excess allene in an NMR tube. The presence of the product was verified by NMR spectroscopy, see below.

Method II: A solution of Ir[N(SiMe$_2$CH$_2$PPh$_2$)$_2$](η^2-C$_3$H$_4$), **14**, (0.044 g; 0.058 mmol) in benzene-d_6 was sealed under excess allene in an NMR tube. The presence of the product was verified by NMR spectroscopy, see below.

Method III: The alkyl halide complexes [Ir[N(SiMe$_2$CH$_2$PPh$_2$)$_2$](CH$_2$R)X (**2**, R = H, X = I; **3**, R = H, X = Br; **4**, R = Ph, X = Br)] in benzene-d_6 were sealed in NMR tubes under excess allene. The formation of the desired product was determined by NMR spectroscopy, see below.

Yield 100% by ^{31}P and ^{1}H NMR by each method. **^{1}H NMR** (C_6D_6, δ, ppm): 0.57, (s, $Si(CH_3)_2$, 12H), 1.25 (tt, H_a, $^{3}J_{P,H}$ = 5.7, $^{4}J_{H,H}$= $^{4}J_{H,H}$ = 2.9), 1.84 (vt, PCH_2Si, 4H, $[^{2}J_{H,P}+^{4}J_{H,P}] \div 2$ = 5.7), 5.79 and 6.17 (t and t, H_b and H_c, $^{4}J_{H,H}$ = 2.9), 6.95-7.10 (m, *m,p*-$P(C_6H_5)_2$), 7.55-7.65, (m, *o*-PC_6H_5). **$^{31}P\{^{1}H\}$ NMR** (C_6D_6, δ, ppm): -6.71 (s, CH_2PPh_2).

***fac*-Ir[N(SiMe$_2$CH$_2$PPh$_2$)$_2$](PMe$_3$)(η^2-C$_3$H$_4$), 16**

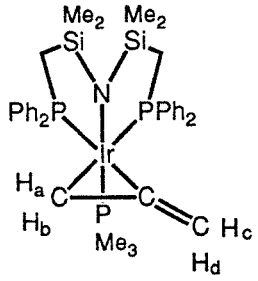

Method I

Allene was condensed onto a solution of Ir[N(SiMe$_2$CH$_2$PPh$_2$)$_2$](C$_8$H$_{14}$), **1**, (50 mg; 0.060 mmol) in toluene (10 mL). After stirring for half an hour excess allene, liberated cyclooctene and the solvent were removed *in vacuo*. The resulting oil was extracted with toluene and trimethylphosphine was condensed onto the solution. The mixture was stirred for one hour and the solvent and the excess trimethylphosphine were removed *in vacuo*. The resulting powder was extracted with benzene-d_6 and the phosphorus-31 and proton NMR spectra were recorded.

Method II

Allene was condensed onto a solution of Ir[N(SiMe$_2$CH$_2$PPh$_2$)$_2$](η^2-C$_3$H$_4$), **14**, (0.031 g; 0.041 mmol) in toluene (10 mL). After stirring for half an hour, trimethylphosphine was condensed onto the metallacyclopentane generated in situ. The mixture was stirred for one hour

and the solvent, the excess reagents, and the liberated cyclooctene were removed *in vacuo*. The resulting powder was taken up in toluene and left to stand at room temperature to crystallize.

^{1}H NMR (C_6D_6, δ, ppm): -0.27, (s, SiCH_3, 3H), 0.29 (s, SiCH_3, 3H), 0.60, (s, SiCH_3, 3H), 0.70 (s, SiCH_3, 3H), 0.36 (d, P(CH_3)$_3$, 9H, $^2J_{H,P}$ = 9.7), 1.8-2.0 (m, PCH_2Si), 2.25 (m, PCH_2Si), 2.96 (m, PCH_2Si), 1.5, 2.4 (m, H_a and H_b), 5.5 and 5.53 (m, H_c and H_d), 6.6-7.9 (m, *o,m,p*-P(C$_6H_5$)$_2$). **^{31}P{^{1}H} NMR** (C_6D_6, δ, ppm): -49.82 (d, *P*Me$_3$, $^2J_P^{cis}$ = 15, $^2J_P^{cis}$ = 14), -4.89 (d, CH_2*P*Ph$_2$, $^2J_P^{cis}$ = 14, $^2J_P^{cis}$ = 11), 3.18 (d, CH_2*P*Ph$_2$, $^2J_P^{cis}$ = 15, $^2J_P^{cis}$ = 11)

7. References.

(1) Bafus, D. A.; Brown, T. L.; Dickerhoff, D. W.; Morgan, G. L. *Rev. Sci. Instrum.* **1962**, *33*, 491.

(2) Corey, E. J.; Kim, C. U.; Takeda, M. *Tettrahedron Lett.* **1972**, *42*, 4339.

(3) Inhoffen, H. H.; Pommer, H.; Meth, E.-G. *Justus Liebigs Ann. Chem.* **1949**, *565*, 45.

(4) Herdé, J. L.; Senoff, C. V. *Inorg. Nucl. Chem. Lett.* **1971**, *7*, 1029.

(5) van der Ent, A.; Onderlinden, A. L. *Inorg. Synth.* **1973**, *14*, 92.

(6) Fryzuk, M. D.; MacNeil, P. A. *Organometallics* **1983**, *2*, 355.

(7) Fryzuk, M. D.; MacNeil, P. A. *Organometallics* **1983**, *2*, 682.

(8) Fryzuk, M. D.; MacNeil, P. A.; Rettig, S. J. *Organometallics* **1985**, *4*, 1145.

(9) Fryzuk, M. D.; MacNeil, P. A.; Rettig, S. J. *Organometallics* **1986**, *5*, 2469.

(10) Fryzuk, M. D.; MacNeil, P. A.; Massey, R. L.; Ball, R. G. *J. Organomet. Chem.* **1989**, *368*, 231.

(11) Fryzuk, M. D.; Huang, L.; McManus, N. T.; Paglia, P.; Rettig, S. J.; White, G. S. *Organometallics* **1992**, *11*, in press.

(12) Fryzuk, M. D.; McManus, N. T., Unpublished results.

(13) Joshi, K. Ph D Thesis, University of British Columbia, 1990.

APPENDIX A

X-RAY CRYSTALLOGRAPHIC ANALYSIS

1. Experimental details.

A. Crystal data.

Empirical Formula	$C_{39.5}H_{45}BrIrNP_2Si_2$
Formula Weight	924.04 g mol^{-1}
Crystal Colour, Habit	orange, prism
Crystal Dimensions (mm)	0.150 x 0.300 x 0.450
Crystal System	triclinic
Number of Reflections Used for Unit Cell Determination (2θ range)	25 (32.7 – 39.2°)
Omega Scan Peak Width at Half-height	0.42
Lattice Parameters:	a = 11.044 (2) Å b = 19.520 (3) Å c = 10.062 (1) Å α = 89.99 (1) Å β = 109.72 (1) Å γ = 76.50 (1) Å V = 1978.1 (5) Å3
Space Group	$P\bar{1}$ (#2)
Z value	2
D_{calc}	1.551 g cm^{-3}
F_{000}	918
μ (MoKα)	45.29 cm^{-1}

B. Intensity measurements.

Diffractometer	Rigaku AFC6S
Radiation	MoKα (λ = 0.71069 Å)
Temperature	21°C
Take-off Angle	6.0°
Detector Aperture	6.0 mm horizontal
	6.0 mm vertical
Crystal to Detector Distance	285 mm
Scan Type	ω - 2θ
Scan Rate	32.0° min^{-1} (in ω)
	(8 rescans)
Scan Width	(1.26 + 0.35 tanθ)°
2 θ_{max}	60.0°
Number of Reflections Measured	Total: 12 097
	Unique: 11 538 (R_{int} = 0.037)
Corrections	Lorentz-polarization Absorption
	(trans. factors: 0.53 - 1.00)
	Secondary Extinction
	(coefficient: 143.85 x 10^{-9})

C. Structure solution and refinement.

Structure Solution	Patterson Method
Refinement	Full-matrix Least-squares
Function Minimized	$\Sigma w (\lvert F_o \rvert - \lvert F_c \rvert)^2$
Least-squares Weights	$\frac{4 F_o^2}{\sigma^2 F_o^2}$
p-factor	0.00
Anomalous Dispersion	All non-hydrogen atoms
No. Observations (I > 3.00 σ(I))	7070
No. Variables	454
Reflection / Parameter Ratio	15.57
Residuals: R; R_w	0.033; 0.028
Goodness of Fit Indicator	1.54
Max Shift / Error in Final Cycle	0.27

Maximum Peak in Final Diff. Map 1.57 e$^-$ Å^{-3}

Minimum Peak in Final Diff. Map –1.16 e$^-$ Å^{-3}

2. Tabulated data.

Table A.Ia. Final atomic coordinates (fractional) and B_{eq} (Å^2).

Atom	*x*	*y*	*z*	B_{eq}[a]
Ir(1)	0.39919 (2)[b]	0.20100 (1)	0.46200 (2)	2.636 (8)[c]
Br(1)	0.22549 (5)	0.26836 (3)	0.22100 (5)	4.22 (3)
P(1)	0.5473 (1)	0.26445 (6)	0.4386 (1)	2.86 (6)
P(2)	0.2194 (1)	0.17473 (6)	0.5055 (1)	2.78 (5)
Si(1)	0.3370 (1)	0.40674 (7)	0.4692 (2)	4.09 (7)
Si(2)	0.1181 (1)	0.34419 (7)	0.5332 (2)	3.92 (7)
N(1)	0.2698 (3)	0.3457 (2)	0.5226 (4)	3.2 (2)
C(1)	0.4661 (5)	0.3582 (2)	0.3946 (5)	3.7 (2)
C(2)	0.0882 (4)	0.2542 (2)	0.4927 (5)	3.5 (2)
C(3)	0.4083 (6)	0.4593 (3)	0.6173 (7)	6.7 (4)
C(4)	0.2141 (6)	0.4715 (3)	0.3239 (8)	7.3 (4)
C(5)	0.1079 (6)	0.3659 (3)	0.7094 (7)	6.1 (4)
C(6)	- 0.0219 (5)	0.4067 (3)	0.3963 (7)	6.7 (4)
C(7)	0.6964 (4)	0.2577 (3)	0.5953 (5)	3.3 (2)
C(8)	0.7933 (5)	0.1950 (3)	0.6338 (5)	4.5 (3)
C(9)	0.9053 (5)	0.1870 (3)	0.7554 (6)	5.7 (3)
C(10)	0.9205 (6)	0.2424 (4)	0.8390 (6)	6.2 (4)
C(11)	0.8251 (6)	0.3046 (4)	0.8015 (6)	6.6 (4)
C(12)	0.7152 (5)	0.3124 (3)	0.6798 (6)	5.2 (3)
C(13)	0.6171 (4)	0.2428 (2)	0.2980 (4)	3.1 (2)
C(14)	0.5526 (5)	0.2092 (3)	0.1849 (5)	4.8 (3)
C(15)	0.6001 (6)	0.1935 (3)	0.0753 (5)	5.5 (4)
C(16)	0.7110 (5)	0.2129 (3)	0.0751 (5)	5.3 (3)
C(17)	0.7747 (5)	0.2472 (3)	0.1844 (6)	5.4 (3)
C(18)	0.7298 (5)	0.2617 (3)	0.2968 (5)	4.4 (3)
C(19)	0.2586 (4)	0.1293 (2)	0.6782 (4)	2.8 (2)

C(20)	0.3071 (5)	0.0571 (3)	0.7007 (5)	3.7 (3)
C(21)	0.3385 (5)	0.0210 (3)	0.8322 (5)	4.2 (3)
C(22)	0.3235 (5)	0.0579 (3)	0.9430 (5)	4.3 (3)
C(23)	0.2784 (5)	0.1303 (3)	0.9256 (5)	4.6 (3)
C(24)	0.2463 (4)	0.1660 (3)	0.7946 (5)	3.7 (2)
C(25)	0.1234 (4)	0.1195 (2)	0.3866 (5)	3.1 (2)
C(26)	0.1301 (5)	0.1090 (3)	0.2540 (5)	4.6 (3)
C(27)	0.0490 (6)	0.0709 (3)	0.1619 (6)	6.1 (4)
C(28)	-0.0381 (6)	0.0446 (3)	0.2037 (6)	5.9 (4)
C(29)	-0.0466 (6)	0.0557 (3)	0.3333 (6)	5.6 (3)
C(30)	0.0328 (5)	0.0927 (3)	0.4254 (5)	4.5 (3)
C(31)	0.3705 (4)	0.2808 (2)	0.5894 (5)	3.1 (2)
C(32)	0.4405 (6)	0.2770 (3)	0.7270 (6)	4.3 (3)
C(33)	0.4516 (8)	0.0914 (4)	0.3635 (7)	7.2 (4)
C(34)	0.5415 (8)	0.0993 (3)	0.4602 (8)	8.7 (5)
C(35)	0.5394 (5)	0.1215 (3)	0.5998 (5)	3.6 (2)
C(36)	0.6069 (8)	0.0964 (5)	0.7260 (8)	5.8 (4)
C(37)	0.543 (3)	0.480 (5)	0.011 (3)	16 (4)
C(38)	0.49 (1)	0.433 (2)	0.030 (3)	25 (3)
C(39)	0.346 (6)	0.444 (3)	0.003 (3)	13 (3)
C(40)	0.313 (7)	0.494 (3)	-0.014 (4)	18 (3)
C(41)	0.334 (6)	0.549 (2)	-0.035 (2)	26 (3)

Table A.Ib. Hydrogen atom coordinates (fractional) and B_{iso} (Å^2).

Atom	*x*	*y*	*z*	B_{iso}
H(1)	0.5375	0.3829	0.4223	4.4
H(2)	0.4228	0.3642	0.2914	4.4
H(3)	0.0268	0.2598	0.3945	4.2
H(4)	0.0437	0.2432	0.5565	4.2
H(5)	0.4783	0.4275	0.6949	8.1
H(6)	0.4460	0.4935	0.5835	8.1
H(7)	0.3382	0.4845	0.6514	8.1
H(8)	0.2583	0.5042	0.2963	8.8

H(9)	0.1751	0.4464	0.2423	8.8
H(10)	0.1439	0.4981	0.3564	8.8
H(11)	0.1755	0.3308	0.7827	7.4
H(12)	0.1233	0.4130	0.7284	7.4
H(13)	0.0196	0.3654	0.7101	7.4
H(14)	-0.0123	0.4551	0.4102	8.0
H(15)	-0.0212	0.3949	0.3019	8.0
H(16)	-0.1061	0.4031	0.4048	8.0
H(17)	0.7832	0.1553	0.5747	5.3
H(18)	0.9732	0.1421	0.7813	6.9
H(19)	0.9990	0.2371	0.9248	7.5
H(20)	0.8347	0.3440	0.8612	7.9
H(21)	0.6490	0.3579	0.6530	6.2
H(22)	0.4714	0.1963	0.1823	5.8
H(23)	0.5541	0.1684	-0.0026	6.6
H(24)	0.7446	0.2022	-0.0032	6.4
H(25)	0.8536	0.2617	0.1837	6.5
H(26)	0.7780	0.2856	0.3757	5.3
H(27)	0.3198	0.0302	0.6222	4.5
H(28)	0.3711	-0.0306	0.8449	5.0
H(29)	0.3450	0.0327	1.0354	5.2
H(30)	0.2690	0.1567	1.0059	5.5
H(31)	0.2144	0.2176	0.7830	4.4
H(32)	0.1919	0.1282	0.2237	5.5
H(33)	0.0547	0.0631	0.0677	7.3
H(34)	-0.0945	0.0177	0.1397	7.0
H(35)	-0.1100	0.0371	0.3621	6.7
H(36)	0.0253	0.1003	0.5189	5.4
H(37)	0.416 (5)	0.333 (3)	0.772 (6)	9 (2)
H(38)	0.505 (5)	0.237 (3)	0.768 (5)	5 (1)
H(39)	0.430 (5)	0.079 (3)	0.282 (5)	5 (1)
H(40)	0.608 (7)	0.119 (3)	0.772 (6)	4 (2)
H(41)	0.676 (6)	0.048 (3)	0.738 (6)	9 (2)

H(42)	0.5483	0.3860	0.0681	30.5
H(43)	0.2973	0.4078	0.0016	15.4
H(44)	0.2209	0.5046	-0.0149	20.5
H(45)	0.2796	0.5973	-0.0608	31.0

[a] $B_{eq} = \frac{8}{3}\pi^2 \Sigma\Sigma U_{ij} a_i * a_j * (a_i \bullet a_j)$

[b] numbers in parentheses indicate the estimated standard deviation in the least significant digit

[c] all atoms are assigned an occupancy of 1 except those associated with the lattice toluene, C(37) - C(41)

Table A.II. Selected bond lengths (Å) with standard deviations.

Atom	Atom	Distance	Atom	Atom	Distance
Ir (1)	Br (1)	2.6401 (7)	Si (2)	N (1)	1.720 (4)
Ir (1)	P (1)	2.339 (1)	Si (2)	C (2)	1.883 (5)
Ir (1)	P (2)	2.337 (1)	Si (2)	C (5)	1.857 (6)
Ir (1)	C (31)	2.053 (4)	Si (2)	C (6)	1.860 (6)
Ir (1)	C (33)	2.389 (6)	N (1)	C (31)	1.460 (5)
Ir (1)	C (34)	2.230 (6)	C (31)	C (32)	1.330 (7)
Ir (1)	C (35)	2.039 (5)	C (32)	H (37)	1.19 (6)
P (1)	C (1)	1.820 (5)	C (32)	H (38)	0.92 (5)
P (1)	C (7)	1.834 (4)	C (33)	C (34)	1.174 (9)
P (2)	C (13)	1.833 (4)	C (33)	H (39)	0.83 (4)
P (2)	C (2)	1.829 (5)	C (34)	C (35)	1.476 (8)
Si (1)	N (1)	1.716 (4)	C (35)	C (36)	1.265 (9)
Si (1)	C (1)	1.893 (5)	C (36)	H (40)	0.63 (5)
Si (1)	C (3)	1.866 (6)	C (36)	H (41)	1.05 (6)
Si (1)	C (4)	1.853 (6)			

Table A.III. Selected bond angles (degrees) with standard deviations.

Atom	Atom	Atom	Angle	Atom	Atom	Atom	Angle
Br(1)	Ir (1)	P (1)	88.20 (3)	N (1)	Si (1)	C (3)	111.5 (2)
Br(1)	Ir (1)	P (2)	86.73 (3)	N (1)	Si (1)	C (4)	113.0 (2)
Br(1)	Ir (1)	C (31)	97.2 (1)	C (1)	Si (1)	C (3)	111.9 (2)
Br(1)	Ir (1)	C (33)	95.0 (2)	C (1)	Si (1)	C (4)	105.8 (3)

Br(1)	Ir (1)	C (34)	119.9 (2)	C (3)	Si (1)	C (4)	106.3 (3)
Br(1)	Ir (1)	C (35)	159.4 (1)	N (1)	Si (2)	C (2)	108.6 (2)
P (1)	Ir (1)	P (2)	160.61 (4)	N (1)	Si (2)	C (5)	112.2 (2)
P (1)	Ir (1)	C (31)	79.4 (1)	N (1)	Si (2)	C (6)	112.4 (2)
P (1)	Ir (1)	C (33)	105.9 (2)	C (2)	Si (2)	C (5)	110.7 (2)
P (1)	Ir (1)	C (34)	90.6 (2)	C (2)	Si (2)	C (6)	104.9 (2)
P (1)	Ir (1)	C (35)	96.0 (1)	C (5)	Si (2)	C (6)	107.9 (3)
P (2)	Ir (1)	C (31)	82.6 (1)	Si (1)	N (1)	Si (2)	136.4 (2)
P (2)	Ir (1)	C (33)	93.2 (2)	Si (1)	N (1)	C (31)	111.6 (3)
P (2)	Ir (1)	C (34)	108.2 (2)	Si (2)	N (1)	C (31)	111.7 (3)
P (2)	Ir (1)	C (35)	95.3 (1)	P (1)	C (1)	Si (1)	123.2 (2)
C (31)	Ir (1)	C (33)	166.9 (2)	P (2)	C (2)	Si (2)	124.1 (2)
C (31)	Ir (1)	C (34)	141.4 (2)	Ir (1)	C (31)	N (1)	117.3 (3)
C (31)	Ir (1)	C (35)	103.4 (2)	Ir (1)	C (31)	C (32)	123.7 (4)
C (33)	Ir (1)	C (34)	29.2 (2)	N (1)	C (31)	C (32)	118.9 (4)
C (33)	Ir (1)	C (35)	64.4 (2)	C (31)	C (32)	H (37)	110 (3)
C (34)	Ir (1)	C (35)	40.1 (2)	C (31)	C (32)	H (38)	119 (3)
Ir (1)	P (1)	C (1)	110.9 (2)	H (37)	C (32)	H (38)	130 (4)
Ir (1)	P (1)	C (7)	115.5 (1)	Ir (1)	C (33)	C (34)	67.9 (4)
Ir (1)	P (1)	C (13)	117.4 (1)	Ir (1)	C (33)	H (39)	133 (4)
C (1)	P (1)	C (7)	106.7 (2)	C (34)	C (33)	H (39)	144 (4)
C (1)	P (1)	C (13)	102.7 (2)	Ir (1)	C (34)	C (33)	82.9 (5)
C (7)	P (1)	C (13)	102.3 (2)	Ir (1)	C (34)	C (35)	62.9 (3)
Ir (1)	P (2)	C (2)	112.1 (1)	C (33)	C (34)	C (35)	127.2 (8)
Ir (1)	P (2)	C (19)	115.3 (1)	Ir (1)	C (35)	C (34)	76.9 (3)
Ir (1)	P (2)	C (25)	119.4 (1)	Ir (1)	C (35)	C (36)	149.3 (5)
C (2)	P (2)	C (19)	105.7 (2)	C (34)	C (35)	C (36)	133.7 (6)
C (2)	P (2)	C (25)	100.8 (2)	C (35)	C (35)	H (40)	114 (7)
C (19)	P (2)	C (25)	101.7 (2)	C (35)	C (36)	H (41)	116 (3)
N (1)	Si (1)	C (1)	108.1 (2)	H (40)	C (36)	H (41)	127 (7)

APPENDIX B

KINETIC DATA

Each kinetic run was performed using a solution of Ir[N($SiMe_2CH_2PPh_2$)$_2$](CH_2Ph)Br, **4**, (29 mg; 0.034 mmol) in benzene-d_6 in NMR tubes. Allene (218 mm Hg in 62.443 mL; 0.740 mmol; 22 equivalents) was condensed onto the frozen solutions (77 K) in the NMR tubes and the tubes were sealed and kept frozen until the kinetic experiments were ready to be started. The decrease of the signal due to the starting material in the phosphorus-31 NMR spectrum (singlet at δ 0.01 ppm) was monitored as a function of time. The time for each run was recorded after 128 of 256 transients were collected. A delay of one second between pulses was used to allow time for relaxation of the phosphorus nuclei and therefore allow for accurate integrations. The integrations were converted to percentages and the percentages are listed in the tables below. The *k* values were obtained from slopes of the lines obtained from the plots of $\ln\left[\frac{(T_t - T_\infty)}{(T_0 - T_\infty)}\right]$ (where T_t, T_0 and T_∞ are the percentage of the starting material at time t, time naught and at infinite time, respectively) versus time shown after each data table. The values of *k* are the observed pseudo-first order rate constants and thus have the units of min^{-1}.

Table B.I. Run 1: Kinetic data at T = 35.0 ± 0.1 °C.

Δ t (min)	[Ir(PNP)(CH_2Ph)Br] (%)	$\ln\left[\frac{(T_t - T_\infty)}{(T_0 - T_\infty)}\right]$ ( )
6	99.1	-0.009
24	99.1	-0.009
51	97.3	-0.028
72	95.4	-0.047

103	92.9	-0.074
134	91.1	-0.093
164	89.3	-0.113
191	87.2	-0.137
231	85.0	-0.163
261	83.1	-0.185
293	80.9	-0.211
321	79.5	-0.229
352	78.0	-0.248
425	74.1	-0.299
491	70.4	-0.351
602	64.6	-0.436
662	61.2	-0.490
722	58.5	-0.536
∞	0.0	- ∞

slope = - 7.40 (6) x 10^{-4} min^{-1}

y-intercept = 6 (2) x 10^{-3}

corr = -0.9995

k = 7.40 (6) x 10^{-4} min^{-1}

$t_{1/2}$ = 937 (2) min

Table B.II. Run 2: Kinetic data at T = 35.3 ± 0.2 °C.

Δ t (min)	[Ir(PNP)(CH_2Ph)Br] (%)	$\ln\left[\frac{(T_t - T_\infty)}{(T_0 - T_\infty)}\right]$ ( )
7	100.0	0.000
72	94.9	-0.053
132	89.0	-0.117
192	84.7	-0.167
252	79.8	-0.226
312	78.7	-0.240

372	73.1	-0.314
432	67.7	-0.389
492	64.8	-0.434
552	60.5	-0.503
612	57.7	-0.550
665	54.6	-0.606
1450	23.3	-1.456
2830	7.5	-2.593
∞	0.0	- ∞

slope = - 9.4 (1) x 10^{-4} min^{-1}

y-intercept = 2 (1) x 10^{-2}

corr = -0.9986

k = 9.4 (1) x 10^{-4} min^{-1}

$t_{1/2}$ = 737 (8) min

Table B.III. Run 3: Kinetic data at T = 35.3 ± 0.1 °C.

Δ t (min)	[Ir(PNP)(CH_2Ph)Br] (%)	$\ln\left[\frac{(T_t - T_\infty)}{(T_0 - T_\infty)}\right]$ ( )
7	100.0	0.000
96	91.0	-0.094
186	83.4	-0.182
276	76.2	-0.272
366	67.9	-0.388
456	61.9	-0.480
546	56.0	-0.580
636	51.1	-0.672
726	46.0	-0.776
816	41.6	-0.878
906	39.6	-0.926
996	37.9	-0.971

1176	32.1	-1.137
1416	26.7	-1.319
∞	0.0	- ∞

slope = - 9.6 (3) x 10^{-4} min^{-1}

y-intercept = 3 (2) x 10^{-3}

corr = -0.9957

k = 9.6 (3) x 10^{-4} min^{-1}

$t_{1/2}$ = 7.2 (2) x 10^{2} min

Table B.IV. Run 4: Kinetic data at T = 45.2 ± 0.1 °C.

Δ t (min)	[Ir(PNP)(CH_2Ph)Br] (%)	$\ln\left[\frac{(T_t - T_\infty)}{(T_o - T_\infty)}\right]$ ( )
9	100.0	0.000
66	85.7	-0.154
126	75.3	-0.284
186	65.1	-0.429
246	57.6	-0.552
306	49.0	-0.713
366	43.2	-0.839
426	38.7	-0.949
486	32.2	-1.133
546	28.9	-1.241
606	25.1	-1.382
666	22.1	-1.510
726	19.0	-1.661
786	16.8	-1.784
846	12.6	-2.071
∞	0.0	-∞

slope = - 2.34 (4) x 10^{-3} min^{-1}

y-intercept = 0.02 (2)

corr = -0.9984

k = 2.34 (4) x 10^{-3} min^{-1}

$t_{1/2}$ = 296 (5) min

Table B.V. Run 5: Kinetic data at Temp = 45.2 ± 0.1 °C.

Δ t (min)	[Ir(PNP)(CH_2Ph)Br] (%)	$\ln\left[\frac{(T_t - T_\infty)}{(T_0 - T_\infty)}\right]$ ( )
7	100	0.000
67	85.3	-0.159
127	74.5	-0.294
187	64.2	-0.443
247	55.6	-0.587
307	48.7	-0.719
367	41.9	-0.870
427	36.7	-1.002
487	31.2	-1.165
547	27.2	-1.302
607	23.1	-1.465
667	20.4	-1.590
727	17.2	-1.760
787	15.3	-1.877
847	13.6	-1.995
∞	0.0	-∞

slope = - 2.40 (1) x 10^{-3} min^{-1}

y-intercept = 0.009 (6)

corr = -0.9998

k = 2.40 (1) x 10^{-3} min^{-1}

$t_{1/2}$ = 289 (1) min

Table B.VI. Run 6: Kinetic data at T = 55.2 ± 0.2 °C.

Δ t (min)	[Ir(PNP)(CH_2Ph)Br] (%)	$\ln\left[\frac{(T_t - T_\infty)}{(T_0 - T_\infty)}\right]$ ( )
13	96.8	-0.033
48	85.7	-0.155
81	76.2	-0.271
122	65.8	-0.418
165	57.2	-0.558
192	51.1	-0.671
225	46.3	-0.771
260	40.5	-0.904
290	37.3	-0.987
319	33.7	-1.087
600	11.7	-2.144

slope = - 3.57 (3) x 10^{-3} min^{-1}

y-intercept = 2.5 (8) x 10^{-2}

corr = -0.9996

k = 3.57 (3) x 10^{-3} min^{-1}

$t_{1/2}$ = 194 (2) min

Table B.VII. Run 7: Kinetic data at T = 55.1 ± 0.2 °C.

Δ t (min)	[Ir(PNP)(CH_2Ph)Br] (%)	$\ln\left[\frac{(T_t - T_\infty)}{(T_0 - T_\infty)}\right]$ ( )
8	97.7	-0.023
42	85.1	-0.161
72	71.9	-0.330
102	63.3	-0.458
132	54.9	-0.599
162	47.7	-0.740

192	41.7	-0.874
222	35.5	-1.034
252	31.7	-1.150
282	25.7	-1.359
312	22.8	-1.478
342	20.5	-1.586
372	17.3	-1.755
402	14.3	-1.947
432	13.8	-1.982
462	9.7	-2.331
492	9.6	-2.342
∞	0.0	- ∞

slope = - 4.87 (7) x 10^{-3} min^{-1}

y-intercept = 4 (2) x 10^{-2}

corr = -0.9984

k = 4.87 (7) x 10^{-3} min^{-1}

$t_{1/2}$ = 142 (2) min

Table B.VIII. Run 8: Kinetic data at T = 55.2 ± 0.2 °C with added 1,4-cyclohexadiene.

Δ t (min)	[Ir(PNP)(CH_2Ph)Br] (%)	$\ln\left[\frac{(T_t - T_\infty)}{(T_o - T_\infty)}\right]$ ( )
10	100.0	0.000
55	89.6	-0.110
100	82.8	-0.189
145	82.8	-0.189
190	75.4	-0.283
235	70.6	-0.348
280	61.2	-0.490
325	54.9	-0.599
370	50.1	-0.691

415	43.3	-0.837
460	32.1	-1.138
505	31.3	-1.161
550	29.6	-1.218
∞	0.0	- ∞

slope = - 2.4 (1) x 10^{-3} min^{-1}

y-intercept = 0.10 (5)

corr = -0.9812

k = 2.4 (1) x 10^{-3} min^{-1}

$t_{1/2}$ = 2.9 (1) x 10^{2} min

Table B.IX. Run 9: Kinetic data at T = 55.0 ± 0.2 °C with added 1.4-cyclohexadiene.

Δ t (min)	[Ir(PNP)(CH_2Ph)Br] (%)	$\ln\left[\frac{(T_t - T_\infty)}{(T_0 - T_\infty)}\right]$ ( )
9	100.0	0.000
54	91.0	-0.094
99	88.2	-0.125
144	82.4	-0.194
189	76.7	-0.265
234	73.5	-0.308
279	68.8	-0.374
324	62.0	-0.478
369	59.0	-0.527
414	55.1	-0.596
459	4.8	-0.718
504	46.2	-0.773
549	44.1	-0.819
594	39.1	-0.939
639	35.5	-1.036
684	35.4	-1.038

729	30.5	-1.188
∞	0.0	- ∞

slope = - 2.08 (4) x 10^{-3} min^{-1}

y-intercept = 4 (1) x 10^{-2}

corr = -0.9969

k = 2.08 (4) x 10^{-3} min^{-1}

$t_{1/2}$ = 334 (7) min

Table B.X. Kinetic data summarized.

Run (#)	Temp. (°C)	slope (min^{-1})	y-intercept ( )	correl'n ( )	k (min^{-1})	$t_{1/2}$ (min)
1	35.0 (1)	-7.40 (6) x 10^{-4}	0.006 (2)	-0.9995	7.40 (6) x 10^{-4}	937 (2)
2	35.3 (2)	-9.4 (1) x 10^{-4}	0.02 (1)	-0.9986	9.4 (1) x 10^{-4}	737 (8)
3	35.3 (1)	-9.6 (3) x 10^{-4}	0.03 (2)	-0.9957	9.6 (3) x 10^{-4}	720 (20)
4	45.2 (1)	-2.34 (4) x 10^{-3}	0.04 (2)	-0.9969	2.34 (4) x 10^{-3}	296 (5)
5	45.2 (1)	2.40 (1) x 10^{-3}	0.03 (1)	-0.9989	2.40 (1) x 10^{-3}	289 (1)
6	55.2 (2)	-3.57 (3) x 10^{-3}	0.025 (8)	-0.9996	3.57 (3) x 10^{-3}	194 (2)
7	55.1 (2)	-4.87 (7) x 10^{-3}	0.04 (2)	-0.9984	4.87 (7) x 10^{-3}	142 (2)
8	55.2 (2)	-2.4 (1) x 10^{-3}	0.10 (5)	-0.9812	2.4 (1) x 10^{-3}	290 (10)
9	55.0 (2)	-2.08 (4) x 10^{-3}	0.04 (1)	-0.9969	2.08 (4) x 10^{-3}	334 (7)